CHALMERS
UNIVERSITY OF TECHNOLOGY

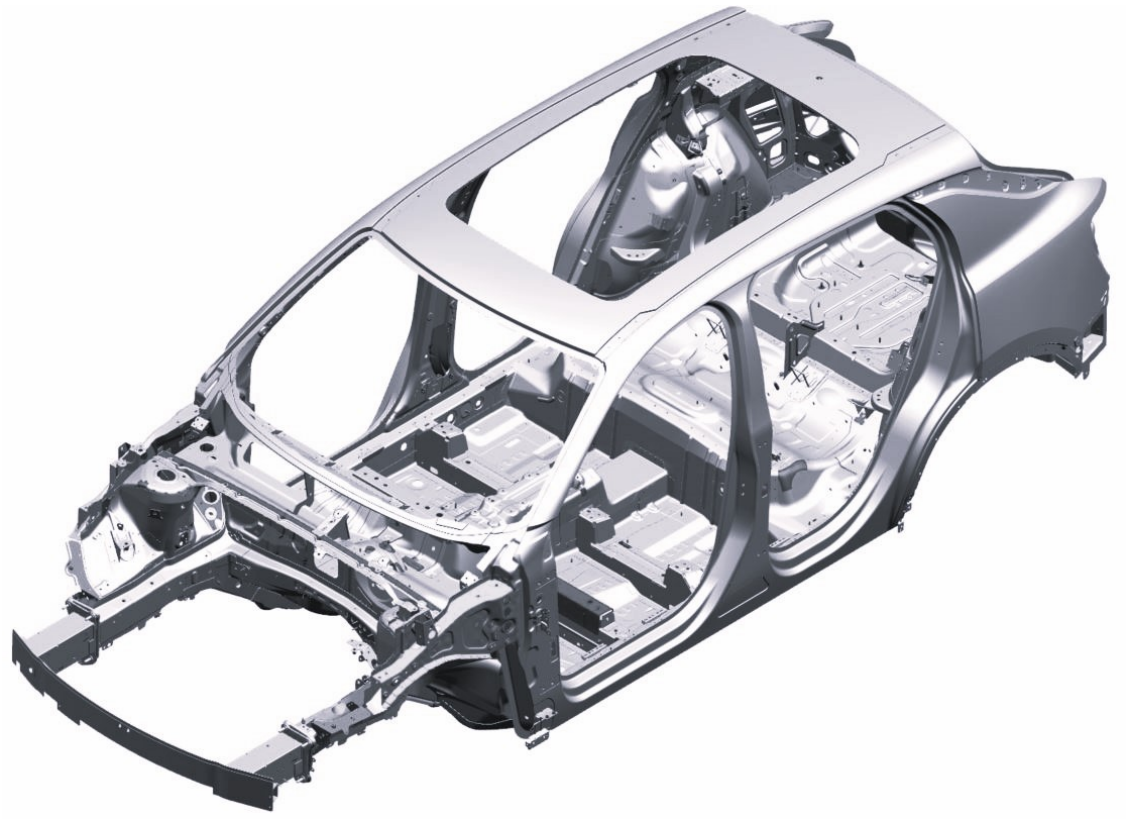

Optimizing Body Structures Designs to Minimize Environmental Impact

ADITYA KULKARNI
ANIRUDH MOSALE VISHWANATH

DEPARTMENT OF INDUSTRIAL AND MATERIAL SCIENCES

CHALMERS UNIVERSITY OF TECHNOLOGY
Gothenburg, Sweden 2024
www.chalmers.se

Master's Thesis 2024

Optimizing Body Structure Designs to Minimize Environmental Impact

ADITYA KULKARNI
ANIRUDH MOSALE VISHWANATH

CHALMERS
UNIVERSITY OF TECHNOLOGY

Department of Industrial and Material Sciences
Division of Production Engineering
Chalmers University of Technology
Gothenburg, Sweden 2024

‘Optimizing Body Structure Designs to Minimize Environmental Impact’

Industry supervisor:
CHRISTOPHER BERGHOFF, *Senior System Engineer, BIW & CAD, Zeekr Technology Europe*

University supervisor:
ARPITA CHARI, *Doctoral student, Production Systems, Industrial and Materials Science, Chalmers University of Technology*

Examiner:
MÉLANIE DESPEISSE, *Associate Professor, Production Systems, Industrial and Materials Science, Chalmers University of Technology*

Master’s Thesis 2024
Department of Industrial and Material Sciences
Division of Production Engineering
Chalmers University of Technology
SE-412 96 Gothenburg
Telephone +46 31 772 1000

Typeset in LaTeX
Printed by Chalmers Reproservice
Gothenburg, Sweden 2024

‘Optimizing Body Structure Designs to Minimize Environmental Impact’

ADITYA KULKARNI
ANIRUDH MOSALE VISHWANATH
Department of Industrial and Materials Science
Division of Production Engineering
Chalmers University of Technology

Abstract

Industries emitted a record 36.2 billion tons of CO_2e emissions in 2022, highlighting the need for sustainable products and manufacturing processes. In view of this, the study was aimed at enhancing the sustainability of automotive Body In White (BIW) structures by exploring alternative designs.

Hence, this thesis aims to investigate and provide insights into the feasibility and advantages, if any, of transitioning from presently used materials and manufacturing process at Zeekr, to an alternative option for sustainable component development. The study enlists comparative solutions to enhance sustainability in BIW structures, with a central focus on mitigating CO_2 emissions. The core proposal involves redesigning of existing automotive body structure components using alternative materials and suitable manufacturing processes.

The thesis is divided into two phases; Phase 1 and Phase 2. Phase 1 begins with theoretical calculations and Euro NCAP-based and RCAR load cases, followed by Computer Aided Drawing (CAD) in Catia V5, Computer Aided Engineering (CAE) simulations (in Ansys, Abaqus and LS-Dyna), and finally Life Cycle Inventory (LCI) analysis. These were carried out for two existing simplified geometries of body structure components; side sill/ rocker and front crash box. The aim here was to better understand the affecting parameters and their effects on predefined performance standards. This serves as a stepping stone for Phase 2.

In Phase 2, we strategically re-designed the front Crash Management System (CMS) to reduce CO_2 impact while maintaining structural performance, guided by Phase 1 insights.CAE simulations were employed to refine the designs, allowing for a thorough assessment of materials and manufacturing processes. Through Life Cycle Assessment (in OpenLCA), resulting CO_2e emissions from current and re-designed parts were studied and the better option among the two was recommended for possible vehicle integration.

Keywords: sustainability, body structure designs, steel, aluminium, biw, manufacturing processes, life cycle assessment.

Acknowledgements

We would like to express our deepest gratitude to our supervisors, Christopher Berghoff, Arpita Chari and Qi Fang, for their invaluable guidance, support, and encouragement throughout the entire process of researching and writing this thesis. Their expertise, patience, and insightful feedback have been instrumental in shaping the direction of this work. We are also indebted to our examiner, Mélanie Despeisse and department head at Zeekr Technology Europe, Magnus Lindvall for their valuable input and constructive criticism. Additionally, we extend our heartfelt appreciation to Martin Larsson for his assistance and contributions to this thesis. We would like to thank our family and friends for their unwavering support, understanding, and encouragement during this challenging journey. Their belief in us has been a constant source of motivation. Finally, we wish to extend our sincere appreciation and gratitude to the administration of Zeekr Technology and the BIW & CAD team for granting us this invaluable opportunity. Additionally, we express our gratitude to our respective departments at Chalmers University of Technology for their support in allowing us to pursue this topic. Without the collective support of these individuals and teams, this research endeavour would not have been possible.

Aditya Kulkarni, Gothenburg, June 2024
Anirudh Mosale Vishwanath, Gothenburg, June 2024

List of Acronyms

Below is the list of acronyms that have been used throughout this thesis:

CMS	crash management system
LCA	life cycle assessment
BIW	body in white
CAD	computer aided design
GWP	global warming potential
FRP	fiber reinforced plastic
PHS	press hardened steel
MCDA	multi criteria decision analysis
DFM	design for manufacturing
LCI	life cycle inventory
LCIA	life cycle impact assessment
MPDB	mobile progressive deformable barrier
BEV	battery electric vehicle
MOI	moment of inertia
N.A.	neutral axis
RER	rest of europe
ROW	rest of world
GLO	global
GCS	global coordinate system

Contents

List of Figures

List of Tables

1
Introduction

1.1 Background

In 2022, energy-consuming industries released a record high 36.2 billion tons of CO_2-emissions [1]. Though the vehicles with an electrical motor themselves are more eco-friendly in the user phase with zero tailpipe CO_2 emissions than an internal combustion engine [2], it is now important to ensure the material and manufacturing processes involved in producing these vehicles are sustainable too. This is required to make the whole product's life cycle sustainable.

Zeekr Technology Europe (Zeekr), is now interested in studying and improving the sustainability of BIW designs. The goal was to achieve this through alterations in manufacturing processes, using appropriate materials and utilising green energy [4]. This would then involve a comparative analysis of current BIW concepts being used to the proposed concepts, to choose the more sustainable one, thereby improving the environmental impact of the whole product. Body structures today are often made of different materials (e.g., steel, aluminium, FRP) and these parts are typically produced by stamping, casting, extrusion and many more. A combination of these materials and processes can make the vehicle both lighter and stronger.

Zeekr has already developed parts from steel (PHS or Press Hardened Steel) and aluminium (6063 T7 & 7003 T6) which, in this thesis, are referred to as 'current parts'. However, there is now an opportunity to explore alternative materials and consider other manufacturing processes while maintaining the desired performance. This exploration could potentially lead to a decrease in the product's overall contribution to environmental impact.

This thesis intends to propose an alternative solution, hereafter referred to as the 'redesigned parts', which entails utilizing a different material and/ or manufacturing process for the current part. The redesigned part will incorporate the chosen material and manufacturing technique, which will then be carefully modelled and evaluated against relevant load cases (load cases required to understand the behaviour of the parts selected). These load cases will be assessed through theoretical calculations followed by 3D CAD of the part i.e., the redesigned part. To gauge its overall performance, the redesigned part will be subjected to CAE simulation under the specified load cases. This analysis seeks to ascertain whether the redesigned part can effectively substitute the current part. Subsequently, the environmental impacts

of both the current and redesigned parts will be examined to determine which has a lesser environmental impact.

1.2 Aim

The aim was to study and compare the environmental impact of BIW concepts (i.e. various designs) by redesigning a current part with alternative materials and manufacturing processes. Following thorough modelling, calculations, simulation and Life Cycle Assessment (LCA), the objective was to recommend and comment on the part that has lower CO_2e emissions and which is the most suitable for the vehicle with respect to the desired performance parameters.

1.3 Research questions

When an alternative material and process is being considered to replace a part, there will be design changes which need to be incorporated. This is because of the material's intrinsic properties like its strength, flowability, ductility and more. These parameters form the basis for the first research question;

1. *How can the current parts be redesigned when different materials and processes are considered?*

Following the re-design, it is necessary to perform CAE simulations on the redesigned part to evaluate the performance under load cases to assess whether it can match (or possibly outperform) the current part. Referring to performance, the evaluation typically includes maintaining the existing part's load-bearing capacity, as well as examining the stresses and tensions induced in the part. Several parameters, such as thickness, weight, and material composition, offer flexibility for adjustment and optimization. This inquisition leads to the second research question;

2. *What essential parameters must be met to retain the same performance of the current part?*

Upon evaluating the performance characteristics of the redesigned part and confirming its suitability to the current part, an examination of several parameters such as thickness, weight, and material composition becomes imperative to understand the environmental impacts of the two parts. This analysis aims to determine which part (or component) is more sustainable and could be seamlessly incorporated into the vehicle. This investigation leads us to the final question of the thesis;

3. *Which attributes affect the CO_2e emissions of these two parts, i.e. re-designed or current and why?*

1.4 Delimitations

1. For cradle-to-gate LCA, emission from ore mining until raw material (coil or ingots/ billets) will be estimated using standard dataset values.
2. For LCA and LCI, only CO_2e emission will be the main focus under the Midpoint impact category (ReCiPe 2016). The same will be calculated for the final result and recommendations will be based on this.
3. The complete car body is not part of the thesis; be it for alternate material or process recommendation, performance analysis or LCA.
4. CMS sub-assembly (and by extension, its components) is symmetric about ZX and XY planes (Section 2.2).
5. A uniform cross-section for the bumper beam is assumed, excluding all slots, cutouts, and notches in the initial modelling. However, any features that could affect structural integrity are included.
6. Design For Manufacturing (DFM) was not part of the scope. However, a pragmatic design approach was always employed.
7. All references to the manufacturing process and data sourcing for LCA and LCI in this thesis pertain specifically to eastern China datasets, from ore mining to finished goods.
8. The steel stamped sill is an assembly of 'flat plate' and 'C Section', spot-welded together along the flanges.
9. For CAE simulations, steel-stamped components such as sills, crash boxes, or bumper beams are modelled without spot welds/ conventional welds. Furthermore, the type of welding considered for LCA will be arc welding (but separate for aluminium and steel).
10. When discussing steel, its primary manufacturing process is stamping, specifically direct hot stamping. For aluminium, the concurrent manufacturing process is extrusion.
11. The use of sheet metal inherently necessitates a welding process. Zeekr's portfolio includes sheet metal gauges ranging from 1.8mm to 4.2mm, which imposes certain design limitations.

1.5 Use of generative AI

This thesis employs the advantages of AI tools as permitted by Chalmers under 'Regulations for the use of AI tools in thesis work' [69]. The extent of use of AI in this thesis was limited to;

- Paraphrasing: employed to reduce the length of sentences and/ or change sentence structure.
- Rephrasing: employed when authors wished to borrow or cite a statement, hypothesis, or theory from other literature works.
- Rewording: employed when a synonym was deemed necessary rather than using two or three words.

Two AI tools were used for the above purpose: ChatGPT [70] & Perplexity.ai [71]. Generated texts were always critically reviewed before accepting into the thesis.

2
Theory

This section provides insights into the theory required to understand the thesis better.

2.1 BIW structures

BIW are sheet metal components like pillars, rockers, roof panels, hoods and so on that are joined together through welding, brazing or through fasteners before the vehicle body goes to the paint shop. BIW structure of a car amounts to almost one-third of the car's total weight[41]. There are many kinds of BIW structures and some of them are; unibody, monocoque, frame structure, and space frame design.

The car referred to in this thesis is assumed to have a 'hybrid unibody structure'. A unibody structure is that which carries the engine and chassis and therefore is considered a consolidated unity of the body. These structures are often made of stamped steel and extruded aluminium parts which are spot welded or fastened together.

BIW structures are engineered to enhance crashworthiness by absorbing and dissipating energy during a collision, thereby preserving the integrity of the passenger compartment and ensuring the protection of occupants. For a car's body structure to be crash-worthy, it has to satisfy a few requirements [20];

- The body structure should be stiff & deformable to absorb kinetic energy.
- The side structures and door should be efficiently designed to minimise intrusion.
- The structure should possess sufficient bending and torsional stiffness for efficient ride and handling.
- Minimise high-frequency vibrations that give rise to harshness[20].

The BIW structure that was the main focus of this thesis was the CMS. *CMS* is a structural assembly which serves the purpose of absorbing energy at the onset of the crash and guides the remaining crash force to the surrounding body structure at low and high-speed crashes, but the damage cannot be avoided during a high-speed crash. The component can avoid damages to the vehicle, thus avoiding the disintegration of the body structure and ensuring the survival of the occupant[36]. CMS consists of two parts: a bumper beam and a pair of crash boxes.

In light of this, other structural components had to be studied, to better understand the crash management system. These components were the crash box, bumper beam and sill.

Crash box is a structural component designed to collapse, absorbing energy during a crash, this helps in protecting the occupant and reducing the amount of damage to the surrounding structural components during a low-speed crash. In a high-speed crash, the crash box absorbs energy before the crash force is taken up by the front rail to reduce the crush impact[52]. Crash boxes sometimes include a trigger, which is an intentionally designed deformation that helps in the efficient collapse during a crash, thereby leading to efficient energy absorption. The 'bead' type of trigger is the one which is usually incorporated in the design as it provides the most efficient crash energy absorption[57] and the same was used in this thesis.

Bumper beam is a crucial structural component of a passenger car's bumper system, serving multiple functions. It absorbs and dissipates impact energy during collisions through bending resistance in low-speed impacts and deformation in high-speed impacts. The bumper beam also protects critical components such as the body, hood, engine, fuel system, cooling system, and safety-related elements like parking lights during collisions.

Side sill or rocker or simply 'sill' is a reinforcing member present on the lower right and the left of the car's door openings to ensure rigidity and also act as a crash structure. A sill usually has an open hollow cross-section, with an upper and a lower flange. A conventional way of designing a sill is to have an inner and outer sill, usually produced by press hardening of steel with a uniform thickness, positioned face to face and spot welded together at the upper and lower flanges. Reinforcements may also be added to further improve the rigidity[51].

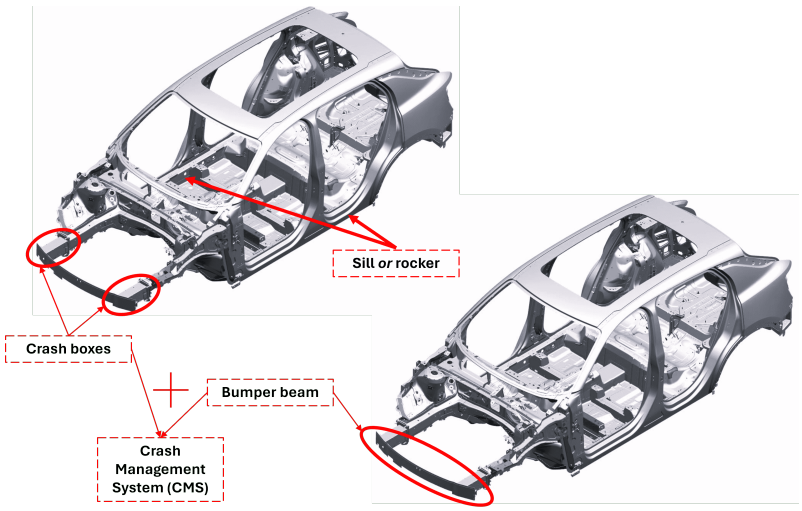

Figure 2.1: Illustration of CMS, crash box, bumper & sill on BIW

2.2 Materials data and manufacturing processes

Understanding the properties, behaviour, and characteristics of materials is essential for making informed decisions throughout the design process of this thesis.

Throughout this thesis, data from Table 2.1 was used wherever necessary. The materials shown below will be used in CAE simulations and theoretical calculations in the following chapters.

Table 2.1: Material matrix
(⊕ are materials used currently by the stakeholder; ⊗ are explored material options)

Material and grade	**E, GPa**	ρ, $\frac{kg}{m^3}$	σ_y, **MPa**	σ_u, **MPa**
Steel (PHS),Usibor 1500[28][29]⊕	200	7850	1050	1553
DP800[46]⊗	200	7850	620	800
Aluminium, 7003 T-6[32]⊕	70	2900	310	390
Aluminium, 6063 T-7⊕	68	2700	190	230
Aluminium, 6063 T-6[31]⊗	68	2700	200	260
Aluminium, 7108 T-6[30]⊗	69	2900	290	350

PHS is often available in the form of sheets. 'Press hardening' process is a hot forming process that employs steel sheets to be formed into complex shapes that have ultra-high strength, by heating the blanks to 1000°C, hot forming it and then rapidly quenching it to $\approx$ 200°C. This facilitates down-gauging (usage of thinner sheets) to reduce weight whilst supporting the aim of achieving high crashworthiness.

The parts considered in this thesis, are either manufactured by the process of extrusion or stamping.

- *Stamping* of metal is a process where a sheet metal is formed into a desired shape with the help of a punch and die. The sheet metal is pressed against the die with a punch to form the desired shape.

- *Extrusion* is a process where a metal is heated to a high temperature and forced through a die with a specific cross-section under high pressure.

2.3 Crash tests and load cases

After designing and manufacturing a vehicle and its components, it is essential to validate their compliance with safety standards and requirements through crash testing, specifically impact testing in various scenarios.

Notably, many organisations conduct and provide results for the said impact test cases. Out of the many, this thesis will draw insights based on two reputed crash impact testing organisations: Euro NCAP and RCAR.

The European New Car Assessment Programme (Euro NCAP), is a voluntary vehicle safety rating system. Euro NCAP provides European consumers with information regarding the safety of passenger vehicles[15]. Out of 3 main tests for occupant safety, this thesis focuses on the side impact tests.

Another organisation which performs crash tests is the RCAR. RCAR is an international association of automotive research centres that research repair procedures and processes, safety features and any new upcoming technology. RCAR's front impact test is focused in this thesis.

From these crash test results, a study of loads and forces can be undertaken. Conversely, loads and forces can also be determined from these tests. The two load cases that were the major focus of this study were the buckling load case and the 3-point bending load case. These load cases originate from two of the major impact tests: the frontal impact and the lateral or side pole impact. The following sub-section will deal with the attributes that were considered for calculating and considering these loads, and by extension, their respective impact test cases.

2.3.1 Front impact crash test

On frontal impact, the BIW structures such as the CMS, experience buckling loads. A structure is said to undergo buckling when an axial load is applied to the structure. A detailed description, types of buckling and the use-case for this thesis are briefly explained in Section 2.4.

RCAR defines case setup for a frontal crash test at low speeds of 15kmph with +/- 1kmph, 16 kmph becomes the max speed the test can be run at to cover tolerance, to understand the effects of the crash on the structure of the vehicles and to learn how the energy absorbing members are deformed[58]. This thesis employs RCAR's case setup and standards for CMS's load case setup.

2.3.2 Side or lateral impact test

The side pole impact test mimics a 3-point bending test with the sill acting as a beam and the pole acting as a point-load roller which applies the bending load at the centre of the sill. As the sill (or the beam) is fixed between the A and C pillars, it

can be assumed that the sill is 'simply supported' at these ends. The loads that are generated under 3-point bending cases are compressive and tensile.A more detailed explanation of bending and its load cases can be found in Section 2.4.

This thesis employs EuroNCAP's 'side pole impact test' case setups and standards for sill's load case setup. Euro NCAP side impact test is performed with a deformable barrier and a side pole.

During the side pole impact test, the car moves sideways at 32 km/h against a rigid, narrow pole, simulating a collision with a roadside object like a pole or tree. This test is crucial for assessing occupant protection, as the high forces involved cause localized deformation and deep penetration into the vehicle (intrusion)[34].

This test is particularly crucial for Battery Electric Vehicles (BEVs) as batteries are placed between two sills and hence, studying intrusion becomes paramount, so that the cells do not get damaged and cause a risk of fire.

2.4 Crash mechanics

Crash mechanics encompasses the study of how vehicles behave during collisions, including the deformation of vehicle components, energy absorption, and the impact on occupants. This thesis does not delve into the latter topic but will discuss mainly on deformation and energy absorption of body structure components.

This thesis delves into the realm of crash mechanics within the context of BIW design; particularly deflection/ bending/ intrusion and buckling.

Calculations and simulations of crash mechanics mainly involve the application of force and the measurement of deflection. All these quantities are vector quantities, meaning they have both magnitude and direction. This imperatively calls for an understanding of the magnitude and direction of forces.

The literature study of bending and buckling supplements the understanding of the magnitude, while the direction is frequently determined by the real-life application of components. Therefore, for direction references, the following Figure 2.2 serves as the datum, representing the global coordinate system (GCS) in relation to Zeekr's 3D CAD models. Henceforth, all mentions of coordinate systems, planes, axes and directions will be in reference to Figure 2.2.

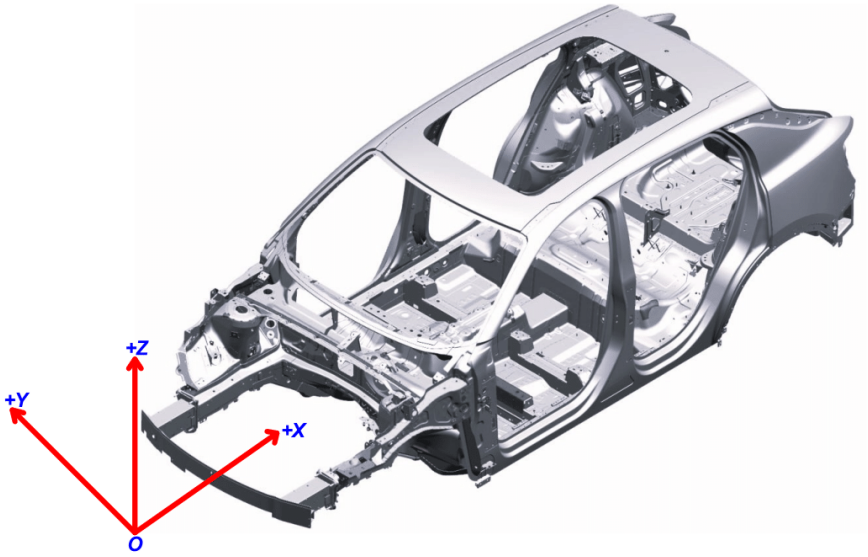

Figure 2.2: Global coordinate system

When a force or load is applied to an object, it induces deformation, which can be categorized as either elastic or plastic. This thesis focuses on plastic deformation, necessitating an examination of the types of deformation induced by various loads and forces in different BIW structures mentioned above. Accordingly, this study includes two essential types of forces: buckling forces in crash boxes and bending forces (compressive and tensile) in sills and bumpers.

Buckling in crash box

Buckling occurs when external forces on a column reach a threshold value, initiating a new deformation mode before the original one, resulting in a switch to this new deformation type. As a geometry- and material-dependent phenomenon[43], understanding buckling is essential for comprehending crash box behaviour. This study employs the 'rectangular column buckling' theory, as the crash boxes under investigation have a rectangular cross-section.

There are two possible ways a column can buckle,

- Global/ Euler's buckling: where the deformation is concentrated in one point, and the column fails by bending[43].
- Local buckling: fails by local deformation, in which wrinkles are formed and buckles progressively one after another[43].

In a square/ rectangular column, three types of buckling might occur; Stable type, Unstable type 1 and Unstable type 2. For efficient energy absorption during buckling, a stable type of buckling is preferred and this thesis employs a stable type of buckling (the column is crushed by forming multiple buckles[44]). The image below shows the different types of buckling modes respectively.

Figure 2.3: 3 types of buckling in a square column[44]

In theory, it is complex to mathematically determine the maximum load-bearing capacity of an axially compressed thin wall column because of the local instabilities that are present in the column which precedes the collapse of the column[39].

The stress at which the column locally buckles is the critical stress of that structure. When the critical stress value is smaller than the yield stress of the material, the collapse is dictated by the geometry of the column. However, if the critical stress is higher than the yield stress of the material, the collapse is dictated by the material properties. Hence, there is a need to opt for the right geometry-material combination which will ensure proper energy absorption[39].

The column's maximum stress-bearing capacity is also influenced by the material properties and the geometry. Another aspect of columns under buckling is their maximum load-bearing capacity.

Bending of beams

The concept of bending of beams is crucial to understanding the behaviour of the sill and the bumper beam under loading.

There are shear forces and bending moments which are set up in the beam under the influence of load, and due to this, the beam undergoes deformation. The deformation of the beam is resisted by the material of the beam, this resistance or stress caused by bending moments is called bending stresses[50].

From Table 2.2, consider sections AB and CD, perpendicular to the beam's axis. When the beam bends, layer AC becomes A'C', shortening, while layer BD becomes B'D', elongating. Between layers AC and BD is a neutral layer that neither shortens nor expands, maintaining the same length as NN and N'N'[50].

Beam cross section before bending	Beam cross section after bending
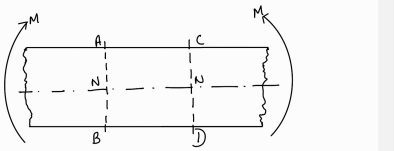	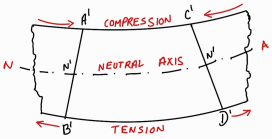

Table 2.2: Cross section of a beam before and after bending

The layers above the neutral layer have shortened and are under compression, while the layer below has elongated and is under tension. The topmost layer (AC) experiences the most compressive stress, and the bottom-most layer (BD) experiences the maximum tensile stress. The tensile or compressive stress experienced by each layer depends on its distance from the neutral layer, according to the theory of simple bending[50].

It is important to understand the type of beam being dealt with. Each beam has its support conditions and these affect how the forces and moments are being formed under load. For this thesis, the sill and the bumper are considered to be simply supported beams. These concepts form a basis for how to approach and calculate the stresses and deflection for the bending of a beam.

2.5 Framework of life cycle assessment study

LCA is the concept of intuitively understanding a product's life cycle. Baumann and Tillman (2012), the literature around which the LCA study of this thesis is based, states that a product's life cycle is followed from its 'cradle' where raw materials are extracted from natural resources through production and use to its 'grave', the disposal. However, in this thesis, the approach is limited to a cradle-to-gate, life cycle from resource extraction (cradle) to Zeekr factory's out gate of Zeekr.

Typical LCA methodology encompasses a thorough, multi-step process, including goal and scope definition, inventory analysis, impact assessment, and interpretation, as shown in the Figure 2.4 [49].

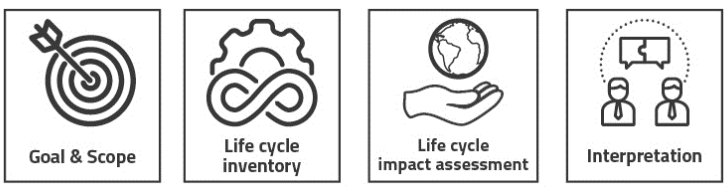

Figure 2.4: Typical LCA methodology

A. Goal and scope definition

To conduct an LCA study, the project's goal and scope have to be defined. According to ISO standard 14041:1998, the goal statement should specify the intended application of the LCA study, the motivation behind it, and the targeted audience [53].

Defining the scope of a study encompassed defining system boundaries, choice of impact categories, functional unit, method of impact assessment and type of LCA. The main components of goal and scope definitions are;

- Flow chart and system boundary:
  A flowchart of the system under study will aid in understanding the processes and products involved.
- Functional unit:
  A functional unit serves as a reference unit to compare different products and processes in a comparative study.

B. Life cycle inventory

LCI is the data-collection component of an LCA study. Broadly speaking, LCI endeavours to take account of everything involved in the product or service, tracking all the inputs and outputs such as raw materials, energy, water, and emissions. During the inventory analysis, a system model was built according to the defined goal and scope. This model represented the flow of technical systems within a system boundary.

The LCI approach in this thesis involved the following three generic steps:

- Construction of flow model according to the system boundaries defined in the goal and scope.
- Data collection for all the activities such as raw materials, energy associated with the activities, products, emissions to water and air, and solid waste.
- Calculation of the amount of resource used and pollutant emitted in reference to the functional unit.

The results from inventory analysis were the mass and energy balance of the system. Environmentally relevant flows were considered, ignoring the ones that are not harmful to the environment like water vapour and surplus heat emitted.

C. Life cycle impact assessment

In every LCA study, the phase addressing environmental impacts is called life cycle impact analysis (LCIA). During LCIA, data from the LCI is used to calculate environmental loads relative to the functional unit.

These loads are translated into inventory results to understand environmental impacts. The LCIA quantifies and transforms inventory data into more environmentally relevant information, focusing on environmental impacts rather than just emissions and resource use.

The major elements that were addressed and considered during LCIA were,

- Classification: it is where the inventory parameters are sorted according to the type of environmental impacts they contribute to.
- Characterisation: it involves calculating the relative contributions of emissions and resource consumption to each type of environmental impact. This step characterizes resource consumption and emission contributions for each impact type[43].

To define and understand these impact categories, the ReCiPe 2016 method was followed through this thesis (illustrated in Figure 2.5). This method translates the inventory data to several impact scores through predefined characterisation factors.

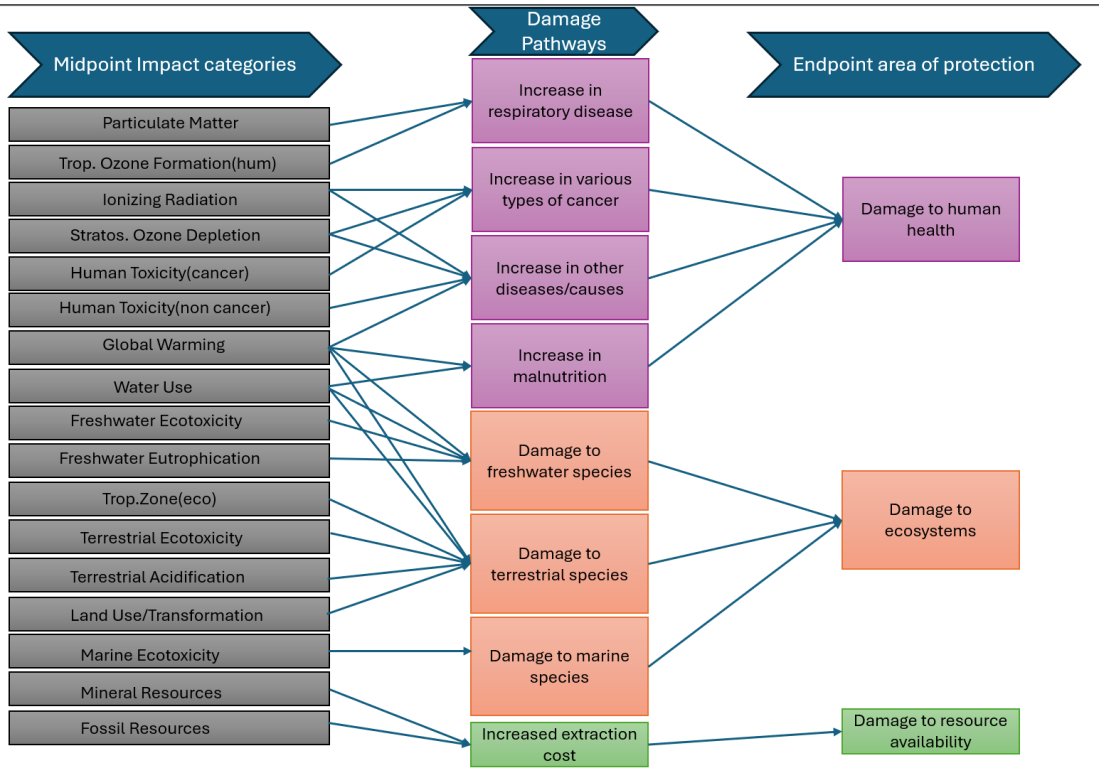

Figure 2.5: Impact categories from ReCiPe 2016

With the LCIA method in place, it then becomes imperative to choose one among the three 'cultural perspectives' [55]. The 'Hierarchist perspective' was chosen for this thesis as the stakeholder's requirement was a framework that strikes a balance between environmental protection and economic/ social development, whilst aiming for fair global outcomes for both current and future generations.

Finally, OpenLCA, which is a free open source software is used for performing LCA study. The software makes use of a database called Eco-invent, a trusted database used by most of the LCA practitioners as it provides access to transparent data, making it easy to understand the sources of environmental impact and enabling informed decision making[56].

The 'Ecoinvent' database was employed as it contains over 17,000 unique datasets [54]. These datasets encompass a broad range of products, services, and processes, spanning from building materials to food, and from resource extraction to waste management. Widely regarded as the largest, most consistent, and transparent database available, it is highly used in the industry.

The datasets in Ecoinvent are primarily divided into;

- GLO (Global)- Where the values of inputs and outputs for a particular process are normalized and weighted w.r.t global average,
- RER (Rest of Europe)- Where the values of inputs and outputs for a particular process are normalized and weighted w.r.t European market average and
- ROW (Rest Of the World)- Which is the difference of normalized and weighted average between GLO and RER.

Most datasets are averaged for Europe (RER), and where this isn't the case, a Global (GLO) average is used. As delineated under Delimitations, all cradle-to-gate manufacturing activities occur in China. Therefore, datasets from the Rest of the World (ROW) were used whenever possible. If normalized data was unavailable for ROW and RER, GLO datasets were used.

D. Interpretation

Interpretation in LCA involves carefully analyzing and understanding the results obtained from the LCIA process. This entails scrutinizing indicators of impact categories (such as GWP) to conclude.

Interpretation aims to offer insights into the environmental performance of the studied system, identify areas for improvement, and support decision-making in alignment with the study's goals and objectives.

3
Methodology

Overview

A mixed-method approach, as described by W. Creswell et al. (2019), entails integrating both qualitative and quantitative research methods and data in a study. Qualitative data typically consists of open-ended responses without predetermined answers, whereas quantitative data generally includes closed-ended answers for preset questions and predetermined parameters.

Within the mixed-method approach, the convergent mixed-methods design was selected. In this design, both forms of data (qualitative and quantitative) were simultaneously collected, aiming to integrate the information and ultimately interpret the overall results [9].

This research methodology faces the challenge of navigating abundant, pertinent, and standardized data. The study requires analyzing both qualitative and quantitative data, making the process time-consuming and demanding. Due to the design's complexity, a clear visual model is essential for understanding the research activities' details and flow.

3.1 Research design

The thesis was divided into two parts: Phase 1 and Phase 2. This separation helped to focus on the main goal and identify important factors in Phase 1. In Phase 1, the objective was to understand how changing the material and design attributes affects the part's (sill and crash box) performance.

In Phase 2, the aim was to study, compare, and potentially enhance the current component (i.e., CMS) through redesign, to recommend a part that reduces $CO2_e$ emissions. Due to the comprehensive scope of this thesis, it was necessary to segment it accordingly.

The Figure 3.1 offers a holistic overview of the structural organization of the content within this thesis. Phases 1 and 2, based on quantitative studies involving theoretical calculations, CAD modelling, and CAE simulations of the sill, crash box, CMS, and LCI, also incorporate elements from literature and qualitative studies.

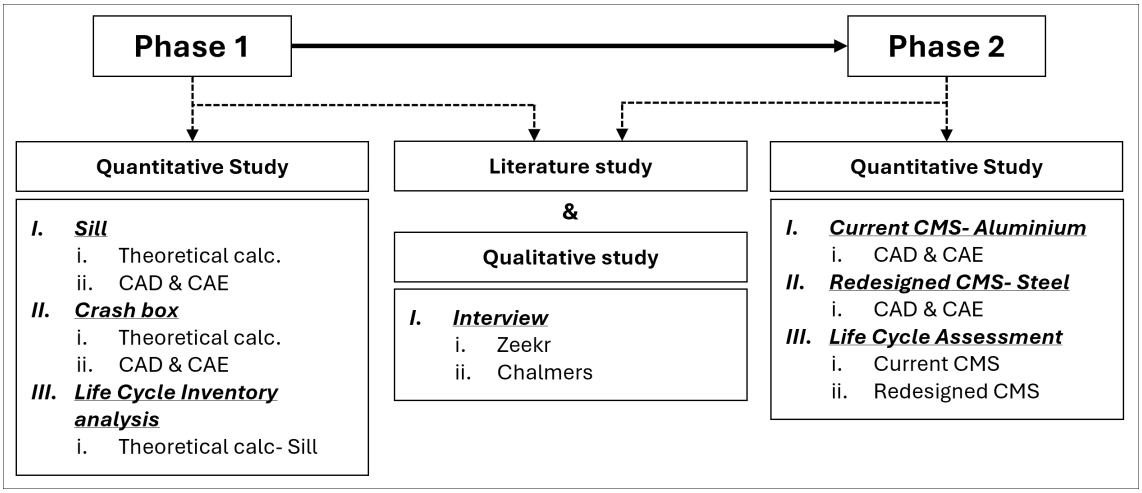

Figure 3.1: Methodology overview

3.2 Parts selection and performance parameters

The primary stakeholder selected CMS as the thesis topic. Before detailed analysis, understanding the function, features, and significance of its parts was necessary. Thus, the bumper beam and crash box of the CMS were chosen for simplification and study in Phase 1.

'Simplification' involved reducing the complexity of the parts' cross-sections by finding alternate BIW structures with similar loads and cross-sectional geometry. The sill was identified as a part with a simpler cross-section and similar load case to the bumper beam, making it the focus of the first part of Phase 1. No suitable proxy was found for the crash box, so the front crash box itself was chosen as the second part.

Using the above information and data from Section 2.2, the matrix in Figure 3.2 was drafted which outlines the parts, materials, and manufacturing processes under investigation in Phases 1 and 2. The table also highlights the 'current parts' that will serve as a baseline for comparing the performance of the 're-designed parts.'

Phase	Part name	Parameters	Current	Re-designed
1	Sill/ Rocker	Material	Steel	Aluminium
		Manufacturing process	Stamping	Extrusion
	Crash box	Material	Aluminium	Steel
		Manufacturing process	Extrusion	Stamping
2	CMS	Material	Aluminium	Steel
		Manufacturing process	Extrusion	Stamping

Figure 3.2: Part, material and manufacturing process matrix w.r.t. each Phase

Now that the part-material-manufacturing process matrix is established, performance parameters can be presented; the key metrics or measurements that are used to evaluate the effectiveness and efficiency of the components under study.

Identifying, tracking and analyzing these performance parameters throughout the design phases enabled us to refine the design and achieve the desired performance outcomes. Table 3.1 gives an overview of parts and their respective performance parameter(s).

It is important to note that the performance parameters discussed are solely focused on the parts themselves, irrespective of the manufacturing process or material used. This approach facilitates a comparison between different design iterations.

Table 3.1: Part specific performance parameters

Relating to	**Part name**	**Parameter**	**Units**	**Criteria (Ideal)**
Phase 1	Sill	Weight, m_{sill}	kg	$m_{sill,redesigned} \leq m_{sill,current}$
		Factor Of Safety, FOS	-	$\geq 1 \leq 2.5$; $FOS_{redesigned} \geq FOS_{current}$
		Intrusion, δ	mm	$\delta_{redesigned} \leq \delta_{current}$
	Crash box	Int. Peak load, P_{max}	kN	$P_{max} \simeq 200$
		Critical stress, σ_{cr}	MPa	$\leq \sigma_{ultimate}$
		Collapse stress, σ_{max}	MPa	$\leq \sigma_{ultimate}$
Phase 2	CMS	Energy absorption, W_e	kJ	Higher the better
		Int. Peak load, P_{max}	N	$P_{max} \simeq 200$
		Weight, m	kg	$m_{redesigned} \leq m_{current}$

3.3 Research process

This section offers a complete overview of the process (or methodology) employed for this thesis, which is grounded in the convergent mixed methods design. All parts within Phase 1 will adhere to this procedural framework.

1. The representative parts provided by the stakeholder were 'simplified' to perform calculations, simulations and analysis to meet the objective of Phase 1.
2. Dimensional values and boundary data were gathered for these simplified current parts using Siemens Teamcentre and Catia V5.
3. Theoretical calculations were performed, as this forms the basis for generating alternative designs.
    - This includes force and load calculations, determining stresses, and studying intrusion/deflection, using MATLAB scripts.
    - Iterations were carried out by varying various attributes of the geometry.
4. Iterations in previous steps are essentially alternative designs for the current parts. From this, the 'current part' was chosen. For each of these alternative designs, performance parameters were calculated.
5. Finalizing among many alternatives was not easy. Hence, Multi Criteria Decision Analysis (MCDA)[45] was employed, to choose the best of the available options.
    - NOTE: The redesigned part will now have to perform at par with the performance parameter values of this current part.
6. 3D CAD model of the current part was constructed in Catia V5.
7. Static structural CAE simulations were performed to validate the theoretical calculations.
8. Now, a new design was initiated with a different material and iterated till the design met the current part's performance parameters (from step 5). This was termed as the 'finalized redesigned part'.
9. Finally, a theoretical LCI analysis was conducted on the current part to understand the effect of various manufacturing processes on CO_2e emissions.
    - NOTE: A complete LCA analysis was not the scope in Phase 1. Only a theoretical LCI study was included.

Phase 1 concludes with the achievement of the objective to understand the functionality, prominent and subtle attributes, and significance of these two (sill and crash box) key components.

3.4 Phase 1 & 2: Literature and qualitative study

3.4.1 Literature study

Qualitative research involves collecting and analyzing non-numeric data, like text, video, or audio, to understand concepts, opinions, or experiences. This is generally done through the means of literature review, studies, observations, interviews, discussions, focus groups, surveys and such. Out of this, interviews and discussions were employed as a part of the qualitative method, along with literature study. A literature study is a method used to gather and synthesize data and information that has been previously published.

The primary sources of information for this research were the published literature and research available through academic databases such as Chalmers Library, Google Scholar, Scopus, and ScienceDirect. There were no restrictions on the publication date or a fixed time frame set during the literature search. A combination of targeted keywords, both individually and collectively, were used in the search for relevant literature which was to the likes of crash mechanics and dynamics, compression, bending and buckling, material properties, design methodology, Life Cycle Assessment, Life Cycle Inventory, DP800, 22MnB5, Press Hardened Steel, sill, rocker, bumper beam, Crash Management System, crash box. Each of these keywords, in combination and individually, resulted in around 1,000,000 to 6,000,000 results. All relevant literature that was collected, referred and studied, was tracked and documented as soft copies on personal computers in the form of files, folders, notes and URLs.

The literature study provided this thesis with many input values for calculations, simulations and decision-making. These inputs were standard values in the form of the material's intrinsic properties such as density, Poisson's ratio, Young's modulus, and crippling coefficient. When it comes to LCA, emission factor, manufacturing process flow and even standard energy consumption of a stationary drilling machine were attained with literature study.

However, the extrinsic properties such as mass, volume, the minimum and maximum gauge of sheet metal allowed, or the output yield of a machine with the supplier and other such stakeholder-specific and sensitive information cannot be attained through literature study. Even if efforts are made to collect component-specific data through literature reviews, surveys, or studies, the results are likely to be skewed and may be considered inconsequential by many readers. This is primarily due to the fundamental necessity for some inputs to be pragmatic rather than purely theoretical.

To address this conundrum, informal qualitative research, specifically one-on-one interviews, was employed to gain an in-depth understanding of individual experiences and perspectives on the subject matter [47]. This included interviews with supervisors, managers, and employees at Zeekr Technology Europe, as well as feedback from Chalmers University's teaching staff.

3.4.2 Qualitative study

One of the qualitative study methods is conducting interviews, which is a widely adopted data collection and data analysis strategy employed across a diverse range of academic and professional disciplines [47]. Qualitative interview approaches have been categorized in various ways, with contemporary literature commonly distinguishing between unstructured, semi-structured, and structured interview formats [48].

The semi-structured interview approach was selected as it combines elements of both structured and unstructured interview formats. This hybrid approach serves as an appropriate foundation, as it provides a set of predetermined questions while also allowing for spontaneous exploration of relevant topics.

The following Table 3.2 gives an overview of interviews, insights and feedback from the respective interviewees. The semi-structured interview format allowed for the development of a thematic framework to guide the discussions, which is outlined in Appendix A.1.

Table 3.2: List of interviews conducted

Interviewee	**Stakeholder from**	**Query explored**
CAE engineer	Zeekr	1. Trigger point placement & validation 2. Design improvements & corrections in CMS structure
Systems engineer	Zeekr	1. Design changes in sill & crash box 2. Finalizing performance parameters 3. Benchmarking values for Phase 2 w.r.t. performance parameters 4. Verification of LCI inputs for Phase 1
CAD engineer	Zeekr	1. Placement of part during design 2. Vehicle's physical attributes 3. Dimensional attributes of representative version's sill & crash box
Product Devp. & CAD prof.	Chalmers	1. Validation of use of Trial-and-Error method
Structural engineering prof.	Chalmers	1. Validation of sill's calculation

3.5 Phase 1: Quantitative study

The objective of Phase 1 was to understand the effect of attributes of sill and crash box on their respective performance parameters. Theoretical calculations were carried out in this phase to lay a stepping stone for Phase 2. This phase culminated by studying and comparing the major contributors of emissions during the manufacturing of steel and aluminium sill, using LCI.

3.5.1 Sill- theoretical calculation

The process flow and activities carried out under Phase 1 for the sill are depicted in Figure 3.3 and elucidated further to provide a better and clear understanding.

Figure 3.3: Generic Phase 1 activities for sill

Theoretical calculations for sill are based on R.K. Bansal (2009) textbook. The textbook deals with the strength of materials and discusses topics such as moment of inertia, shear force, bending moment, stresses and deflections in beams. Activities mentioned in Figure 3.3 were performed in sync with topics from R.K. Bansal (2009). The calculations in this section were performed to determine the theoretical value of intrusion and stresses induced (i.e. tensile, compressive and bending). The non-standard calculation method from the referenced literature is briefly explained in the following sub-sub-sections.

Impact force calculations

Using three general equations of;

Work done, W;

$$W = F.d \tag{3.1}$$

Kinetic Energy, KE;

$$W = Kinetic\ Energy = \frac{1}{2}.m.v^2 \tag{3.2}$$

distance, d;

$$d = V.t \tag{3.3}$$

An equation to calculate 'impact force' is generated, i.e.

$$F_{impact} = W = \frac{m.V}{2.t} \tag{3.4}$$

Neutral axis calculations

The neutral axis (N.A.) is defined as 'an axis within the cross-section of a beam or shaft undergoing bending, that experiences no longitudinal stresses or strains.' [11].
Location: In symmetric, isotropic sections that are initially straight (which is in this case), the neutral axis is located at the geometric centroid.
Importance: Calculating the neutral axis is essential, as fibres on one side of the neutral axis experience tension while those on the opposite side undergo compression. This calculation is necessary for subsequent theoretical analyses. However, to calculate N.A., following are required;

Calculating area of 'sub-divisions'

However, to calculate the neutral axis, it is mandatory to find out the area of 'sub-divisions'. This was done using Eq. 3.5.

$$Area\,of\,rectangle,\ n\ = A_n = breadth * depth\ (in\ mm^2) \tag{3.5}$$

Next, the distance between the bottom-most fibre (OX) and the centre of gravity (cg) of each subdivision had to be determined.

Distance from OX to cg of each subdivison

The distance between the centroid of each subdivision and the reference axis (OX) was denoted as Y_n (in mm), corresponding to the number assigned to each subdivision.

$$Y_n\ =\ Distance\,from\,OX\ +\ cg\,of\,subdivision(n) \tag{3.6}$$

Moment of inertia of each subdivision

Now, MOI of all these subsections were found about OX.
This is given by the formula $A_n.Y_n$, where A_n is the area of the respective subsection.

$$A_nY_n = A_n.Y_n\ (in\ mm^3) \tag{3.7}$$

Finding the neutral axis (N.A.)

The Neutral axis for the whole section was found out by dividing the sum of moments of the subdivision by the sum of areas of these subdivisions.

The neutral axis is represented by the symbol $\bar{Y}$

$$\bar{Y} = \frac{\sum_{i=1}^{n} A_n.Y_n}{\sum_{i=1}^{n} A_n} \tag{3.8}$$

here 'n' are subdivisions of the sill's cross section.

Calculating moment of inertia ($\mathbf{I}_{XX}$)

MOI or simply, I_{XX}, is calculated about the X-axis. MOI of sectional areas, about Neutral Axis passing through their respective cg.

The formula for finding I_{XX} is given by;

$$I_{XX} = I'_{G1} + I'_{G2} + I'_{G3} + ... + I'_{G6} \tag{3.9}$$

where;

$$I'_{Gn} = Parallel\ Axis\ Theorem = I_{Gn} + A_n.h_n^2 \tag{3.10}$$

MOI for a rectangle is given by;

$$I_{Gn} = \frac{b_n.d_n^3}{12} \tag{3.11}$$

wherein b is breadth and d is depth of each subdivision.

A_n is already calculated in previous sections. h_n is the distance between each subdivision's cg and cross section's cg, which is given by the equation.

$$h_n = Distance\,between\,cg\,of\,subdivision(n)\ \pm cg\,of\,cross\,section\,(in\,mm) \tag{3.12}$$

Calculating deflection/ intrusion of sill

Intrusion is the deflection of the beam from its original position due to the application of load (point load in this case). The sill of a car is modelled as a simply supported beam due to its load-bearing characteristics, and the support it receives from the vehicle's front and rear structures.

The sill experiences bending moments and shear forces along its length, characteristic of the behaviour of a simply supported beam under load. The formula for deflection of the simply supported beam is given by [12],

$$Y_{max} = \frac{W.L^3}{48.E.I}\,(in\,mm) \tag{3.13}$$

where; W is the mass of vehicle (in kg), L is the length of beam (in mm), E is the Young's modulus of material (in MPa) and $I\ or\ I_XX$ is the Moment of Inertia (in mm^4).

Bending moment calculations

Figure 3.4 depicts a free-body diagram of the sill, representing the nomenclature and direction of loads, forces and moments. It is to be noted that these attributes are independent of the material and cross-section of the sill.

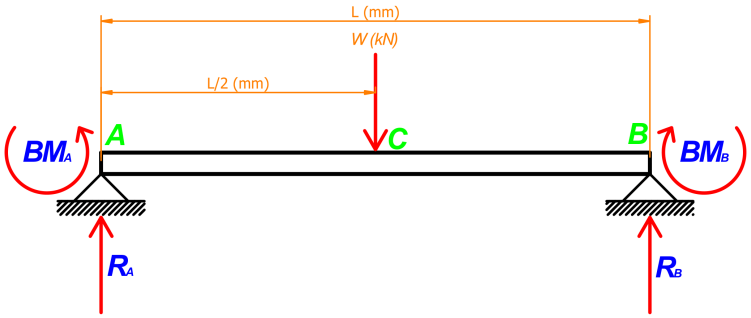

Figure 3.4: Free Body Diagram of sill

The reaction forces at two ends of the simply supported beam AB had to be calculated, before calculating the bending moment. For a simply supported beam to stay in equilibrium, the reaction forces have to counteract the point load. Hence reaction forces for the beam AB are;

$$W = R_A + R_B \tag{3.14}$$

where R_A and R_B are reaction forces at ends A and B respectively. Note that $R_A = R_B$.

The bending moment was calculated using the following sign convention [13];

- Beam is sagging, then 'positive'
- Beam is hogging, then 'negative'

Stress calculations

When there is a point load acting on a beam, the fibres close to the load are shortened in length, meaning they are under compression. The fibres on the far end of the load are said to be under tension. The compression and tensile stresses are maximum on the extreme-most fibre from the N.A. The tensile and compression forces were found by the formula [14];

$$\frac{M}{I} = \frac{\sigma_{max}}{y} \tag{3.15}$$

Here, y is the distance of extreme fibre from neutral axis, essentially, $\bar{Y}_{bottom}$ and $\bar{Y}_{top}$ (in mm), I *or* I_{XX} is the Moment of Inertia (in mm^4), M is the maximum bending moment (in Nm) and σ_{max} is either maximum tensile stress or compression stress, depending on $\bar{Y}_{bottom}$ or $\bar{Y}_{top}$.

Tensile stress

$$\sigma_{max,compression} = \frac{M.\bar{Y}_{top}}{I_{XX}} \; (in\ MPa) \tag{3.16}$$

Compression and bending stress

$$\sigma_{max,compression} = \frac{M.\bar{Y}_{bottom}}{I_{XX}} \; (in\ MPa) \tag{3.17}$$

3.5.2 Sill- CAD modelling and CAE simulations

The data generated in the previous section will be compared with the simulated values of this section. For this, 3D CAD modelling was carried out in Catia v5 with the aid of Siemens Teamcentre to generate various concepts (by varying gauge thickness from 1.8 to 4.2mm), eventually to choose a 'current design'.

The current design was chosen after 'simplifying' the representative steel sill. The steel sill was modelled to imitate the performance parameters of the representative design provided by the stakeholders.

NOTE: Due to confidentiality issues, the representative version of sill cannot be released or displayed in this thesis. Readers are therefore requested to cooperate and contact authors for any query.

With theoretical calculations and 3D CAD models ready for the sill, CAE simulations were carried out in the Ansys workbench. The motive was to record intrusion, and maximum principle stress (i.e. von Misses stress) and to study points of high-stress concentration for all the concepts that were generated.

This exercise was carried out to validate the calculated values and determine whether to use the theoretical values or the simulated ones.

Boundary conditions

Boundary conditions or constraints defined the behaviour at the boundaries of the model domain and incorporated the influence of the outside world into the simulation. The boundaries set for sill's static structural CAE simulation are demonstrated in Figure 3.5. The blue line is an indication of fixed supports. The beam was analysed as a simply supported beam by performing a 3-point bending test. It has to be noted that these boundary conditions were set the same for both aluminium (redesigned) and steel (current) designs. The inner edges of the sill (in Y axis) are treated as though the sill was rested on rollers at those points.

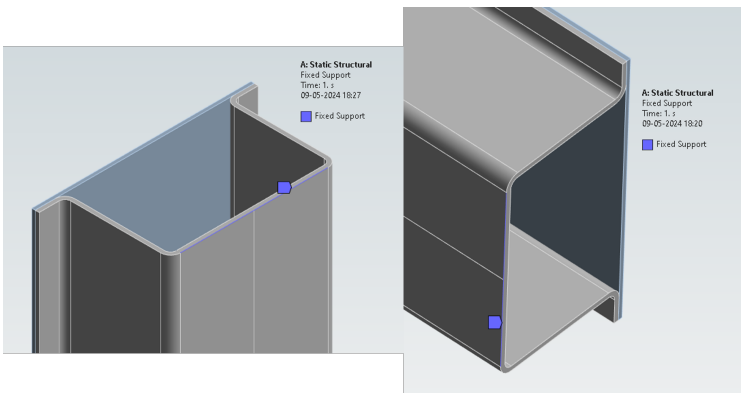

Figure 3.5: CAE: Boundary conditions employed for sill

Loading direction and area

The loading direction specifies the orientation and vector along which external forces (loads) are applied to the model. It was defined using the global coordinate system (Figure 2.2) while the loading area in CAE simulations refers to the specific surface on the model where the load was applied. Figure 3.6 portrays the loading direction and magnitude being applied on the sill. Furthermore, the highlighted area (in red) is the area of impact or loading area.

This area was informed by the requirement that the side pole crash test is required to have a diameter of $\phi 254 \pm 3mm$[19]. This is particularly noteworthy because this section of the pole is anticipated to come into contact with the sill during the crash test. To calculate the impact area, the length of the minor arc of a circle was to be calculated.

The formula for the length of minor arc of a circle is;

$$MinorarcAB = \pi * r * \frac{\theta}{180^\circ} \tag{3.18}$$

$$\pi * \frac{254}{2} * \frac{75^\circ}{180^\circ} = MinorarcAB = 166.25mm \simeq 166mm \tag{3.19}$$

The loading direction (as per GCS) for steel and aluminium sill was on the outermost fibre in;

- +Y direction for LHS sill, and
- -Y direction for RHS sill

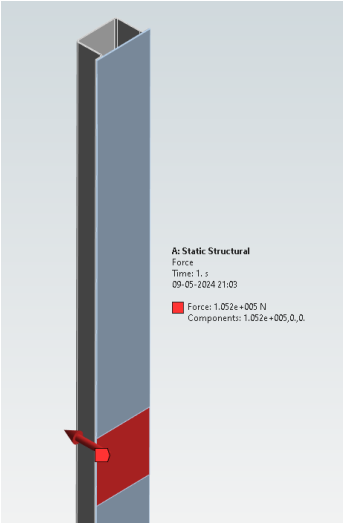

Figure 3.6: CAE: Loading criteria employed for sill

By the end of this process, both calculated and simulated values were generated for the current (steel) and the redesigned (aluminium) sill. A table was drafted for comparative study, which will be discussed in Chapter 4.

3.5.3 Crash box- theoretical calculations

The crash box entailed a different set of calculation procedures. However, the objective of performing theoretical calculations remains the same as before; to compare with simulated values to have a better understanding of attributes and how they affect the performance parameters.

The calculations in this section were performed to determine the theoretical value of critical stress, collapse stress and max load-bearing capacity. The cross-section of the crash box was chosen under the quantitative study using TeamCentre and Catia v5.

When an axial load is applied to a structure, it fails locally due to buckling at a particular stress level, this stress is called critical stress. Critical stress, σ_{cr} is given by the formula;[39]

$$\sigma_{cr} = \frac{k\pi^2 E}{12(1-\nu^2)}(\frac{t}{c})^2 \tag{3.20}$$

k is elastic plate coefficient, E is Young's Modulus of the material, ν is Poisson's ratio of the material, t is thickness of the cross section

The maximum stress-bearing capacity of the column, is called collapse stress σ_{max}, which is given by the formula;[39]

$$\sigma_{max} = (\frac{k_p * E * (t/c)^2}{(1-\nu^2) * \beta * \sigma_y})^n * \sigma_y \tag{3.21}$$

β is material strength coefficient and is given as;

$$\beta = \frac{\sigma_u}{\sigma_y}$$

k_p is Crippling coefficient (in this case the k_p will always be 3.5 as breadth and depth of crash box is not changing, σ_u is Ultimate tensile strength of the material, σ_y is Yield stress of the material.

The max load bearing of the column, when the column starts complete buckling, P_{max} is given by;[20]

$$P_{max} = 2 * [\frac{K_p * E}{\beta * (1-v^2}]^{0.43} * (t^{1.86}) * (C^{0.14}) * (1+\alpha) * (\sigma_y^{0.57}) \tag{3.22}$$

where α is section aspect ratio, and given by;

$$\alpha = \frac{d}{b}$$

3.5.4 Crash box- CAD modelling and CAE simulations

The design of the crash box was done in Catia V5, with the aid of TeamCentre. The model used for simulation was made by simplifying the representative aluminium crash box design provided by the stakeholder. The aluminium crash box was designed as a square tube without any trigger points, to understand and imitate how the crash box would behave under loading. This aluminium crash box was later redesigned into a steel crash box to match the performance.

CAE simulations for the crash box were conducted using Abaqus workbench. The aim was to record the peak load and collapse stresses and to understand how crash boxes behave without the trigger points. Eventually, the results from the CAE simulation were compared with the theoretical calculations. The loading direction depends on how the crash box was placed during design. For the case of buckling analysis, the loading direction was the positive X-axis.

Boundary conditions

Boundary conditions defined the behaviour at the boundaries of the model domain and integrated the influence of external factors into the simulation. The boundaries established for the crash box's static structural CAE simulation are illustrated in Figure 3.7. The speed of the wall was 16km/h (i.e. 4444mm/s) and the weight of the moving wall was 1000kg. These boundary conditions were derived from Euro NCAP's frontal impact load test (refer Sub-section 2.3.1) and the loading case was determined based on insights from qualitative study, i.e. interview.

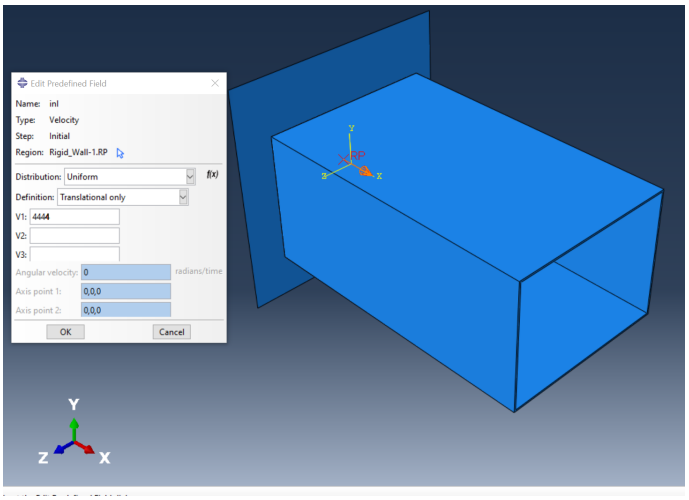

Figure 3.7: Speed of wall in mm/s

By the end of this process, both calculated and simulated values were generated for the current (aluminium) and the redesigned (steel) crash box. A table was drafted for comparative study, which will be discussed in Chapter 4.

3.5.5 Life cycle inventory analysis

As established earlier under Section 3.3, LCI analysis was performed as a final step of Phase 1. It has to be noted that in this phase (1), a 'less elaborate' LCA was performed; which is often termed 'Life Cycle Inventory analysis' or LCI analysis. Essentially stopping after inventory data collection and analysis, from which the results were directly interpreted [24].

This allowed authors to study the major contributing factors to CO_2e emissions during the manufacturing process and helped to generically understand the math and logic involved in LCA study.

A. Goal and scope definition

According to ISO 14041:1998, before conducting any type of LCA, the practitioner must [24]:

- Provide a clear rationale for carrying out the study
  - For Phase 1, the reason was to study the dominant attributes of sill (aluminium and steel) production that affect the CO_2e emissions.
- Decide on the intended application of the LCA study
  - To analyze which is the environmentally preferred part for integration into the vehicle (for Phase 1).
- Declare the intended audience for the LCA findings.
  - BIW and CAD department at Zeekr Technology Europe.

The scope definition and modelling requirements are broadly enlisted below;

- System boundary: In the schematisation of process flows in the following figures, red arrows are input to the process, green arrows are output from the process and grey arrows depict the material flow path. The dotted lines represent the system boundary.
  - Additionally, Figure 3.8 presents the adjusted system boundary for LCI analysis in Phase 1. It is important to note that certain processes have been omitted to align with the study's rationale and adhere to the designated time frame for this thesis. The same has been followed for aluminium sill and can be noticed in Figure 3.9.
  - These exclusions were not arbitrary but rather guided by specific criteria; processes with negligible mass changes or those beyond the influence of stakeholders (in this case, Zeekr) were omitted from the system boundary.
- Functional unit: 1 piece of steel stamped sill produced.

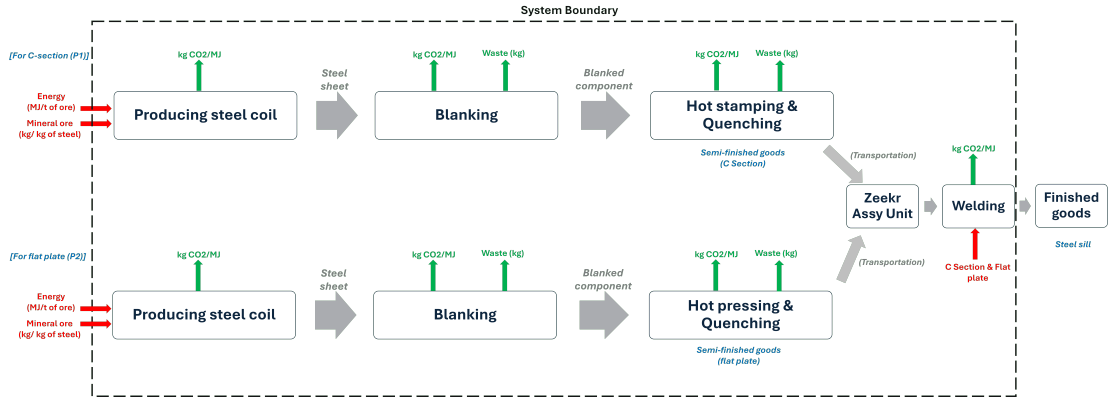

Figure 3.8: System boundary for steel sill LCI analysis

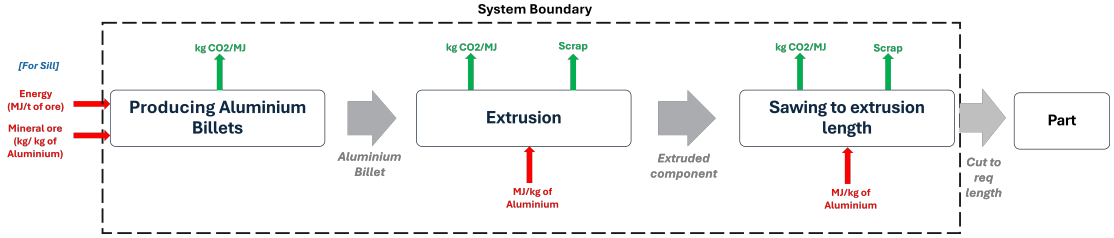

Figure 3.9: System boundary for aluminium sill LCI analysis

According to ISO 14040:1997, it is essential to address and describe all assumptions and limitations in the goal and scope definition. This requirement pertains primarily to significant assumptions and does not extend to individual dataset assumptions[24]. In line with the above standard, the following are the delimitations and assumptions of LCI analysis of Phase 1:

- The LCI model (of sill in aluminium and steel) will use global datasets.
- All data related to inputs and outputs for various processes, ranging from energy usage to emission rates, is gathered solely from Chinese sources, such as articles, journals, and machinery catalogues. This sourcing strategy is informed by the fact that the manufacturing processes for the components examined in this thesis occur entirely within China.
- The Primary source of energy required to produce electricity (to run stationary machines like CNCs, presses, etc) and run the furnace (to produce steel coil, aluminium ingot) is bituminous coal or soft coal.
- An assumption was made that Zeekr produces 50,000 cars annually, necessitating the production of 100,000 sills per year (two sills per car).

B. Life cycle inventory

To meet the aim of this LCI study, the system boundary was converted into variables, i.e. parametric model to gather a clear understanding of affecting parameters. Hence, Figure 3.8 transitions to Figure 3.10 for steel sill and 3.9 transitions to Figure 3.11 for aluminium sill.

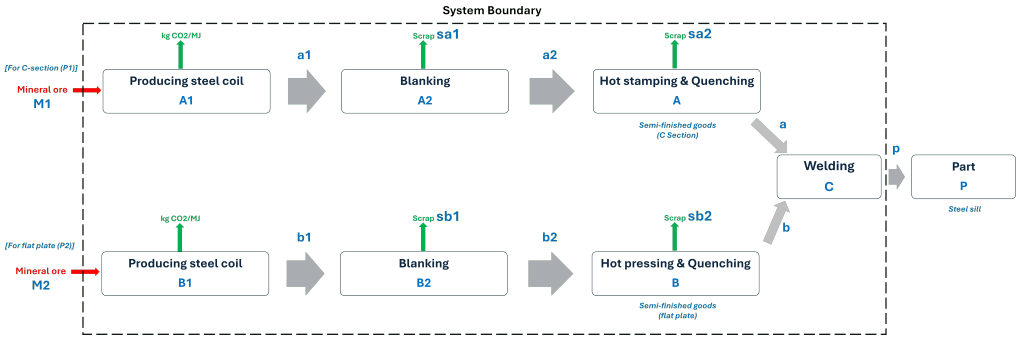

Figure 3.10: System boundary; parametric model for steel sill

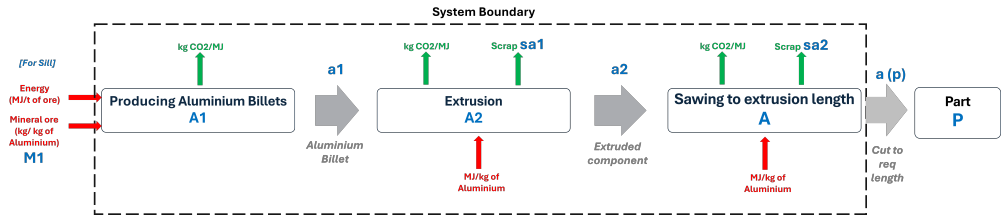

Figure 3.11: System boundary; parametric model for aluminium sill

In Figure 3.10 and 3.11;

M1 is mineral ore required, in kg/year
A1 is the activity corresponding to producing steel coils for C Section & aluminium billets
M2 is mineral ore required for producing steel coils for flat plate, in kg/year
B1 is the activity corresponding to producing steel coils for flat plate
a1 is the main product from A1, in kg/year
b1 is the main product from B1; steel coil, in kg/year
A2 is the activity corresponding to blanking of C Section & extrusion of aluminium sill
B2 is the activity corresponding to blanking of flat plate
a2 is the main product from A2, in kg/year
b2 is the main product from B2; blanked part, in kg/year
sa1 are the scrap produced from A2, in kg/year
sb1 is the scrap produced from B2, in kg/year
A is the activity of hot stamping & quenching of C Section and sawing
B is the activity of hot pressing & quenching of flat plate
sa2 are the scrap produced from A, in kg/year
sb2 is the scrap produced from hot pressing & quenching of flat plate, in kg/year
C is the activity of welding C Section and flat plate
a & b are main products from A and B resp.; C Section & flat plate (SFG), in kg/year
p is the final main product from C; finished product, in kg/year
P is the finished product-sill, in kg

The system depicted in Figures 3.10 and 3.11 were modelled as an array of equations (in Matlab) involving mass flow, energy and emission attributes. All trailing equations form a parametric modular system that illustrates the production of steel stamped and aluminium extruded sill.

System equations

Once the system boundary was finalized, the flows connecting the activities of the modelled system were calculated. To calculate the flows linking the processes an equation system is needed, essentially it is required to describe the relation between different flows [27]. These are system equations. Input data, primarily sourced from literature studies, was used to develop these equations, thereby establishing the relationships between these flows.

Normalizing system equations

Normalizing system equations means describing the inputs and outputs of a process to its main output, by calculating the raw materials and energy needed to produce one kilogram of the main product [26]. The above set of equations had to be normalized w.r.t. each activity's output, i.e. all inputs to and outputs from a particular activity have to be normalized to that activity's main output.

Mass flow relations

Mass flow describes the relationship between inflows and outflows for each activity in a flow chart. It shows the material needed at each step to produce one functional unit [27].

Solving mass flow answers questions like how much material is needed, how much is transported, and what is the scrap from a process. Note that the material balance for a plant or process might differ from that of a specific functional unit due to material usage for other part's production under a process.

Energy equations

Different energy sources may be used in product production. To calculate total energy consumption, these sources cannot be simply combined. Instead, each type of energy is calculated separately [27].

$$Energy\,equation = Norm.\,energy\,input_{activity,n} * Main\,product_{activity,n} \tag{3.23}$$

Emission factor

Instead of calculating the total emissions from a vehicle or industry, emission factors can be used. This involves determining the amount of pollutants per functional unit [27]. These emission factors too were derived from literature study.

$$CO_2e\,Emissions = Energy\,equation_n * Emission\,factor\,of\,CO_2e \tag{3.24}$$

3.6 Phase 2: Quantitative study

The objective of Phase 2 was aligned with the overarching aim of this thesis. This phase involved studying, comparing, and potentially enhancing the current component (i.e., CMS) through a redesign to recommend a part with reduced CO_2e emissions.

The results from Phase 1 indicated that performing theoretical calculations is one of the redundant tasks, as theoretical calculations and CAE simulations yielded almost the same results. Hence in Phase 2, theoretical calculations were avoided but only engaged in necessary calculations (geometrical dimensions, dimensional analysis, impact load calculations, and such). Drawing on the insights gained from Phase 1 and with clearly defined performance parameters and objectives were then used to proceed with Phase 2.

A holistic view of process flow and activities carried out under Phase 2 for CMS are depicted in Figure 3.12. Furthermore, it has to be noted that the performance parameters of the CMS are already specified in table 3.1.

Figure 3.12: Generic Phase 2 activities

3.6.1 Current CMS

Unlike Phase 1, where benchmarked values for the sill and crash box were established by the authors (Step 5 of Section 3.3), Phase 2 did not require benchmarking values as the current CMS design (aluminium crash box and bumper beam) was provided by the stakeholder (Zeekr).

All essential information, data, and statistics were collected during qualitative interviews with the systems, CAE and CAD engineer at Zeekr for benchmarking. The interview questions (see Appendix A.1) were designed to retrieve the performance parameters outlined in Table 3.1.

CAD modelling and CAE simulation

Due to confidentiality, the current CMS's figure is inaccessible for this thesis. Geometrical dimensions from TeamCenter and Catia V5 served as boundary conditions for redesigning the CMS with steel. Since the current CMS was already designed, no remodelling was required. Additionally, unlike Phase 1, the focus here was solely on studying CO_2e emissions themselves and not on the effects of attributes on these emissions.

3.6.2 Redesigned CMS

With the current design's dimensional constraints, benchmarked performance parameters and the aim to study the CO_2e emissions, the aluminium CMS was redesigned using DP800 steel. DP800 was the material chosen because of its ability to deform and absorb energy. All steps from 6 through 9 of Section 3.3 were carried out to design and arrive at the 'redesigned CMS'.

The redesigned CMS was selected following a comparative analysis of results obtained from LS Dyna for the concept's values against the specified performance parameters that were obtained in the benchmarking process of the current CMS.

Upon finalizing the concept, an LCA of the current CMS (i.e., in aluminium) was conducted to establish a benchmark value, as this data was not readily available from stakeholders. Following the completion of the LCA on the current CMS, an LCA on the redesigned CMS was conducted, utilizing similar datasets and impact categories as those employed for benchmarking.

CAD modelling and CAE simulation

Using the dimensional values from benchmarking, 3D CAD concepts were developed in Catia V5. A static structural CAE simulation was then conducted in Abaqus to identify weaknesses. Once the Abaqus results met the requirements, the CMS design concepts were submitted to the CAE team at Zeekr for validation. The CAE engineer used LS Dyna to simulate the frontal impact scenario (Sub-section 2.3.1) on each concept.

This step ensured that all essential checkpoints were addressed from the stakeholders' perspective. It also guaranteed to receive professional and experienced feedback on the CAE simulated results, ensuring that these results would then go on to form a solid base for performing further tasks.

Additional refinements to the design were implemented, including minor fillets and chamfers, to enhance the practicality of the 3D CAD model for seamless integration into the complete BIW structure.

3.6.3 Life cycle assessment

In conducting LCAs for both the current and redesigned CMS, the same databases, impact assessment methods, and impact categories were utilized. Similar assumptions and considerations were also maintained throughout the process. The simulation tool employed for this purpose was OpenLCA.

A. Goal and scope definition

As already illustrated in Figure 2.4 and established in Sub-section 3.5.5, the practitioner is required to follow the steps therein.

- Decide on the intended application of the LCA study
  - To analyze which CMS (current or redesigned) is environmentally preferred to be integrated into the vehicle.
- Provide a clear rationale for carrying out the study
  - For Phase 2, the reason was to study the CO_2 emissions generated from current and redesigned CMS.
- Declare the intended audience for the LCA findings.
  - BIW and CAD department at Zeekr Technology Europe.

The scope definition and modelling requirements are broadly enlisted below;

- System boundary: establishes the criteria for determining which unit processes, inputs, outputs, and environmental impacts are included in the analysis scope. Additionally, it helps determine the required level of detail and data quality, while also specifying spatial, temporal, and functional aspects.
  - Figure 3.13 provides a detailed overview of the process flow (cradle-to-gate) for an aluminium extruded CMS and the corresponding Figure 3.14 depicts the same process for a steel stamped CMS.
- Functional unit: 1 CMS produced.

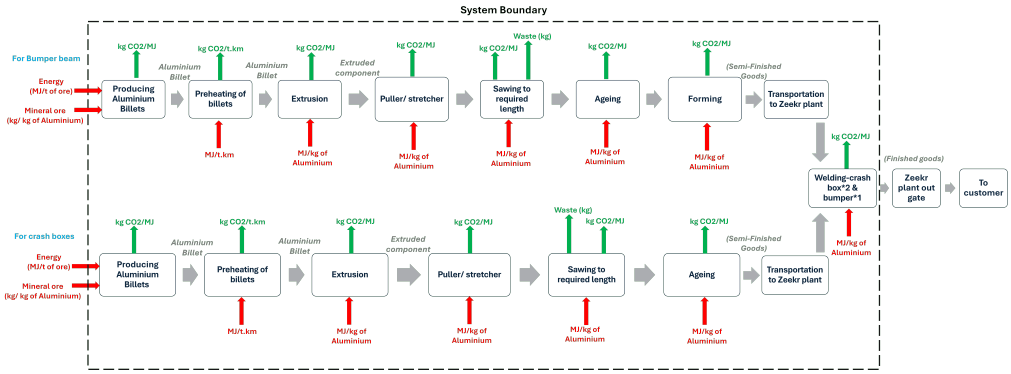

Figure 3.13: Complete process flow for production of aluminium extruded CMS-Bumper & crash box

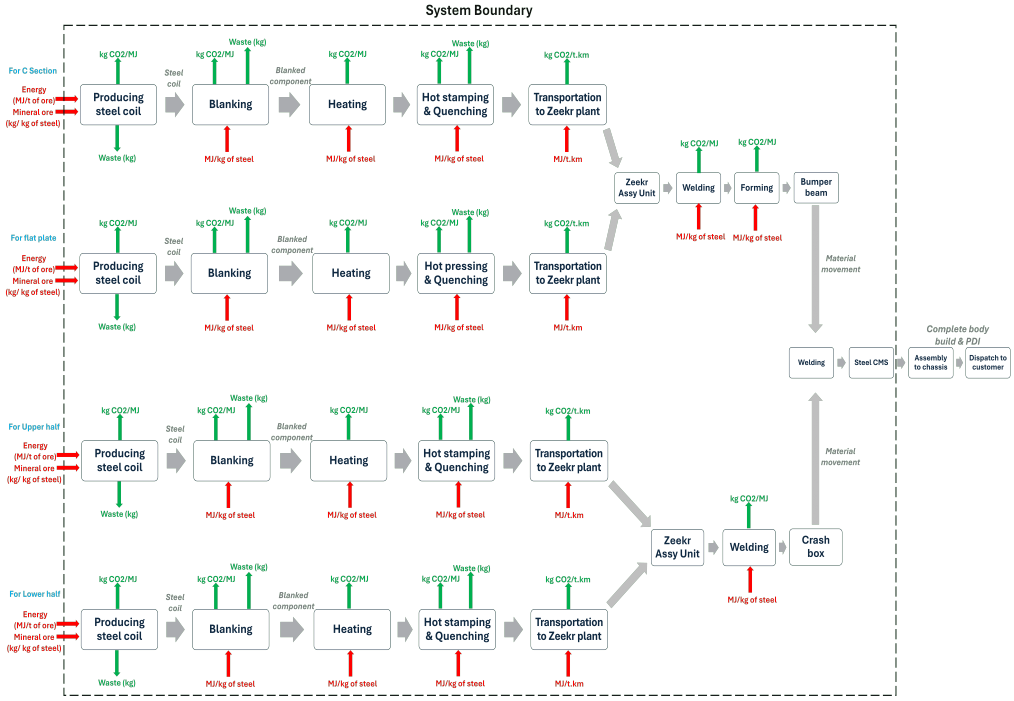

Figure 3.14: Complete process flow for production of steel stamped CMS-Bumper & crash box

As mentioned previously, by ISO 14040:1997, it is crucial to identify and delineate all assumptions and limitations within the goal and scope definition. This directive mainly concerns significant assumptions and does not encompass assumptions pertaining to individual datasets[24].

Consistent with the aforementioned standard, the following are the boundaries and assumptions relevant to the LCA analysis of Phase 2:

- The LCA model (of current and redesigned CMS) will use global datasets from the Ecoinvent database. The datasets that will be considered will belong to ROW, indicating that
- All data concerning inflows and outflows for any process, encompassing energy consumption to emission factors, are sourced exclusively from Chinese-related materials, including articles, journals, and machinery catalogues. This sourcing approach is dictated by the fact that all manufacturing processes for the components discussed in this thesis originate and conclude in China.
- The primary energy source utilized for generating electricity to power stationary machinery such as CNCs, presses, etc., as well as for operating the furnace to produce steel coil and aluminium ingots, is bituminous coal or soft coal.
- The datasets primarily represent RER averages, supplemented by GLO averages as needed. As manufacturing activities are focused in eastern China, ROW datasets were used when available. GLO datasets were utilized in the absence of normalized ROW and RER data.
- Production of steel and aluminium is mainly from primary ore and not from

secondary or tertiary (recycled) resources.
- Inputs or inflows for each process will be determined by an adaption of the 'zero-sum' rule, i.e. the total gains must equal the total losses, in sense, 'the gains' is the weight of necessary output and 'the losses' are scrap from that process.

B. Life cycle inventory

i. Current CMS- aluminium

To perform the sustainability study, Figure 3.13 was modelled in OpenLCA. The following Figure 3.15 gives a holistic view of inputs and outputs for producing one aluminium CMS, i.e. two aluminium (extruded) crash boxes welded to one bumper beam (extruded).

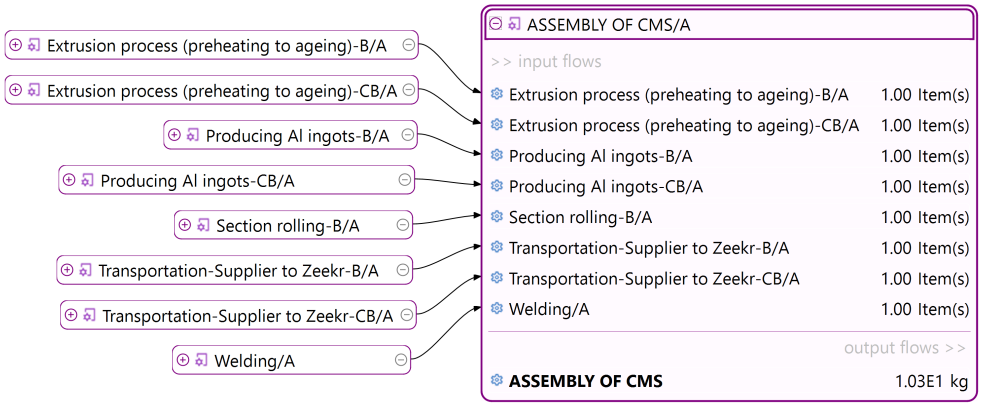

Figure 3.15: Model graph: Aluminium CMS's production process

Bumper beam
The figure referenced as Figure 3.16 depicts the model graph for manufacturing the aluminium extruded bumper beam.

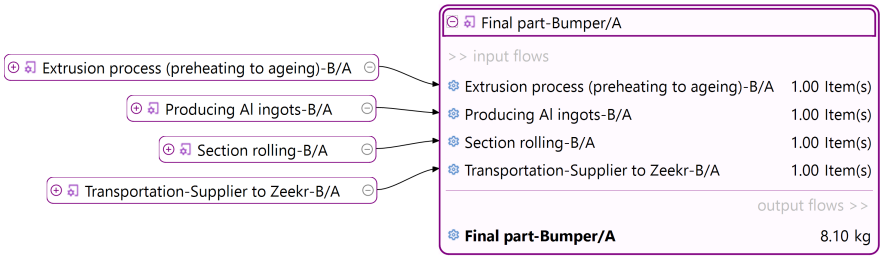

Figure 3.16: Model graph: Aluminium bumper's production process

Refer to Appendix A.2 for detailed information on the inputs and processes involved at each step of the model graph of Figure 3.16.

Crash boxes

The figure referenced as Figure 3.17 illustrates the model graph for manufacturing aluminium extruded crash boxes.

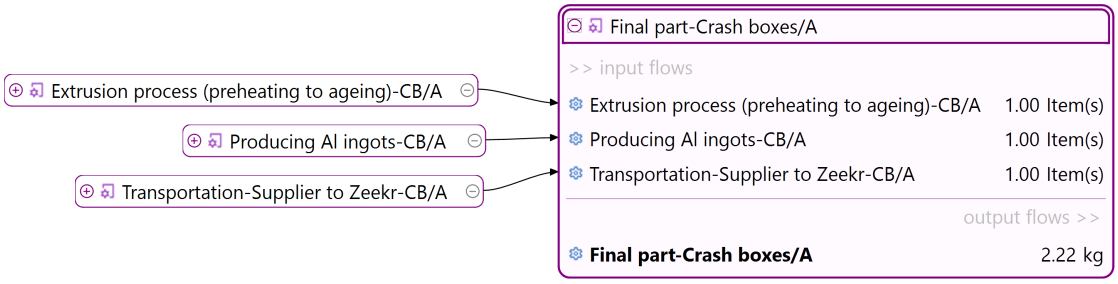

Figure 3.17: Model graph: Aluminium crash box's production process

Please refer to Appendix A.2 for detailed information on the inputs and processes involved at each step of the model graph of Figure 3.17.

CMS assembly- crash boxes and bumper beam

The assembly of CMS is simply done by aluminium arc welding of two crash boxes to the bumper beam.

The dataset (ROW) for the process involved in aluminium arc welding includes;

- Emissions from filler rods and their transport,
- Energy used for arc welding, and
- Emissions from use and production of protective gases

ii. Redesigned CMS- steel

Similar to the method followed for the current CMS, to perform the sustainability study, Figure 3.14 was modelled in OpenLCA. The following Figure 3.18 gives a holistic view of inputs and outputs for producing a single steel CMS, consisting essentially of two steel crash boxes (stamped) welded to one bumper beam (steel stamped).

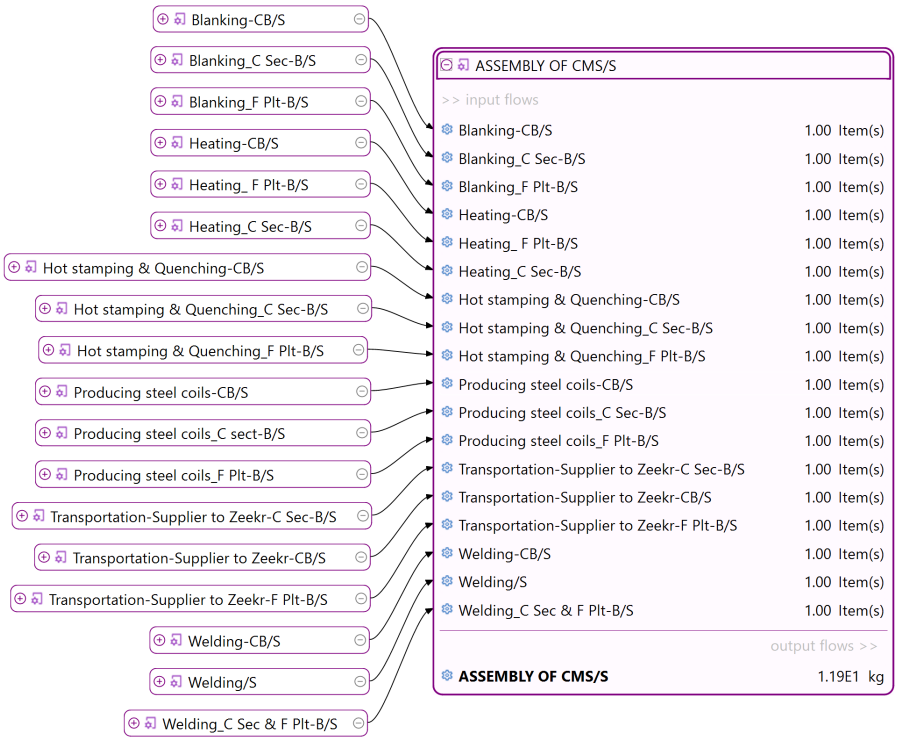

Figure 3.18: Model graph: Steel CMS's production process

Bumper beam

The figure referenced as Figure 3.19 illustrates the model graph for producing the steel stamped bumper beam. Furthermore, as already established under Delimitations, it has to be again noted that the bumper beam is a sub-assembly to welding C Section and flat plate.

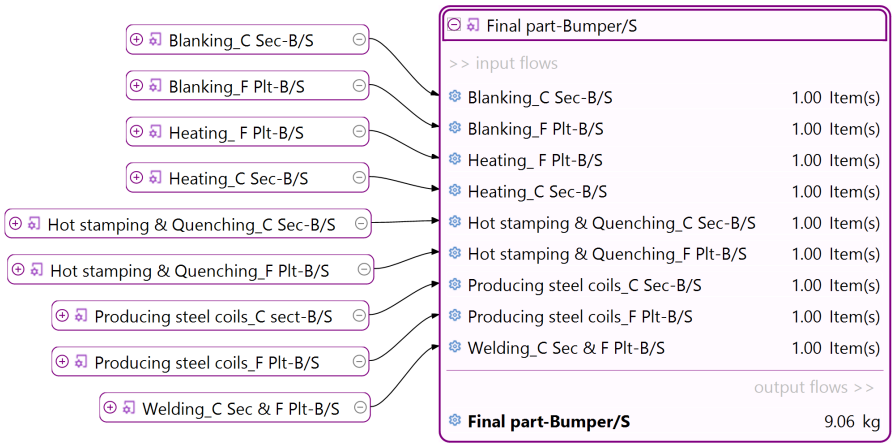

Figure 3.19: Model graph: Steel bumper's production process

Refer to Appendix A.2 for detailed information on the inputs and processes involved at each step of the model graph of the Figure 3.19.

Crash boxes

Figure 3.20 depicts the model graph detailing the manufacturing process for steel-stamped crash boxes.

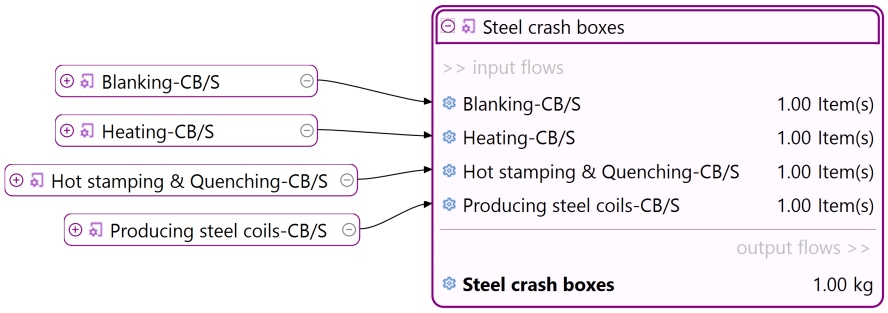

Figure 3.20: Model graph: Steel crash box's production process

Refer to Appendix A.2 for detailed information on the inputs and processes involved at each step of the model graph of the Figure 3.20.

CMS assembly- crash boxes and bumper beam

The assembly of CMS was also done by steel arc welding of two crash boxes to the bumper beam. The dataset (ROW) for the process involved in steel arc welding are same as that of aluminium arc welding.

C. Life cycle impact assessment

As established, the stakeholder's interest was solely in CO_2e emissions, making the selection of the impact category from the 'Midpoint Impact category' a natural choice. GWP served as a key indicator, and a 'Hierarchist perspective' was adopted under the ReCiPe method for performing a comparative LCA study on CMS.

D. Interpretation

Interpretation in LCA analyzes LCIA results and scrutinizes impact indicators like GWP to conclude. This process provides insights into environmental performance, identifies improvement areas, and supports decision-making aligned with the study's goals. In short, these are the results from LCA, hence will be discussed in Chapter 4.

4

Results

This chapter provides the results of studies conducted under Phase 1 and Phase 2. To justify the structure of the thesis and also the methodology employed, the following framework (Figure 4.1) was adopted to present the results. This figure illustrates that, for instance; under Phase 2, the redesigned CMS results for CAD and CAE (for steel) incorporate elements of a quantitative study.

Phases 1 and 2 are based on different quantitative studies that include theoretical calculations, CAD modelling, and CAE simulations of sill, crash box, CMS and LCI (see Figure 3.1). Importantly, both phases also draw on elements from literature and qualitative studies.

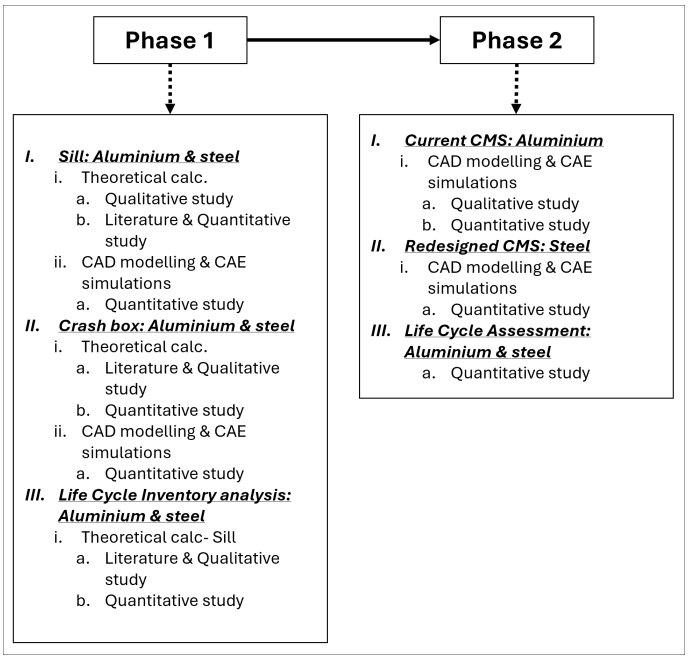

Figure 4.1: Results overview

To clarify, this section follows the chronological order of the parts, as they appeared in the Methodology chapter. These sections are further divided into sub-sections with the categorization of literature study, qualitative study and quantitative study.

Phase 1

The objective of Phase 1 was to understand attributes that affect the performance parameters of each part. As mentioned earlier, Phase 1 entailed the design of the side sill and the crash box with alternative materials;

- Sill: steel (current) to aluminium (redesigned) and
- Crash box: aluminium (current) to steel (redesigned)

This was then followed by an LCI analysis of sill (with aluminium and steel) to understand the effects of attributes on CO_2e emissions. The results from Phase 1 of this thesis are presented below.

4.1 Phase 1: Sill

Due to confidentiality, the representative version cannot be released in this thesis. Therefore, this section will present only the current design and the redesigned components with their respective results.

4.1.1 Theoretical calculations- steel and aluminium

In this subsection, the results of theoretical calculations performed on a simply supported sill with both steel-stamped (current) and aluminium-extruded (redesigned) concepts will be presented.

A. Qualitative study: Steel stamped sill

Following are the input values of Phase 1 that were gathered during interviews with the systems engineer. Also listed below are some of the assumptions and relevant considerations that were made after discussing with the systems engineer and CAE engineer. The list is followed by the cross-section and nomenclature of the sill (Figure 4.2).

- Mass of the vehicle, $m = 2600kgs$
- Velocity of vehicle, $V = 32km/h \; or \; V = 8.9m/s$
- Time taken (delay) for impact, $t = 0.11sec$
- The beam was considered to be simply supported at both ends.
- The length of beam, $L = 2026mm$
- The cross section is further divided into 6 sub-divisions as below;
  - b_1, d_1 is the breadth and depth of subdivision/rectangle $1/A_1$.
  - b_2, d_2 is the breadth and depth of subdivision/rectangle $2/A_2$.
  - b_3, d_3 is the breadth and depth of subdivision/rectangle $3/A_3$.
  - b_4, d_4 is the breadth and depth of subdivision/rectangle $4/A_4$.
  - b_5, d_5 is the breadth and depth of subdivision/rectangle $5/A_5$.
  - b_6, d_6 is the breadth and depth of subdivision/rectangle $6/A_6$.
- Calculated force will be assumed as point load acting at the centre of a simply supported beam; essentially imitating a 3-point-bending test.

- Alternatively, Area A1 will be referred to as the "flat plate" of the steel sill, while Areas A2 to A6 collectively constitute a geometry termed the "C-Section" of the steel sill.
- The material used in this case was PHS, 22MnB5 (from table 2.1).
- That 'thickness' is for varying dimensions of *b4,b5,d1,d2,d3 and d6*. All other dimensions remain constant.
- FOS is calculated by dividing material's ultimate strength by max stress-induced, i.e. $\frac{\sigma_{ultimate}}{\sigma_{max}}$.

The simplified cross-section of the representative version sill is illustrated in Figure 4.2. Also, the parametric values for variables are shown in Table 4.1.

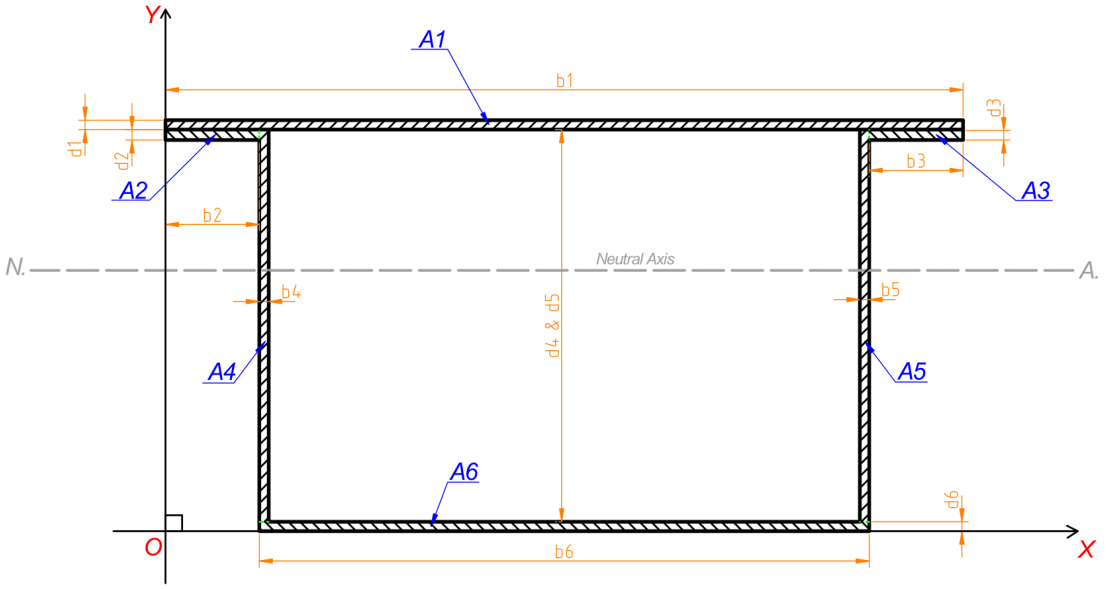

Figure 4.2: Cross-section of sill and its respective nomenclature

Table 4.1: Dimension and values for Steel Sill

Dimension	Value
b1	153 mm
b2, b3	18 mm
b4, b5	1.8 to 4.2 mm
b6	117 mm
d1	1.8 to 4.2 mm
d2, d3	1.8 to 4.2 mm
d4, d5	77-d6 mm
d6	1.8 to 4.2 mm

B. Quantitative study: Steel stamped sill

As one might notice in Table 4.1, the values for few dimensions are varied over a range of 1.8 to 4.2mm. This variation in sheet metal gauges is what gives rise to different concepts; out of which the 'redesigned parts' will finally be chosen.

The calculations adhered to the procedure outlined in Section 3.5.1. Equations from 3.4 to 3.19 were modelled in Matlab as a script, and the corresponding results were generated. Input to equations was from Table 4.1.

Substituting the values from Table 4.1 into the respective equations yields the performance parameters necessary for benchmarking and facilitating a direct comparison.

The impact force or point load needed to be calculated before proceeding with further calculations. Using the readily available input data from literature and qualitative studies, Eq. 3.4 was solved. Consequently, the impact force or point load, F_{impact} or W, acting at the centre of the 2026 mm sill was determined to be **105.2 kN**.

With the impact force, material properties, and cross-section of each concept available, the Matlab script was ready to be executed. All the performance parameter (i.e. results) values that were calculated for steel stamped sill are shown in Table 4.2. This is a result of executing all the steps of Figure 3.3.

Table 4.2: Theoretical calculation results of current steel stamped sill

Thickness	**Induced stress, MPa**		**Deflection, mm**	**FOS, -**
	$\sigma_{tensile}$**, MPa**	$\sigma_{compression}$**, MPa**		
1.8	2664.65	1967.31	95.74	0.79
2.3	2131.71	1555.66	76.22	0.73
2.8	1789.81	1291.05	63.68	0.87
3.3	1552.11	1106.62	54.95	1.00
3.8	1377.48	970.72	48.53	1.13
4.0	1319.99	925.87	46.42	1.18
4.2	1268.04	885.29	44.51	1.23

Furthermore, Figure 4.3 demonstrates how the thickness of the cross-section influences the stress induced in a steel-stamped sill. Meanwhile, Figure 4.4 portrays the impact of thickness on intrusion, specifically concerning PHS 22MnB5 material.

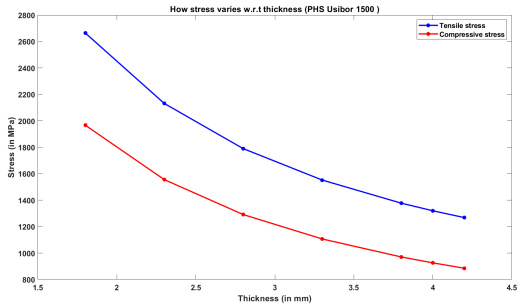

Figure 4.3: Stress behaviour of steel stamped sill with varying thickness

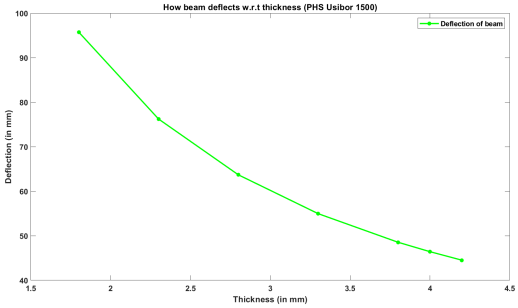

Figure 4.4: Intrusion behaviour of steel stamped sill with varying thickness

It can be observed from Figures 4.3 & 4.4 and Table 4.2 that **as cross-section thickness increases from 1.8mm to 4.2mm, the stress reduces by approximately 52%, thereby increasing FOS and curtails intrusion by almost 53%.**

Deciding on the right thickness for the steel sill was the next step, considering the different thickness options available. MCDA was employed to choose the most dominating dimensions in steel sill.

Multi criteria decision analysis for steel sill

Thirty-six attributes of each steel sill from Table 4.2 were plotted against the Ixx and N.A. These two parameters were determined to be highly influential, and notably, they were the only parameters that could be adjusted in equations 3.15 and 3.15. Also, note that breadth-wise dimensions (b1 to b6) were not considered as they are constrained geometries and served as boundary conditions.

The thirty-six attributes were the result of;

d1 to d6	Depths of sill's cross section
A1 to A6	Areas of sub-divisions in cross section
Y1 to Y6	Distances from OX to cg (centre of gravity) of each sub-division
h1 to h6	Distances b/w each sub-divisions cg & cross section's cg
Ig1 to Ig6	MOI of each sub-division
IG1 to IG6	MOI (per Parallel Axis theorem) of each sub-division

The plots yielded slopes for each of the 36 attributes against Ixx and N.A., resulting in a total of 72 slope values. Attributes with the steepest slopes were categorized as high priority.

From the calculation it was clear that d1,d2,d3 and d6 dimensions (which are modifiable) are dominant. But y1,y4,y5 and y6 are even more dominant attributes. On further analysis it was noticed that y1,y4,y5 and y6 are all majorly dependant on one dimension, i.e. d6.

Hence, it was concluded that the lower-most or farthest fibre from the point of load application is the most vulnerable and dimension d6 is the dominant attribute of the steel stamped sill.

However, referring back to Figure 4.2 it was further deduced that varying or increasing only d6 is not feasible as it would lead to varying cross-section thickness, which is not desirable from a manufacturing perspective.

As a result of this, d2, b4, d6, b5 and d3 had to have the same dimension. In summary, the 'C section' thickness had to be varied with higher thickness while the 'flat plate' could have relatively lower thickness. Varying these dimensions between 1.8 to 4.2mm, led to the generation of different concepts; amongst which one would be chosen and termed 'current sill'.

4.1.2 CAD modelling and CAE simulations- steel

To culminate the quantitative study of steel stamped sill, the results and insights from MCDA were analysed and 7 concepts were generated which were now based on representative version sill and were also simplified. Out of these, concept 4 was then finalized as the 'current steel stamped sill', as it met the required performance parameters (outlined in Table 3.1).

This now means that the 'redesigned sill' will have to exceed (or at least meet) the performance parameters of concept 4. The concepts that were generated to choose the current sill and their descriptions along with their performance parameter values are tabulated in Table 4.3.

Table 4.3: Assessing performance parameters for current steel stamped sill (PHS, 22MnB5 Material). *FPt is Flate Plate thickness; CSt is C Section thickness*

Concept	**Concept descp.**	**Deflection, mm**	**Weight, kgs**	**FOS, -**
1	FPt=2.3mm; CSt=1.8mm	47.50	14.25	1.07
2	FPt=1.8mm; CSt=2.3mm	46.95	15.44	1.02
3	FPt=2.3mm; CSt=2.3mm	41.98	16.62	1.12
4	FPt=2.3mm; CSt=2.8mm	38.35	18.53	1.20
5	FPt=2.3mm; CSt=3.3mm	35.28	21.31	1.32
6	FPt=2.3mm; CSt=3.8mm	32.76	23.63	1.4
7	FPt=1.8mm; CSt=3.8mm	35.25	22.47	1.08

To reiterate the objective, the reason for conducting both theoretical calculations and CAE simulations was to validate the notion that while CAE simulations offer

efficiency and practical results beyond theoretical calculations alone, it's essential to empirically establish this premise rather than merely assuming it as an axiom.

Additionally, concept 4 underwent minor modifications, introducing corner radii to the C Section to eliminate sharp edges and facilitate mesh generation in Ansys. These adjustments were made to enhance the design's practicality and realism. Figure 4.5 shows the CAD model of concept 4, i.e. the 'current sill' in different views.

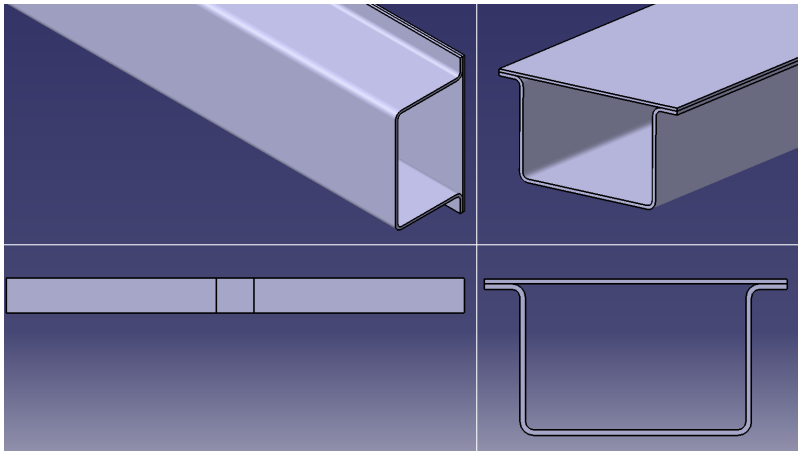

Figure 4.5: Different views of current sill: Steel stamped sill

On following the same procedure and beginning with the same cross-section as that of the current sill but with aluminium 7108 T-6 as material (refer Table 2.1), results were gathered that are tabulated in Table 4.4.

Table 4.4: Theoretical calculation for aluminium 7108-T6 sill

Thickness	**Induced stress, MPa**		**Deflection, mm**	**FOS, -**
	$\sigma_{tensile}$**, MPa**	$\sigma_{compression}$**, MPa**		
1.8	2664.65	1967.31	291.39	0.79
2.3	2131.71	1555.66	231.97	0.73
2.8	1789.81	1291.05	193.81	0.87
3.3	1552.11	1106.62	167.26	1.00
3.8	1377.48	970.72	147.72	1.13
4.0	1319.99	925.87	141.28	1.18
4.2	1268.04	885.29	135.46	1.23

It can be observed from Table 4.4 and 4.2 that **as cross-section thickness increases from 1.8mm to 4.2mm, the induced stresses and FOS of aluminium sill remains the same, although intrusion increases drastically by nearly 200%.**

Stresses followed the relation in Eq. 3.15, dependent on cross-section (Ixx) and forces (M), but not material properties, leading to unchanged stress values. In contrast, Eq. 3.13 includes Young's Modulus (E), resulting in significant variations in sill intrusion, as shown in tables 4.4 and 4.2.

These results indicated that varying the cross-sectional area and not just the thickness, was necessary for the redesigned sill. Sole reliance on theoretical calculations was insufficient, as they can be inconclusive and time-consuming with each change in cross-section.

Based on these insights, the focus shifted to CAE simulation outcomes over theoretical calculations to validate aluminium-based concepts for performance comparable to steel sills. However generating 3D CAD models was essential before these simulations.

4.1.3 CAD modelling and CAE simulations- aluminium

C. Quantitative study: Aluminium extruded sill

To ensure that the 'redesigned sill' (aluminium extruded) performs on equal par with the current sill (steel stamped), the redesigned sill had to meet the performance parameters of concept 4 in Table 4.3. Given this, 19 concepts in total were generated. Concept 19 was then finalized as the 'redesigned aluminium extruded sill'. The concepts and their descriptions along with their performance parameter values are tabulated in Table 4.5. Also, Figure 4.6 shows the CAD model of concept 19, i.e. the 'redesigned sill' in different views.

Table 4.5: (1/2)Assessing performance parameters for redesigned aluminium extruded sill (Aluminium 7108 T-6 and 7003 T-6).
*FPt is Flate Plate thickness; CSt is C Section thickness; Wy is webs in Y drxn; Wz is webs in Z drxn; R is corner radius along length; ** is mesh size limitation for student license*

Concept	Concept descp.	Deflection, mm	Weight, kgs	FOS, -
	Al 7108 T-6			
1	FPt=2.3mm; CSt=2.8mm	111.07	7.01	0.26
2	FPt=1.8mm; CSt=3.8mm; Wy=1*1mm	106.59	7.44	0.27
3	FPt=4.2mm; CSt=4.2mm	85.18	9.63	0.34
4	FPt=CSt=1.8mm; Wy=2*2.5mm	71.63	12.39	0.4

Table 4.6: (2/2) Assessing performance parameters for redesigned aluminium extruded sill (Aluminium 7108 T-6 and 7003 T-6)

Concept	Concept descp.	Deflection, mm	Weight, kgs	FOS, -
5	FPt=CSt=4.2mm; Wy=Wz=2*2.5mm	69.78	14.74	0.41
	Al 7003 T-6			
6	Complete solid	24.11	54.55	1.29
7	Wall t=20mm	29.62	36.99	0.98
8	Wall t=10mm; Wy=4*10mm	33.06	34.85	0.88
9**	FPt=CSt=4.2mm; Wz=Wy=2*2.5mm	-	25.5	-
10	Wall t=20mm; R=20mm	32.60	35.22	0.95
11	Wall t=20mm; R=20mm; Wy=20mm	29.04	36.30	1.07
12	Same as 11; with cavity on ends of FPt	30.95	33.57	0.94
13	Same as 12; with more cavities on Wy	36.10	28.30	0.80
14	Same as 13; with elongated cavities in Y drxn.	32.88	27.54	0.95
15	Same as 14; with b1 as 163mm (ref 4.1)	30.69	29.07	1.04
16	Same as 14; with d4/d5 as 83.8mm (ref 4.1)	28.46	28.01	1.05
17	Same as 14; with shorter cavities	32.28	28.83	1.10
18	Same as 17; with elongated cavity on FPt	39.42	23.49	0.8
19	Same as 17; with no cavity protruding on FPt	31.93	28.10	1.14

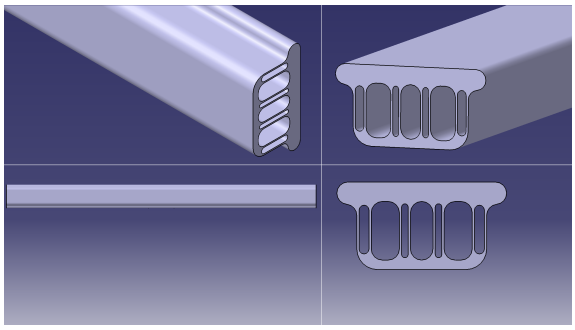

Figure 4.6: Different views of redesigned Aluminium sill

This concludes the presentation of results from the literature study, as well as the quantitative and qualitative studies conducted under Phase 1 for both steel and aluminium sills.

4.2 Phase 1: Crash box

A. Literature and qualitative study

The existing crash box was benchmarked and the Figure 4.7 and 4.8 shows the cross-section of the existing crash box. For Phase 1 of this thesis, the crash boxes were considered to be hollow rectangular columns without any geometrical changes throughout.

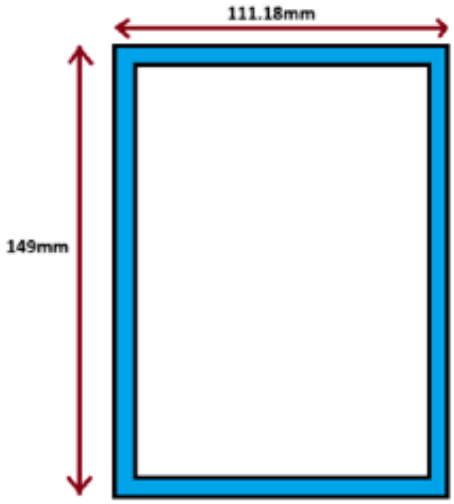

Figure 4.7: Crash box's side values, d=111mm, b=149mm

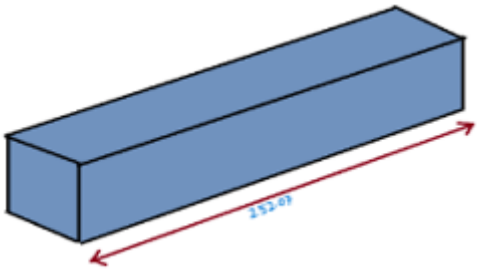

Figure 4.8: Length of the crash box, l=252

4.2.1 Theoretical calculation- steel and aluminium

B. Quantitative study

The existing crash box made of aluminium 6063-T7 (current), was redesigned with DP800 steel(redesigned) as the alternative material.

Steel stamped crash box

For the crash box with DP800 as a material, the thickness was varied from 1.5mm to 2.7mm, with a 0.3mm increment. The variation in thickness for the steel box was done to find a suitable thickness value that matches the performance of the aluminium crash box.

Incorporating the theory of buckling mentioned in section 2.4 and the process of solving shown in section 3, the values for critical stress, collapse stress and the peak loads was obtained for corresponding thickness.

For DP800 steel, Table 4.7, shows the critical stress, collapse stress and the max load-bearing capacity value.

Table 4.7: Theoretical calculation results of steel stamped crashbox

Thickness, mm	**Induced stress, MPa**		**Peak load, KN**
	$\sigma_{Critical}$**, MPa**	$\sigma_{max/Collapse}$**, MPa**	
1.5	118.15	261.43	178.16
1.8	170.14	305.81	250.09
2.1	231.59	349.17	333.13
2.4	302.48	391.66	427.05
2.7	382.83	433.41	531.6

Aluminium extruded crash box

For the aluminium 6063-T7 crash box, Table 4.8, shows the critical stress, collapse stress and the max load-bearing capacity value.

Thickness, mm	**Critical stress, MPa**	**Collapse Stress, MPa**	**Peak load,KN**
2.7	127.83	141.44	180.13

Table 4.8: Buckling values for Aluminium 6063-T7 crash box

Comparing the critical stress, collapse stress and peak loads of the Aluminium crash box and the DP800 steel crash box having a thickness of 1.5mm has values close to the aluminium crash box values.

The performance parameter which is of importance here is the peak load-bearing capacity. The values are dependent on both the geometry of the column and the material properties, hence an appropriate combination of geometry and material has to be chosen.

4.2.2 CAD modelling and CAE simulation- aluminium

The CAD model of the aluminium crash box is shown in Figures 4.9. It is modelled as a rectangular column with a constant thickness

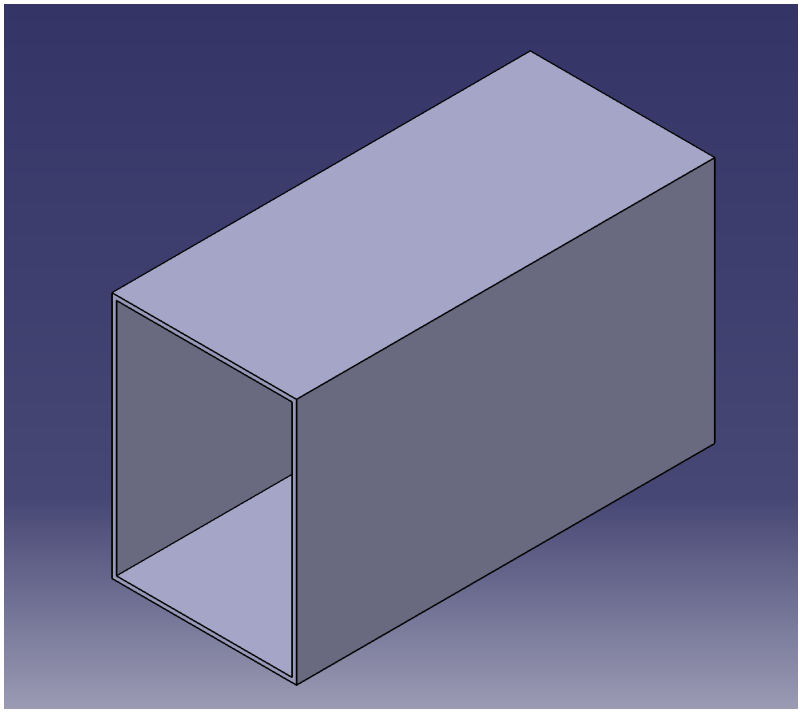

Figure 4.9: CAD model of aluminium crashbox, thickness = 2.7mm

Figure 4.10 presents the values for peak load for the aluminium crash box.

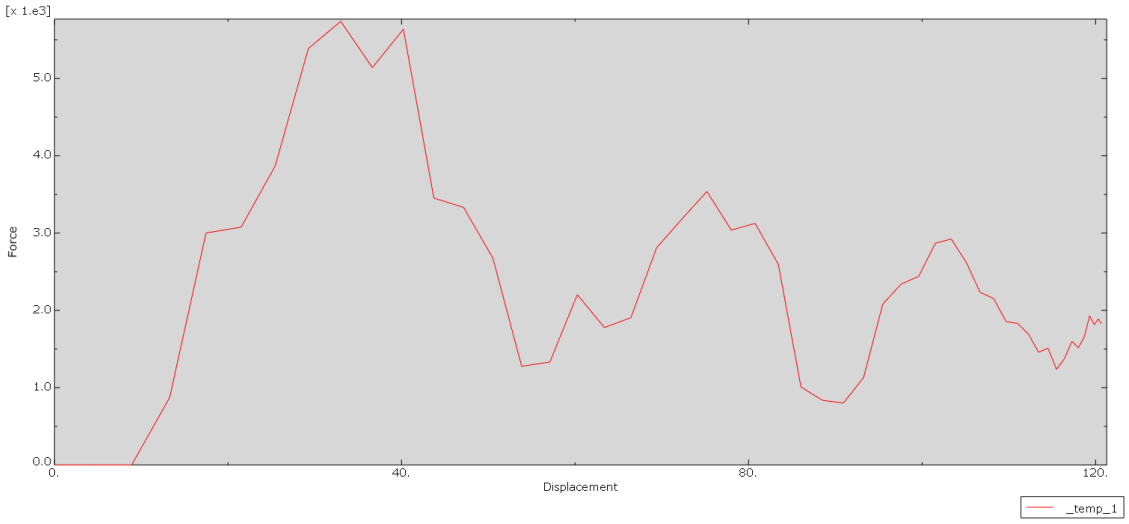

Figure 4.10: Force-Displacement graph for aluminium crash box

Figure 4.11 shows the collapse stress registered by the Abaqus software for the aluminium crash box.

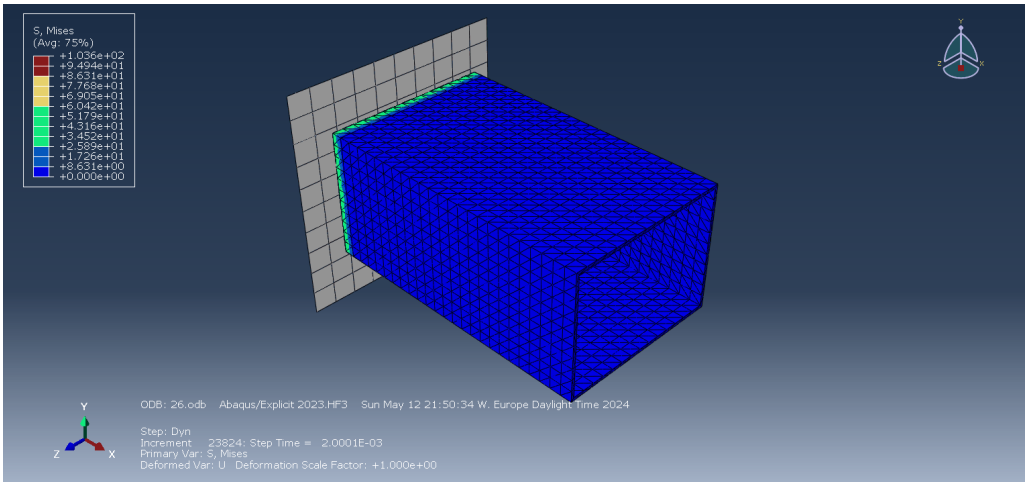

Figure 4.11: Collapse stress registered in Abaqus for aluminium crash box

The collapse stress is found to be 103.6MPa.

4.2.3 CAD modelling and CAE simulation- steel

C. Quantitative study: Steel crash box

The CAD model of the steel crash box is shown in the Figure 4.12.

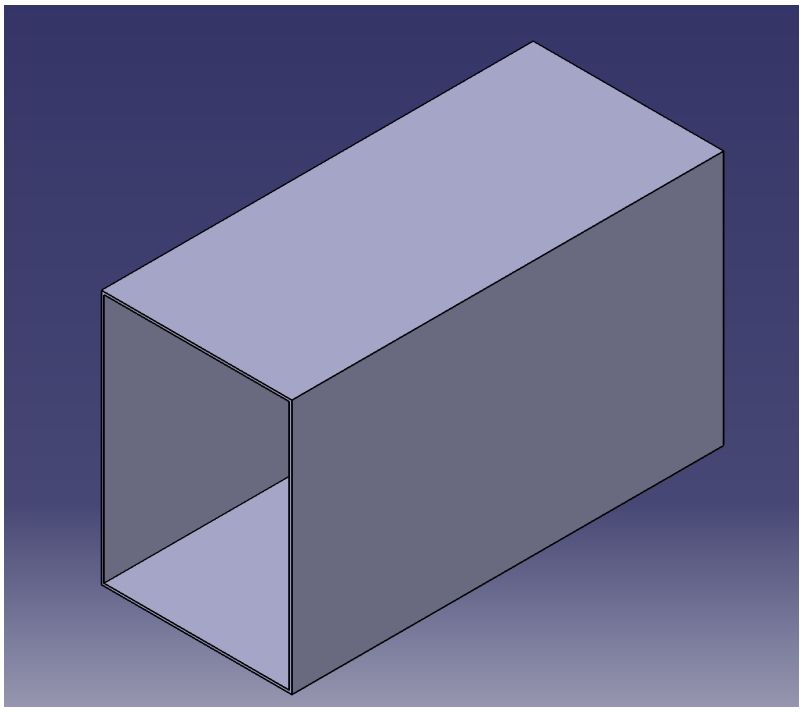

Figure 4.12: CAD model of steel crash box, thickness = 1.5mm

Figure 4.13 presents the values for peak load for the steel crash box.

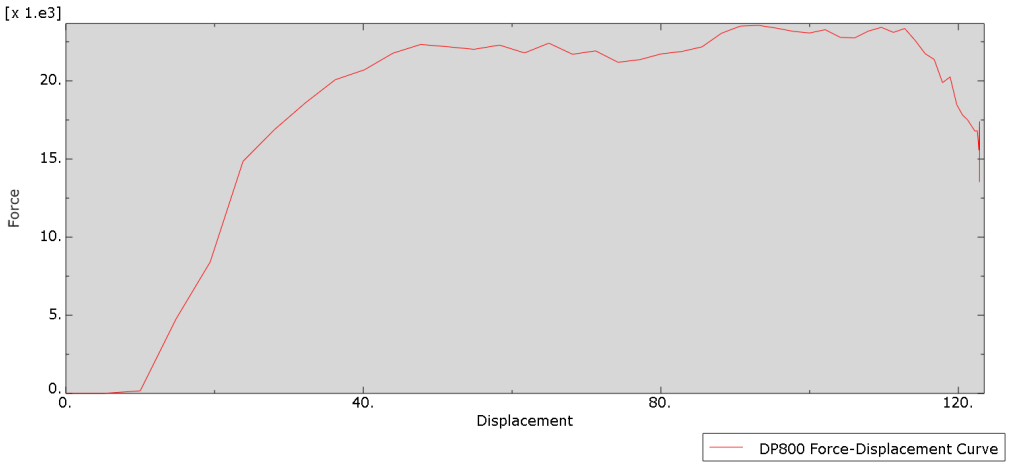

Figure 4.13: Force-Displacement graph for steel crash box

The results for the collapse stress of the crash boxes is presented below,

Figure 4.14 shows the collapse stress registered by the Abaqus software for the aluminium crash box.

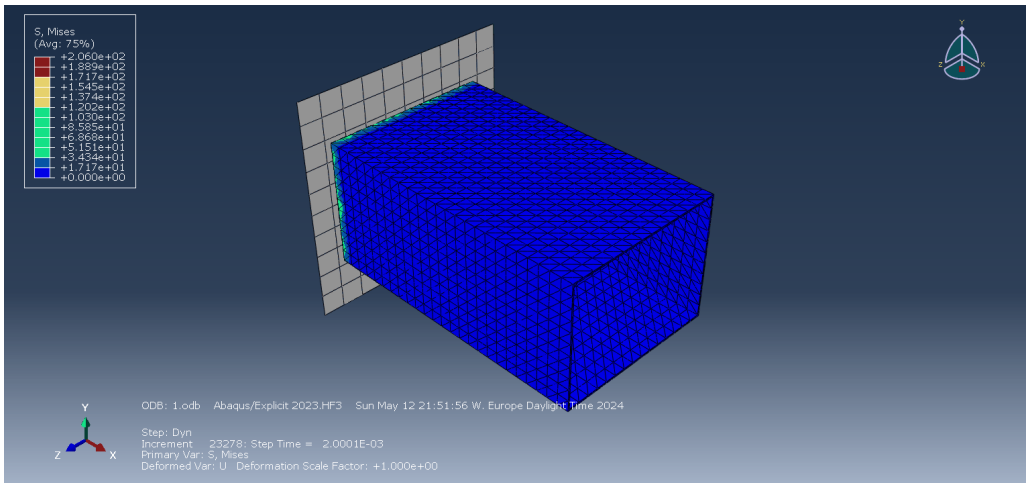

Figure 4.14: Collapse stress registered in Abaqus for the steel crash box

The collapse stress for the steel crash box is found to be 206MPa.

The collapse stress values registered by the Abaqus software for the aluminium and steel crash box are close to the theoretically calculated collapse stress values for the DP800 crash box with 1.5mm thickness and the aluminium crash box with 2.7mm thickness. The collapse stress values from abaqus and the values for stresses and load from theoretical calculations will form the basis for design consideration of the

crash boxes. The values for the collapse stress calculated theoretically and values for the same which was simulated are close, proving the design of the crash box.

The peak load values for the steel DP800 and aluminium 6063-T7 crash boxes from Abaqus are skewed, Steel has a peak load of 20KN while aluminium has a peak load of 5KN, both of these need to reach a value of around 200KN according to the calculated values and the standards mentioned by the stakeholder. The peak load values do not reach the required value during the simulation might be because of not considering material imperfections during the simulation.

Hence, the decision was made to advance to Phase 2, disregarding the simulated peak load values of the crash boxes. The focus shifted to the close correlation between the theoretically calculated collapse stress and the simulated collapse stress values. This correlation validated the design of the crash box, demonstrating that the crash boxes initially behaved as intended. As previously mentioned, peak load values are the primary performance parameter for comparing the two crash boxes. Based on the closely matched peak load capacities from the theoretical calculations, DP800 steel with a thickness of 1.5mm was selected for the redesigned crash box in Phase 2.

4.3 Phase 1: Life cycle inventory analysis

As detailed in Section 3.1, LCI analysis was conducted on the aluminium and steel sills to identify the manufacturing process parameter that contributed most significantly to the CO_2e emissions during the manufacturing phase of these sills.

A. Literature and qualitative study

To calculate the mass flow for the production of aluminium and steel sill, basic data was gathered from a literature study. These basic data are shown in Tables 4.9 and 4.10

Data label	Data value
Scrap rate during extrusion[60]	14.2%
Amount of ore needed to produce 1kg of aluminium [61]	4 kgs
Coal energy required to produce 1kg of aluminium ingot [62]	155 MJ
Energy consumed for extruding 1kg aluminium [63]	2.05 MJ
Energy consumed for sawing 1 part [64]	0.0538 MJ

Table 4.9: Input values for Phase 1 aluminium sill

Data label	Data value
Scrap rate during blanking [68]	15%
Scrap rate during stamping [68]	29%
Amount of ore needed to produce 1kg of steel [66]	1.66 kgs
Coal energy required to produce 1kg of steel coil [65]	26.7 MJ
Energy consumed for blanking steel[67]	0.38 MJ
Energy consumed for stamping steel[67]	0.66 MJ

Table 4.10: Input values for Phase 1 steel sill

The above values that were gathered from the literature study were verified with a systems engineer during an interview that was conducted under qualitative study. The production rate, the weight of the sill and the parameters mentioned above in Table 4.10 and 4.9 are required to calculate the CO_2e emissions.

Using table values and system equations that were built in the Sub-section 3.5.5, the following results are presented.

B. Quantitative study

4.3.1 Aluminium sill

Figure 4.15 illustrates the material and energy inputs required for the production of 100,000 sills. Following the steps outlined in Sub-section 3.5.5, which include generating and normalizing the system equations, constructing mass flow and energy equations, and calculating the CO_2e emissions using the emission factor for each step, the amount of CO_2e released in the production of a single aluminium sill was determined.

Total CO_2e emissions from the manufacturing process of aluminium sill were 498.66 kg.

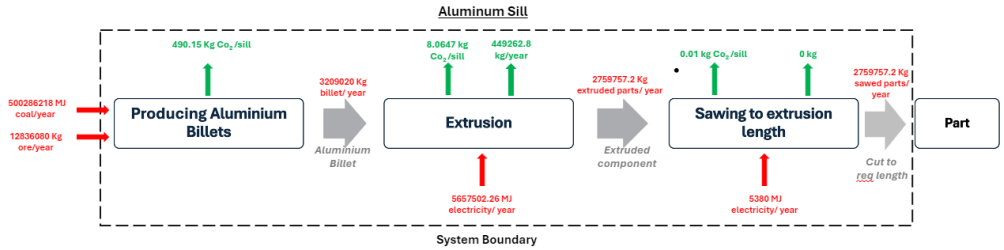

Figure 4.15: Inputs and output values from each production step considered in the making of aluminium sill

4.3.2 Steel sill

The flow chart in Figure 4.16, represents the process flow for the manufacturing of the steel sill. The weight of material and energy which is given as input for each process is for the manufacturing of 100,000 sill. As mentioned for aluminium sill, following the steps in Section 3.5.5, the CO_2e emission for each of the processes involved in the manufacturing of the steel sill is obtained.

Total CO_2e emissions from the manufacturing process of steel sill were 81.92 kgs.

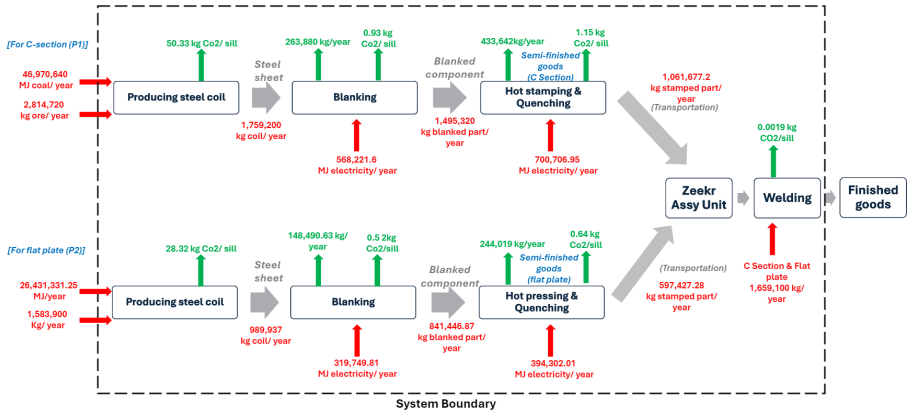

Figure 4.16: Inputs and output values from each production step considered in the making of steel sill

After performing LCI analysis on both the aluminium and the steel sill, major CO_2e emissions were from the process of manufacturing materials, while processes like stamping and extrusion did not contribute significantly to the total emissions. This can be noted in Figure 4.17, which compares the CO_2e emissions of both steel sill and aluminium sill.

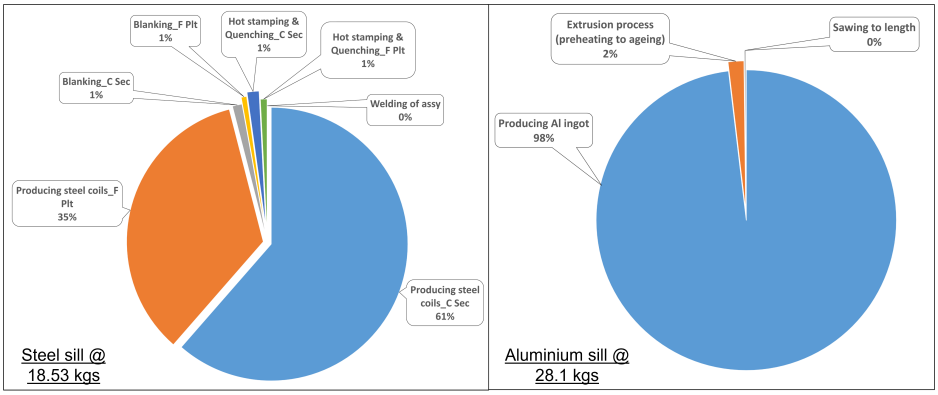

Figure 4.17: Analysis of the contribution of each manufacturing process to CO_2e emissions: Current (steel) sill v/s redesigned (aluminium) sill

The pie chart on the left is of steel sill weighing 18.53 kg. The major contributors to the CO_2e emissions during the manufacturing of steel sill was the production of steel coil for the C-section and for the flat plate, together accounting for 96% of the total CO_2e emission. While only 4% of the emissions were from downstream processes such as blanking, heating, etc.

Similar results were observed for the manufacturing of aluminium sill too (pie chart on right), where it was observed that the production of aluminium billets accounted for 98% of the total CO_2e produced from the process and the remaining 2% was a function of the extrusion process.

Phase 2

The objective of Phase 2 was to perform a comparative study of CO_2e emissions from the current and redesigned CMS. In this phase, the CMS (comprising a bumper and two crash boxes) was redesigned from aluminium to steel. Subsequently, an LCA study was conducted to analyze the impact of respective manufacturing processes on CO_2e emissions. The findings of LCA from Phase 2 of the thesis are outlined below.

4.4 Phase 2: Current CMS- aluminium

A. Qualitative study

To reiterate the part-material-manufacturing process matrix and quantity off used for the current CMS are as follows;

- One bumper with aluminium 7073 T-6 produced by extrusion process
- Two crash boxes with aluminium 6063 T-6 produced by extrusion process

Benchmark values of the current CMS are tabulated in Table 4.11. As stated, the values are the result of the interviews that were carried out with CAD and CAE engineers at Zeekr.

Table 4.11: Aluminium CMS benchmarking values against performance parameters

Parameter	Units	Benchmarked value	Ideal criteria for redesigning
Energy absorption, W_e	kJ	18.19	$W_{e,redesigned} \geq W_{e,current}$
Peak load, P_{max}	kN	189.98 @ 21.2mm	$P_{max} \simeq 200$
Weight, m_{CMS}	kg	10.32	$m_{CMS,redesigned} \leq m_{CMS,current}$
Eq. CO_2 emissions, CO_2e	kg	-	$CO_2e_{redesigned} \leq CO_2e_{current}$
Weight, m_{bumper}	kg	8.1	$m_{bumper,redesigned} \leq m_{bumper,current}$
Weight (of 1), $m_{crashbox}$	kg	1.11	$m_{crashbox,redesigned} \leq m_{crashbox,current}$

Table 4.12 is an excerpt from the previous table to highlight the performance parameters of the current CMS that will be compared against the redesigned CMS. Only the equivalent CO_2e emission's benchmark value is omitted as this particular value was part of the quantitative study and was determined in the following sections.

Table 4.12: Benchmark values of current CMS with 7003 T-6 (for bumper) and 6063 T-7 (for crash boxes) material

Concept	Concept descp.	Int. Peak load, kN	Energy absorbed, kJ	Weight, kg
Baseline	-	189.98 @ 21mm	18.19	10.32 [8.1+(2*1.11)]

Figure 4.18 is a representation of the current CMS's energy absorption capacity depicted using the load v/s distance plot. A set of points was provided, derived from interviewing the CAE engineer for benchmarking the current CMS. These points were constructed into a plot by the authors to facilitate better understanding.

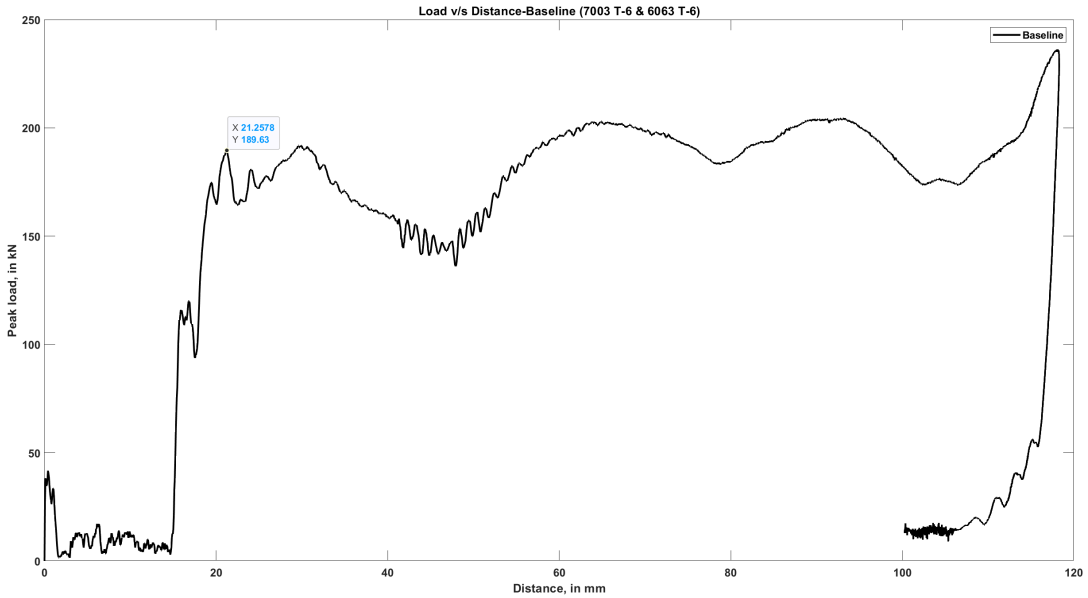

Figure 4.18: Plot depicting initial peak load against collapse distance for current design

Although the plot in Figure 4.18 represents the deformation of both the crash box and bumper, the energy absorption primarily depends on the crash box. Therefore, analyzing the current and redesigned bumper beams separately was necessary to ensure their performance is comparable.

B. Quantitative study

The current bumper was analysed with a '3-point-bending' load case setup, the performance parameters of which were benchmarked by simulating in Abaqus for the capability to endure peak load. The peak load registered at 32.5kN, at which the bumper beam showed an intrusion of about 17.6mm. Furthermore, Figures 4.19 and 4.20 are snippets from Abaqus illustrating loading conditions and peak load plots.

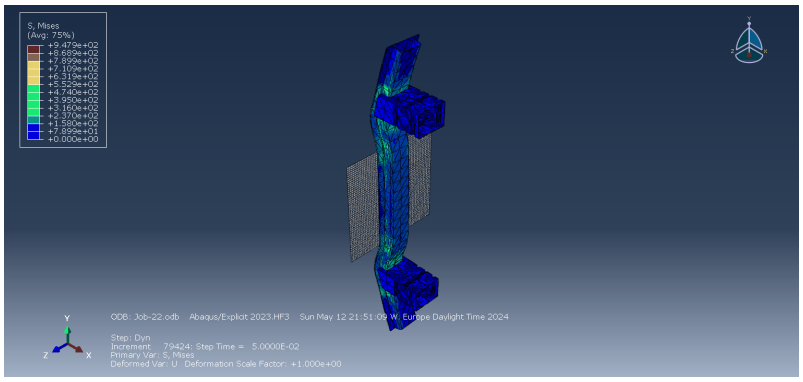

Figure 4.19: Aluminium (current) bumper's loading condition in Abaqus

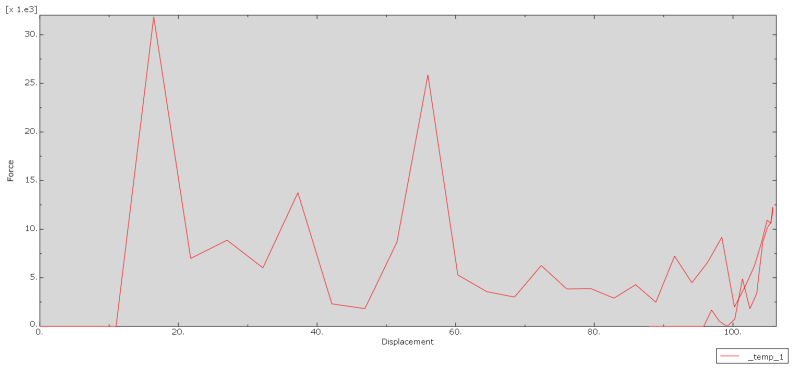

Figure 4.20: Aluminium (current) bumper's energy curve plot

4.5 Phase 2: Redesigned CMS- steel

To reiterate the part-material-manufacturing process matrix and quantity off used for the redesigned CMS are as follows;

- One bumper with DP 800 steel produced with stamping process
- Two crash boxes with DP 800 steel produced with stamping process

CAD modelling and CAE simulations

C. Quantitative study

To ensure that the 'redesigned' CMS (steel stamped) performs on equal par with the current CMS (aluminium extruded), the performance parameters of Table 4.12 had to be met. Given this, 8 crash box concepts were generated in total. DP 800 with 'M design w bead,t=1.5mm' crash box was then finalized to be a part of the redesigned steel stamped CMS.

The concepts and their descriptions along with their performance parameter values are tabulated in Table 4.13.

Table 4.13: Assessing performance parameters for redesigned steel stamped CMS (with DP 800 material). *All values correspond to one crash box only*

Concept	Int. Peak load, kN	Energy absorbed, kJ	Weight, kgs
DP 800			
Box design,t=2.7mm	201.40 @ 32.5mm	20.34	12.78 [9.06+(2*1.86)]
Box design,t=1.5mm	77.73 @ 27.7mm	14.72	12.0 [9.06+(2*1.47)]
M design,t=2.5mm	344.48 @ 30.5	19.37	12.7 [9.06+(2*1.82)]
M design,t=2mm	243.60 @ 28.6mm	19.52	12.24 [9.06+(2*1.59)]
M design w bead,t=2mm	272.87 @ 30.6mm	19.49	12.28 [9.06+(2*1.61)]
M design w bead,t=1.5mm	189.72 @ 30mm	19.44	11.96 [9.06+(2*1.45)]

It is to be noted that unlike for crash box, only one bumper design was generated (weighing 9.06 kgs) and the same was paired up with 8 crash box designs for analysis in LS Dyna. This bumper was modified until it met the peak load-bearing capacity of the current bumper design, i.e. 32.5kN. Figure 4.21 shows that the redesigned bumper (with DP800 material) also has a peak load bearing capacity of about 31.5kN but at which point the beam showed an intrusion of about 22.5mm.

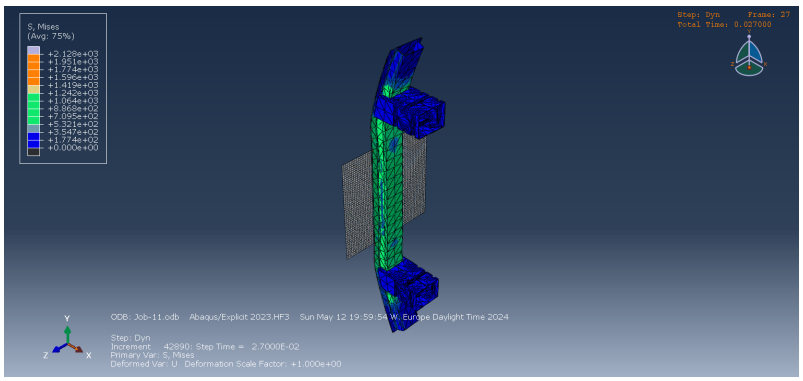

Figure 4.21: Steel (redesigned) bumper's loading condition in Abaqus

Figure 4.22 is a snippet illustrating the loading condition of the redesigned bumper in Abaqus while Figure 4.23 demonstrates CAD model of the redesigned bumper beam in different views.

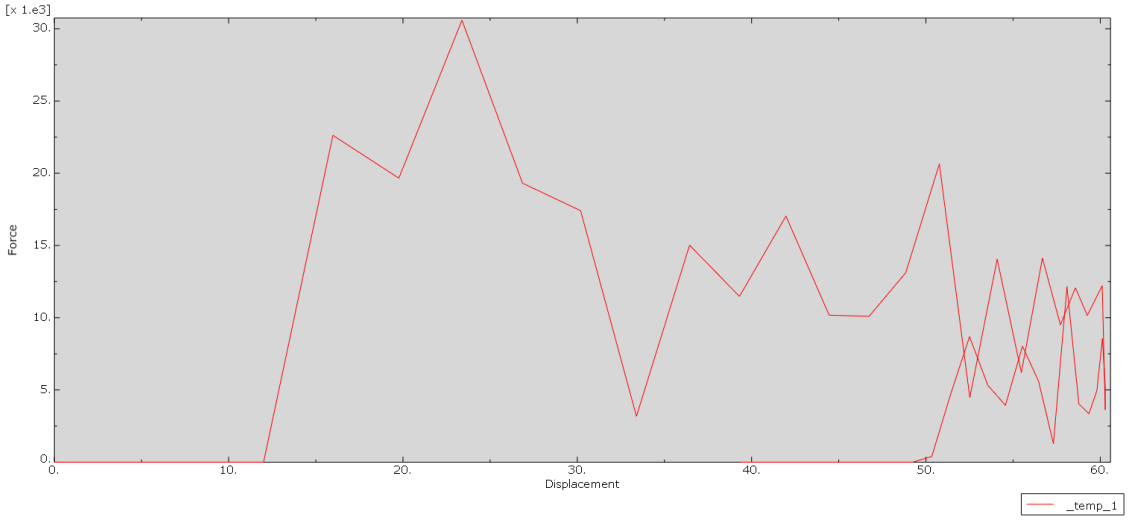

Figure 4.22: Steel (redesigned) bumper's energy curve plot

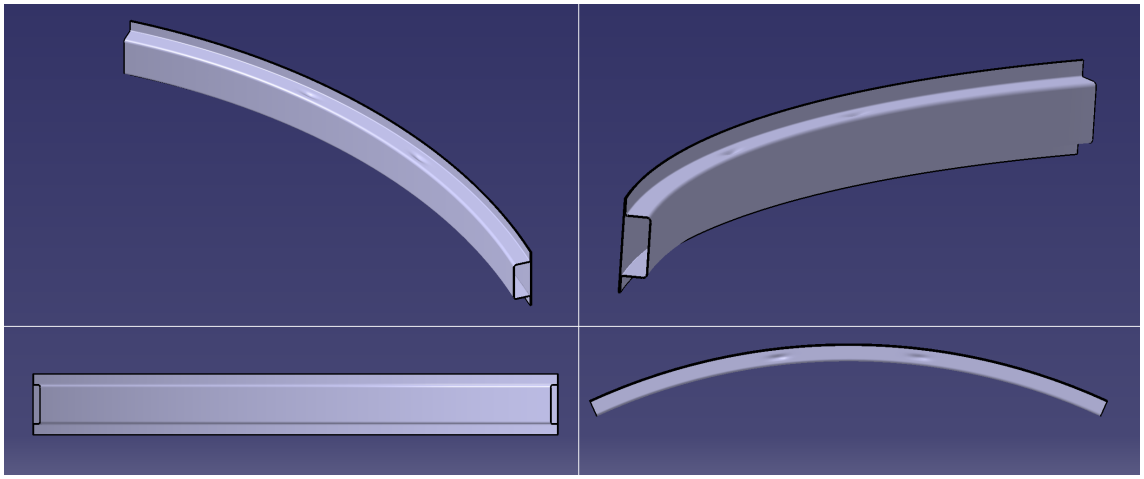

Figure 4.23: Different views of redesigned bumper: Steel stamped

The crash boxes were modelled in 3 different designs which differed geometrically with the major difference being the trigger points: M design with bead (Figure 4.24) was the design which helped meet the performance of the current CMS. Furthermore, these designs were varied in cross-section thickness, thereby generating 8 crash box designs.

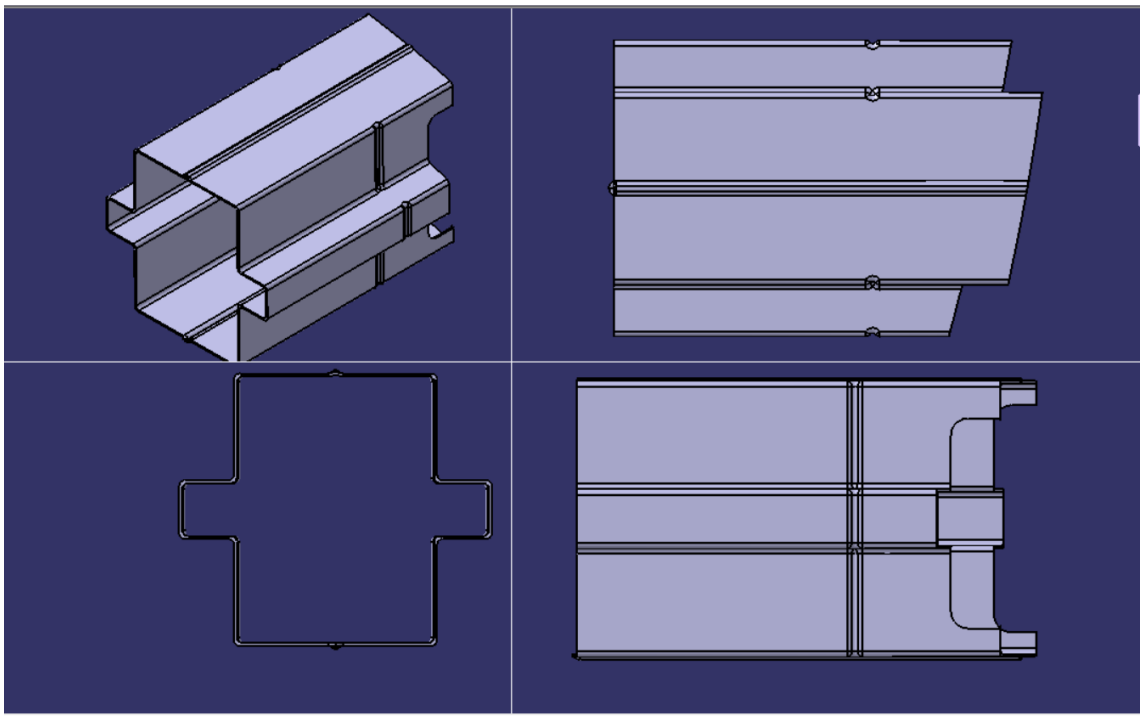

Figure 4.24: Various views of steel M bead design crash box

With the bumper and crash box designs ready, the CMS was ready to be analysed in LS Dyna. Figures 4.25 depict the force-displacement diagram for the CMSs simulated in LS Dyna with DP 800 material. Trailing Figure 4.26 illustrates various views of redesigned CMS. The chosen redesigned CMS is 'M design w bead-1.5mm' or the yellow curve as it closely resembles the baseline, i.e. black cruve.

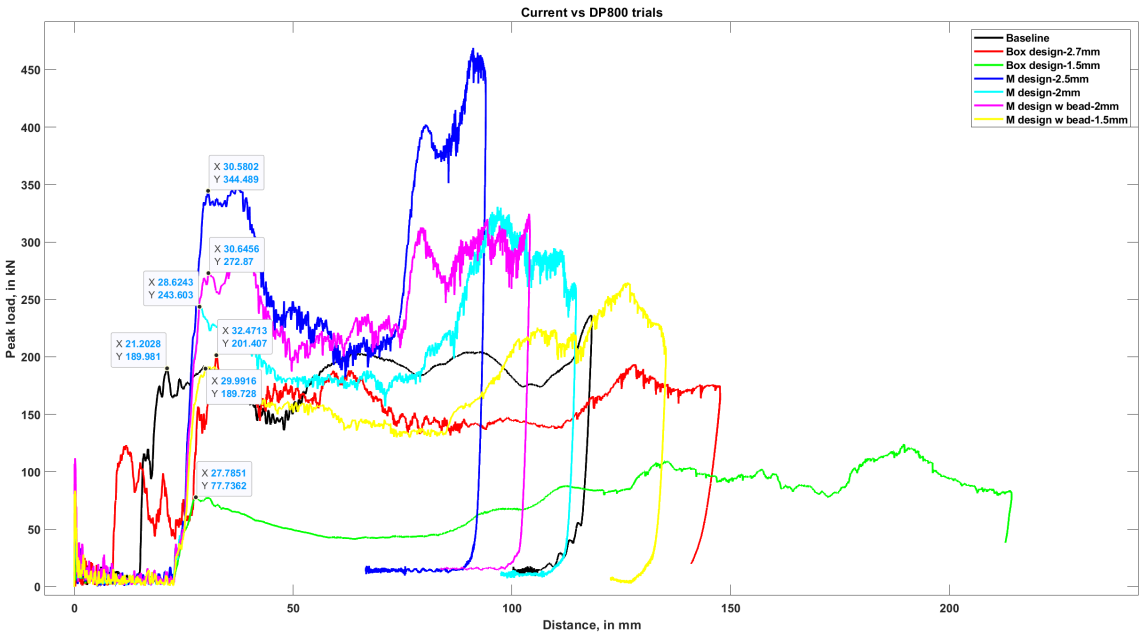

Figure 4.25: Force v/s distance plot for redesigned CMS with DP800 material

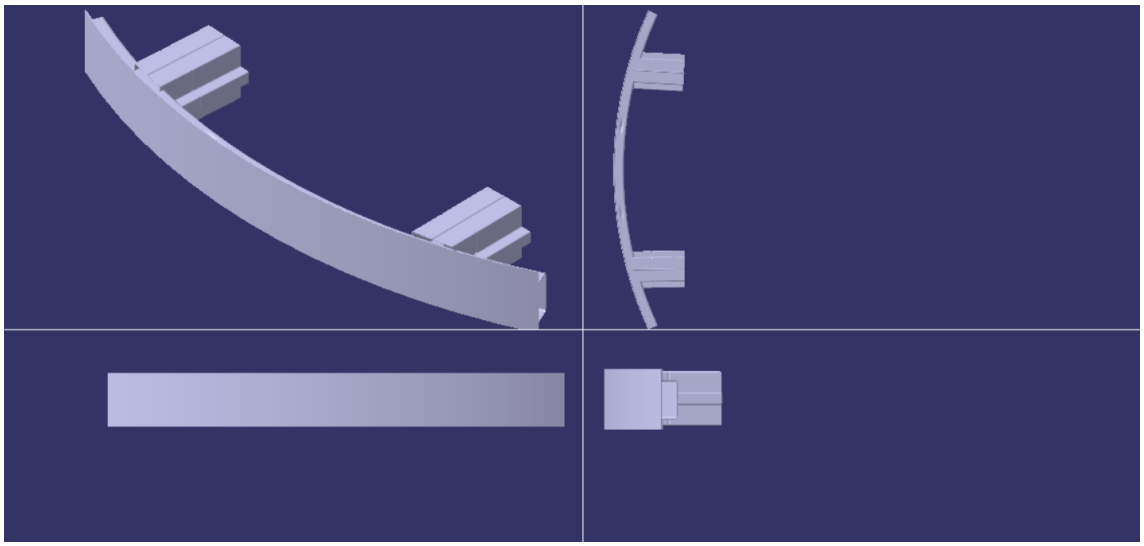

Figure 4.26: Various views of redesigned steel CMS with M design with bead crash box

Finally, Table 4.14 tabulates the performance parameters of redesigned CMS.

Table 4.14: Performance parameter values of redesigned CMS with DP 800 steel

Concept	Concept descp.	Int. Peak load, kN	Energy absorbed, kJ	Weight, kg
Redesigned	-	189.73 @ 30mm	19	11.96 [9.06+(2*1.45)]

4.6 Phase 2: Life cycle assessment

A. Quantitative study

Using datasets, system boundaries, process flows and methods established under Section 3.6.3, the results of the current and redesigned LCA are presented in this section. Modelling and solving all the models under Sub-section 3.6.3, generated results of the LCA study for the current and redesigned CMS.

4.6.1 Current CMS- aluminium

Figure 4.27 illustrates the mass flow and corresponding CO_2 emissions from each manufacturing unit process involved in the production of an aluminium CMS (refer Figure A.2 for sankey diagram).

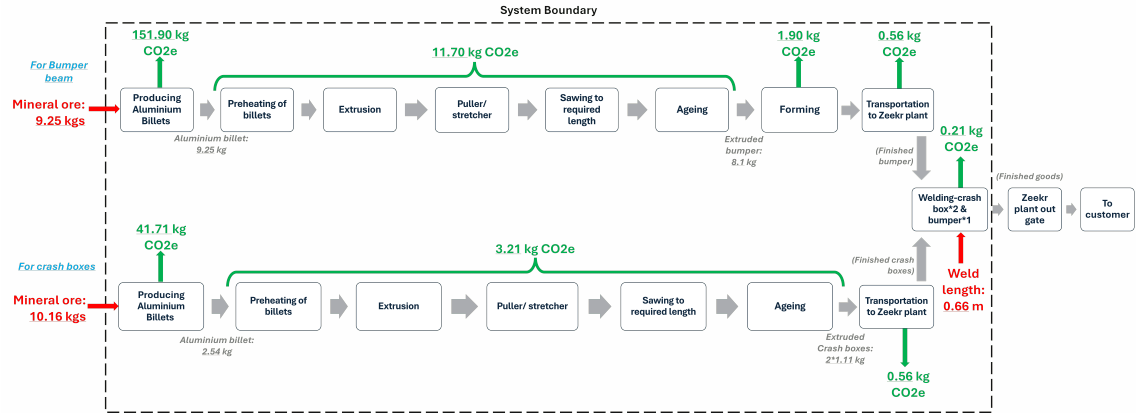

Figure 4.27: Process flow for current CMS with mass flow and CO_2e emissions for each unit process

4.6.2 Redesigned CMS- steel

Figure 4.28 depicts the mass flow and equivalent CO_2 emissions from each manufacturing unit process involved in making an aluminium CMS (refer Figure A.3 for sankey diagram).

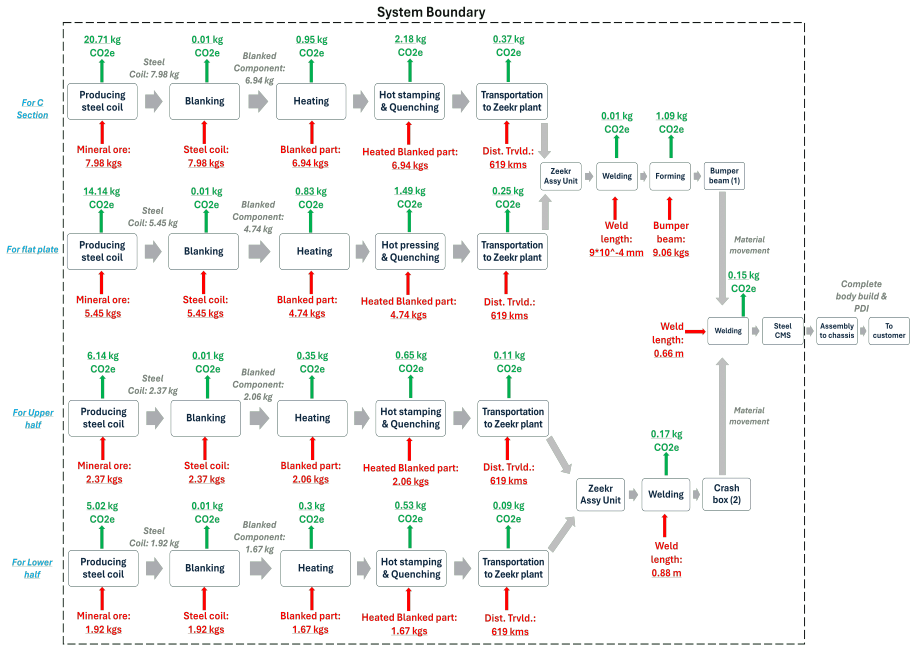

Figure 4.28: Process flow for redesigned CMS with mass flow and CO_2e emissions for each unit process

Figure 4.29 compares the CO_2e emissions (in weight percentage) from current and redesigned CMS. Furthermore, Table 4.15 shows a comparison of total emissions in kgs.

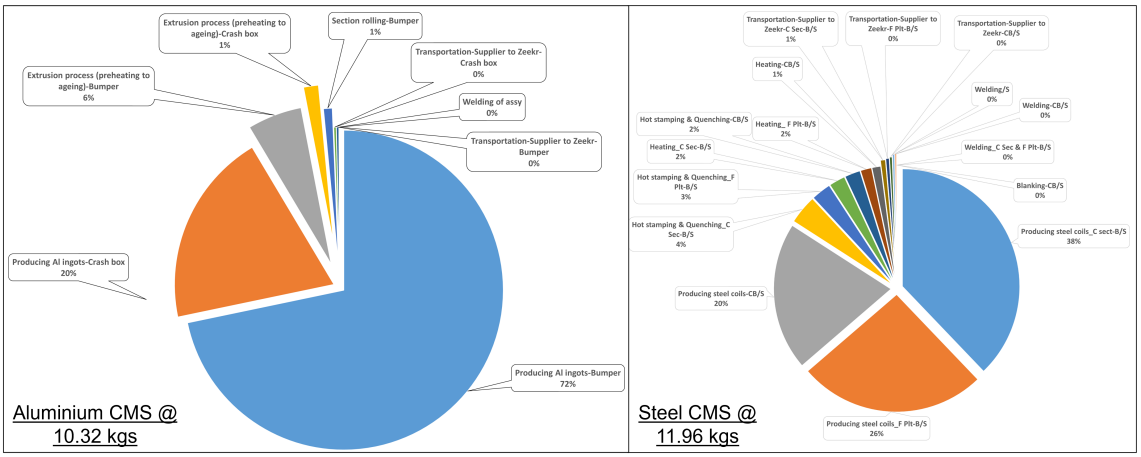

Figure 4.29: Analysis of the contribution of each manufacturing process to CO_2e emissions: Current (aluminium) CMS v/s redesigned (steel) CMS

CMS version	Weight, kgs	Total CO_2e, kgs	Major contributor
Current (Al)	10.32	211.78	Producing al ingots @ 92%
Redesigned (Steel)	11.96	54.73	Producing steel coils @ 84%

Table 4.15: Attributes comparison matrix of current and redesigned CMS with its major contributors

5
Discussion

This chapter presents and discusses the methods used, answers to the research questions, the research gap addressed, quality of research, research related to previous work, limitations of this thesis and finally the future work required.

5.1 Literature study

As mentioned in Section 3.4.1, the literature study included articles and scientific papers without any restrictions on the publication date. This approach was necessary because there were few papers focused on buckling theoretical calculations, so searching without date restrictions provided the best chance of finding useful articles. Most of the articles and papers concentrated on FEM-based buckling analysis rather than theoretical calculations, this could be because of not using the right keywords.

There was plenty of data available for bending of beam problems and LCA. For the LCI analysis, all the data gathered came from the literature study (see Tables 4.9 and 4.10). Each author had a different approach to the required data, making it difficult to choose the correct data. Therefore, keywords from specific literature were used to search for similar papers and articles, and reviewing the references in certain literature led to other sources that were more useful for this thesis.

R.K. Bansal's (2009) work significantly informed the theoretical calculations of the sill and the general analysis of beams under load. The approach outlined in Section 3.5.1 was substantially guided by this literature study, which extensively covers crash mechanics and related topics, particularly from the standpoint of numerical solutions.

5.2 Qualitative study

The qualitative study for this thesis involved interviews with different stakeholders and was divided into two categories: internal stakeholders (engineers at Zeekr Technology Europe) and external stakeholders (professors at Chalmers University of Technology). The purpose of interviewing the internal stakeholders was to understand the methods used in the company and to gain insights on how to improve

the results obtained during the thesis. Interviews with the external stakeholders aimed to assess whether the problem-solving approaches and concepts were appropriate from an academic standpoint and whether proper research techniques were employed.

The internal stakeholders consisted of individuals with significant industrial experience and a thorough understanding of the thesis topic, who had been part of the company for a considerable time and could provide the necessary guidance to conclude the thesis successfully. The external stakeholders were professors from previous courses who had extensive and varied experience related to the thesis topic. Information obtained from both internal and external stakeholders complemented each other's knowledge, helping to keep the thesis on track and reach a successful conclusion.

The questions framed for the interviews were precise and addressed the specific issues needing clarification. It was ensured that all questions asked were honest and unbiased, which contributed to the successful completion of the thesis. The questions were designed to answer the three research questions of the thesis and were kept as direct as possible to avoid misinterpretation. All important points from the interviews were noted and included in the thesis after obtaining consent from the interviewees.

Although the qualitative study in this thesis provided a roadmap for navigating lesser-known areas, such as the placement and design of trigger points, inputs for Phase 1 LCI, validation of theoretical calculations of the sill, and benchmarking performance parameters for Phase 2; the quantitative study formed the crux of this thesis. The literature study and qualitative study served as supporting pillars for conducting the quantitative studies.

5.3 Quantitative study

The quantitative study in this thesis integrates theoretical calculation, CAD modelling, simulations, and LCA. The quantitative study formed the crux of this thesis. Initially, theoretical calculations were conducted to identify the attributes affecting performance parameters. Based on these calculations, models were created with careful consideration of dimensional attributes. Subsequently, simulations were performed to correlate the values obtained from the theoretical calculations with the simulation results. These three steps—theoretical calculation, modelling, and simulation are essential to conducting the LCA. This sequence ensures that the part being studied meets the performance parameters, allowing for a comprehensive LCA.

The data gathered from literature and qualitative methods proved invaluable in performing the quantitative study. The combination of all three studies: literature review, qualitative methods, and quantitative analysis was necessary to answer the three research questions of the thesis effectively.

5.4 Addressing research questions

The thesis centred around addressing the following three research questions.

5.4.1 Research question: 1

How can the current parts be redesigned when different materials and processes are considered?

In phase 1, the existing sill and crash box design were benchmarked using steel and aluminium. To make a part sustainable, material change can have a huge impact on the sustainability of the product. After the material change, the parts were redesigned to maintain the expected performance. The current sill design used PHS, known for its fully martensitic microstructure, which makes it exceptionally hard with very high yield and ultimate strength. This property significantly reduces deflection/ intrusion during side crashes.

According to the formula of deflection (Eq. 3.13), deflection or intrusion depends on the material's Young's Modulus and the beam's moment of inertia (MOI), which is influenced by the beam's cross-section. Choosing the optimal beam cross-section can minimize deflection. The term beam refers to the sill as it depicts a simply supported beam.

The redesign of the current sill utilized aluminium 7108-T6 and 7003-T6 due to their high tensile strength from precipitation hardening and satisfactory extrudability. Interviews indicated that 7003-T6 offers superior extrudability and availability compared to 7108-T6, leading to its selection for the redesigned part. It is important to note that aluminium alloys have a lower Young's modulus compared to steel.

Referring back to the deflection formula in Eq. 3.13, Young's modulus is inversely proportional to deflection. Thus, aluminium's lower Young's modulus increases deflection values. The only controllable parameter for deflection is the MOI, which depends on the beam's cross-sectional design.

The current crash box design uses 6063 T-7 aluminium alloy, characterized by its fine grain structure and evenly dispersed precipitates, which enhance energy absorption and deformation under loading. This alloy is also easily extruded. According to the formulas in Section 3.5.3, the critical stress, collapse stress, and peak load values for the current design were benchmarked. Young's modulus and the thickness of the crash box directly affect these parameters. Table 4.8 provides the values for critical stress, collapse stress, and peak load for the 6063 T-7 aluminium crash box.

The crash box was redesigned using DP800 material, where DP stands for 'dual phase.' This material's microstructure consists of soft ferrite and very hard martensite phases. During deformation, strain concentrates in the soft ferrite phase, resulting in adequate ductility and energy absorption.

Young's modulus of DP800 is significantly higher than that of aluminium. This higher Young's modulus allows for a reduction in the crash box thickness while meeting the performance values of the current design. Table 4.7 shows the variation in thickness for DP800 and the corresponding values for critical stress, collapse stress, and peak loads. The primary goal was to achieve similar peak load values for both the steel and aluminium crash boxes. The crash box thickness was reduced from 2.7mm to 1.5mm when the material was changed from aluminium to steel.

In Phase 2, the focus was on the CMS, which comprises a bumper beam and two crash boxes. The current design utilized aluminium 7003 T-6 for the bumper beam and aluminium 6063 T-7 for the crash box.

Building on insights from Phase 1, the redesigned steel crash box using DP800 maintained the same thickness while undergoing design modifications. Phase 2 addressed parameters such as initial peak force and crash energy absorption. DP800 steel was chosen for both the crash box and bumper beam redesigns due to its deformation capability and energy absorption characteristics. The bumper beam thickness was adjusted to achieve a comparable initial peak force to that of the aluminium 7003 T-6 bumper beam.

The peak load and performance of the redesigned DP800 steel crash box were aligned with those of the current aluminium 6063 T-7 crash box after design adjustments and incorporating triggers. Both aluminium and steel crash boxes exhibited a peak load capacity of 189 kN and similar energy absorption. The steel CMS achieved its peak load slightly later than the aluminium CMS, suggesting potential for improvement in CMS design.

This study demonstrates the potential for redesigning components by selecting appropriate materials and understanding their behaviour. Effective solutions require not only understanding material properties but also modifying part geometry and design accordingly.

5.4.2 Research question: 2

What essential parameters must be met to retain the same performance of the current part?

A total of 9 performance parameters collectively for sill, crash box and CMS were identified. An ideal criteria for the same was set, based on Quantitative and Qualitative studies. The same are tabulated in Table 3.1.

Values of the redesigned part had to be weighed against parameters enlisted in Table 3.1, as these were essentially the parameters that had to be retained.

In Phase 1, the study of two parts (sill and crash box) was carried out. By employing MCDA (see Section 4.1.1), a conclusion was drawn as to which dimension was most dominantly contributing towards maintaining performance parameters when compared with the current sill.

As 36 attributes of theoretical stress and deflection calculations were discussed and weighed against Ixx and N.A., it can be said with certainty that almost all parameters were included in the MCDA study. The dimensions d1, d2, d3, and d6 (parameterizable) hold significance. However, attributes y1, y4, y5, and y6 exhibit even greater importance. Further analysis revealed that y1, y4, y5, and y6 are primarily dependent on one dimension, namely d6.
With this, it was established that d6, i.e. farthest-most fibre from the point of load application was the most essential parameter to control performance parameters of sill.

In summary, for the current sill design and the redesigned sill, the bottommost fibre was identified as an essential parameter that required focused attention to maintain the necessary performance specifications.

In the crash box, due to its fairly simple cross-section and geometry, there weren't as many attributes as compared to the sill. The only attribute that was parametrizable was the cross-section thickness.

Hence, owning to geometrical and packaging constraints, it was established that based on the choice of material and its grade, only thickness was the parameter that had a significant impact on performance parameters.

It has to be noted here that as the Phase 1 crash box was simplified, the trigger points were not modelled and analysed. Consequently, this was a limitation in the essential parameter study of the crash box in Phase 1.

In contrast to Phase 1, the benchmark parameters were easily available during Phase 2. With an understanding of the essential parameters for each component, the redesign process of the current CMS can be started.

In Phase 2, both the thickness and trigger points of crash boxes were established as essential attributes that affect performance parameters. This can be clearly observed in Figure 4.25.

The design for the steel crash box went through multiple changes to obtain a peak load similar to the aluminium crash box. The design changes were guided by the CAE engineers and design engineers. The M bead designs turned out to be the most

effective, a trigger was introduced in the design to ensure efficient energy absorption and achieve the peak load at the location of the bead. M bead design is made of two steel stamped parts welded together.

The distance at which peak loads were observed was solely dependent on the placement of trigger points. The farther the trigger points were positioned from the bumper, the greater the delay in absorbing the initial peak load. This effect is undesirable as the delay would imply that the impact load is being taken up by the rest of the BIW structure and in turn, passengers have to face the grunt of this impact.

Furthermore, the same Figure 4.29 observed that by increasing the thickness of the cross-section by 0.5mm, resulted in a drastic increase of initial load-bearing capacity. For instance, consider the initial peak load of M design w bead-2mm (purple line) and M design bead-1.5mm (yellow line); although the initial peak load was observed at the same instance, i.e. nearly after a collapse distance of 30mm, the peak load reading difference was nearly 82kN.

On the other hand, the energy absorbed, which is practically represented by the area under the respective curve, was theoretically approximately 18.81 kJ on average per crash box. The margin of deviation from the average energy absorbed was found to be below 8% for each concept, except for the concept 'Box design,t=1.5mm. Therefore, it can be established that all designs, with the exception of the Box design (t=1.5mm), will perform equally well, concerning the energy absorption parameter.

The inclusion of two materials, 22MnB5 and DP800 in Table 4.13, aimed to assess the potential of using 22MnB5 instead of seeking new materials, given its existing presence in Zeekr's portfolio. However, Table 4.13 indicates otherwise. The average initial peak load and energy absorption values for the three 22MnB5 concepts were collectively lower than those for the six DP800 concepts under discussion. Therefore, DP800 and its concepts establish a solid foundation for the performance parameters of the steel CMS.

However, Phase 2 was conducted to compare and study the CO_2e emissions generated by the current and redesigned CMS. Therefore, the case study of essential parameters would be considered unnecessary. Nevertheless, the insights and relationships developed in Phase 1 played a crucial role in smoothly and confidently advancing Phase 2.

5.4.3 Research question: 3

Which attributes affect the CO_2 emissions of these two parts, i.e. redesigned or current and why?

The LCI analysis of the current and redesigned sill was carried out theoretically, by establishing empirical relations and equations (see Section 3.5.5). Figure 4.17 illustrates that the production of raw material necessary for the parts, be it steel or aluminium, significantly impacts CO_2e emissions.

Over 80% of emissions in both cases stem from raw material production, primarily due to the energy source utilized in producing the said raw material, namely bituminous coal. Hence, it can be concluded that raw material production and the energy used to produce this raw material directly impact the Global Warming Potential, i.e. CO_2e emissions. Furthermore, along with raw material production and its energy source, two more indirect essential parameters were identified during the study; ore-to-mineral ratio and scrap percentage.

The ore-to-mineral ratio was a literature study based value (refer Tables 4.9 and 4.10). Any amount of changes in design would not affect this ratio as such values have to be accepted as axioms. However, the scrap percentage can be conditioned by incorporating geometrical changes. Lower scrap percentages would require lower input material, thereby generating lower CO_2e emissions. Albeit, the values chosen for scrap percentages were derived from literature since this data was not readily available with stakeholder.

To summarize, attributes that affect the CO_2e emissions of the re-designed and current sill were raw material production and its energy source, followed by an indirect contribution of ore-to-mineral ratio and scrap percentages.

The LCA of both the current and redesigned CMS was performed using OpenLCA software, guided by empirical relationships and equations. Consistent with Phase 1 findings, the primary source of emissions continues to be raw material production. Figure 4.29 illustrates that despite significant manufacturing processes, emissions from raw material production contribute more than 90% to the total emissions in the aluminium CMS and approximately 80% in the steel CMS.

Hence, it was established that irrespective of the concern regarding the appropriate proxy dataset employed, the major carbon dioxide emission factor is related to raw material production and its energy source. Furthermore, from Table 4.15 it can be observed that the current CMS emits about 4 times more CO_2e emissions than the redesigned CMS, even though the redesigned CMS is 14% heavier than current (aluminium) CMS.

5.5 Research gap addressed

Exploration of research gaps is crucial to finding new questions worth investigating. This section into such gaps regarding sustainability, mechanics of bending and buckling.

After investing considerable effort in researching the aforementioned topics, it's evident that there remain areas where definitive answers elude us. These uncertainties serve as inspiration to delve deeper, posing further questions and exploring additional ideas.

1. Despite the efforts in researching the crash behaviour of a crash box, no literature was found that included theoretical calculations for the buckling of a square/ rectangular crash box. There was a wealth of data concerning stresses and peak loads gathered from FEA simulations for a crash box, but regrettably, none delved into the underlying theory behind these findings. This thesis tries to fill this gap by working on finding the stresses and max load-bearing capacity of the crash box/ a buckling column through theoretical calculations.

2. From the literature survey on LCA, no literature was found which had built an empirical parametric equation system where values for a certain product could be plugged in and the total CO_2e emission for that particular product can be found. This thesis fills that gap by building a set of equations for a car sill, where data can be plugged in and the total CO_2e emissions for that part can be found. This comes into play when the stakeholder decides to compare two or more sills with varying designs and materials.

This thesis primarily serves as a guide for addressing the specific problem faced by the stakeholder. The results obtained are tailored to the stakeholder's needs and are not intended to apply to other products. However, the methodology outlined can be used as a reference for solving numerical problems related to buckling and bending.

The equation system developed for calculating total CO_2e emissions is versatile and can be adapted for various products. Nonetheless, it considers only the steps relevant to this thesis. Readers can follow the same method and modify it to suit their specific requirements.

5.6 Research quality

Research quality is essential to understand and reflect on various aspects of the research process and its outcomes.

Conducting research for this thesis on sustainability study on body structure design has been a source of learning and growth while being both challenging and rewarding. This thesis adopted a convergent mixed method approach both qualitative (interviews) and quantitative data, along with a literature study.

For data collection, the quality of quantitative data gathered was validated by cross-referencing if the papers, articles or websites were trustworthy and if the information from these had been cited before. One of the challenges faced during data collection was making use of the wrong combination of keywords to search for data which resulted in papers and articles, less suitable for this research. This was mitigated later by using the right combination of keywords, which led to better data being collected.

In this thesis, the authors adhered to strict ethical standards by incorporating proper citation practices and complete honesty of data. All of the sources in this thesis are properly cited to ensure the original authors get credit for their work and data. One of the challenges was incorporating a balance for the way the authors approached solving theoretical problems as every author had their method of solving questions and sometimes the approach they used was contradictory.

Finally, through the iterative process of revising and incorporating feedback from supervisors, clarity and consistency in this thesis were achieved. This process ensured the quality of the presentation and the clarity of the findings communicated effectively.

Reflecting on the thesis journey, challenges encountered regarding ethical dilemmas, data collection and methodological approaches have been instrumental in enhancing personal and professional growth. The whole process of research helped authors enhance their skills and provided them with invaluable insights which contributed to their development as researchers.

5.7 Research relation to previous work

This section provides an overview of how this thesis contributes and draws inspiration from the existing literature. Through a diligent examination of the available literature, this thesis seeks to humbly add to the ongoing academic work. Going through the previous literature and findings helps solidify the understanding of and around the topic of research.

Despite thorough research, several gaps remain. Notably, while there is literature which focuses on the FEA method of solving problems, especially related to buckling, there is almost none which explains the theoretical method of solving these buckling problems. Similarly, there is literature on how to solve an LCA problem theoretically, this thesis's contribution is the development of a parametric equation system where users can plug in values to arrive at the answer. This thesis aims to fill gaps like these. However, as with any study, some questions can still be answered or further refined.

By delving into existing literature, this thesis will do justice by incorporating crucial aspects from the previous literature while simultaneously providing new insights that are relevant to this field of study.

5.8 Limitations

While this thesis has contributed crucial insights into the topics of sustainability of body structures and mechanics, it is important to acknowledge its fundamental

limitations. Understanding the limitations is important for precisely interpreting the results and recognising the limits of this thesis's applicability.

In this section, the intention is to discuss the key limitations encountered during this thesis.

1. In Phase 1, the steel sill was redesigned into an aluminium sill. However, the aluminium sill experienced a weight increase of approximately 52% (from 18.53 to 28.1 kg). Although many premium OEMs, such as Ford, Lotus, and BMW, still utilize aluminium sills despite weight being a primary consideration in vehicle manufacturing. This conflicting result is primarily due to the considerations and objectives of Phase 1, where the goal was to study the effect of attributes on performance parameters rather than designing a sill for optimal performance.

2. When the beams were simulated in Ansys, the max stress appeared at the supports. Here, the supports were defined as a line instead of defining over an area. For this reason, 'artificial stresses' were generated at these fixed supports. This could have been avoided by defining the supports as they would appear in real-world conditions.

3. When calculating the deflection and stresses for the sill, the sill was considered to be the part which is directly hit by the pole, but in reality, there are few parts in front of the sill which are in contact with the pole in real life. These components in front of the sill were not considered.

4. In Phase 2 of the thesis, the simulation values of the CMS provide the total force-displacement behaviour which includes the crash box and the bumper beam. The force-displacement behaviour of the bumper beam and the crash box separately is not studied.

5. Aluminium ingots are considered for LCIA in Phase 2 instead of aluminium billets. This was the case as the Ecoinvent database used did not provide us with an option to opt for aluminium billets. This might affect the overall result of the LCA.

6. Considering the actual scrap percentages from the process was an option, but instead, scrap values were derived from literature study.

7. In Phase 1 of the LCI, only the processes involving mass change were taken into account. Including all the steps involved could have provided a better understanding of the impacts caused by these processes.

8. For LCIA in Phase 2, datasets predefined in the Ecoinvent database have been used. This particular database does not contain all the manufacturing processes which were required, in this case, proxies or a predefined process were

used, which is close to the data set required. This may affect LCA results.

9. The design of the crash box and bumper (CMS) can be optimized further. For instance, the initial peak load for baseline starts at 21mm but for all the crash box designs (in Phase 2), the initial peak load was observed after a delay of 9mm collapse distance (at 30mm).

5.9 Future work

Although the thesis findings met the aim, there is still scope for future work on the subject.

Given a broader time frame, it's possible that the comparative LCA study could have been enriched with greater depth and detail. Instead of using proxies for unavailable processes and datasets, one could explore building case-specific processes with more detailed input and output values.

Another approach could involve looking at alternative sources for minerals and ore procurement, owing to ethical aspects. The current source of raw material was assumed from China. Given more time, it would be possible to examine how CO_2e emissions would be affected if the materials were sourced from a country with a greener energy source.

The redesigning of all components could be approached from a 'design for manufacturing' aspect, rather than it just being pragmatic. Exploring this aspect may open up new realms of possibilities to curb CO_2e emissions, due to the introduction of various factors, such as GD&T and yield rate. These factors often control the excessive use of material and hence reduce input material requirements.

6
Conclusions

The goal was to assess and compare the CO_2e emissions of BIW concepts (i.e., various designs) by redesigning current components such as sills, crash boxes, and bumpers, utilizing alternative materials listed in Table 2.1 and manufacturing processes including stamping and extrusion. Through detailed modelling in Catia V5, theoretical calculations, CAE simulations in Ansys, Abaqus, & LS Dyna, and LCA analysis in Open LCA, the aim of recommending and evaluating the CMS with lower CO_2e emissions was successfully achieved, deemed most suitable for the vehicle based on performance parameters outlined in Table 3.1.

Although the redesigned steel CMS weighs approximately 16% more than the current aluminium CMS, it emits around 74% less carbon dioxide emissions. Therefore, a detailed analysis needs to be conducted regarding the replacement of the current CMS with the redesigned CMS, considering the trade-off between weight and sustainability aspects.

Drawing from the findings of this research and reflecting on the research questions, this thesis's conclusion has highlighted several key points:

1. Increase in cross-section thickness of the farthest-most fibre from the point of load application, decreases the induced stress and deflection in sills.

2. The major contributing attributes can be identified by performing a Multi-Criteria Decision Analysis. This approach was established for the sill design in Phase 1.

3. The increase in thickness of the crash box significantly increased the critical and collapse stresses and peak load-bearing capacity of the crash boxes.

4. The CAE simulated results and theoretically calculated values of collapse stress and deflection for the steel and aluminium crash boxes and sill respectively, were nearly identical with only a small delta value.

5. Integration of trigger points on a crash box ensures efficient impact energy absorption and stable collapse. Furthermore, the placement of these points and their geometry also play a vital role in setting an optimum peak initial load.

6. The primary attribute affecting the CO_2e emissions of any component is raw material production and its energy source, followed by the indirect contribution of ore-to-mineral ratio and scrap percentages.

7. Any manufacturing process, even with maximum yield can not significantly reduce CO_2e emissions.

8. When the same automotive BIW component is redesigned from steel to aluminium or vis-a-vis, the aluminium component is often found to have significantly higher CO_2e emissions (with respect to China dataset).

9. The research demonstrated that alternative materials and manufacturing processes can be feasibly implemented in automotive BIW structures to curb CO_2e emissions.

Finally, steel CMS demonstrates a superior sustainability index with lower CO_2e emissions compared to aluminium CMS while maintaining equivalent performance. Although the design of the steel CMS can be further improved through iterations, its integration into the vehicle reduces CO_2e emissions from the manufacturing process of the CMS by approximately 74%.

In summary, this thesis concludes that alternative materials and manufacturing techniques hold promise for enhancing sustainability in automotive BIW structures, with careful consideration of environmental impact, structural performance, and overall feasibility being crucial factors in the transition towards sustainable vehicle development.

Bibliography

[1] United Nations Department of Economic and Social Affairs (Sustainable Development) (2023), '*Goal 9, Dept. of Economic and Social Affairs*' Available at: `https://sdgs.un.org/goals/goal9` (Accessed 23 January 2024).

[2] United States Environmental Protection Agency (EPA) (2023), '*Electric & Plug-In Hybrid Electric Vehicles*' Available at: `https://www.epa.gov/greenvehicles/electric-plug-hybrid-electric-vehicles`. (Accessed 27 January 2024).

[3] David A. Sindrey.(1999), ' *Steel Bumper Systems for Passenger Cars an Light Trucks*', SAE Transactions, Vol. 108, Section 5: JOURNAL OF MATERIALS & MANUFACTURING (1999), pp. 875-883.

[4] Byjus '*What is meant by green energy? Which energy sources can be called as green energy sources and why?*' Available at: `https://byjus.com/question-answer/what-is-meant-by-green-energy-which-energy-sources-can-be-called\-as-green-energy/`. (Accessed 15 January 2024).

[5] Hydro '*High-strength aluminium for automotive applications*' Available at: `https://www.hydro.com/en/media/news/2010/high-strength-aluminium-for-automotive-applications/`. (Accessed 10 April 2024).

[6] J. C. Benedyk.(2010), '*Aluminum alloys for lightweight automotive structures*',Woodhead Publishing Series in Composites Science and Engineering 2010, Pages 79-113

[7] Cooper, H., 2015, '*Research synthesis and meta-analysis: A step-by-step approach (Vol. 2)*'. Sage publications.

[8] John W. Creswell, J. David Crewell. (2018), 'Review of Literature', *Research Design*, pp. 29-30. Sage Publication, Inc., Los Angeles (5th edition).

[9] John W. Creswell and J. David Creswell (2018) *Research Design: Qualitative, Quantitative, and Mixed Methods Approaches*. 5th ed., Los Angeles: SAGE

Publications, Inc.

[10] Dr R. K. Bansal (2010) *A Textbook of Strength of Materials*. Rvd 4th ed., New Delhi: Laxmi Publications (P) Ltd.

[11] Dr R. K. Bansal (2010) *A Textbook of Strength of Materials*, pp. 295-296 Rvd 4th ed., New Delhi: Laxmi Publications (P) Ltd.

[12] Dr R. K. Bansal (2010) *A Textbook of Strength of Materials*, pp. 515-517 Rvd 4th ed., New Delhi: Laxmi Publications (P) Ltd.

[13] Dr R. K. Bansal (2010) *A Textbook of Strength of Materials*, pp. 237-238 Rvd 4th ed., New Delhi: Laxmi Publications (P) Ltd.

[14] Dr R. K. Bansal (2010) *A Textbook of Strength of Materials*, pp. 293-297 Rvd 4th ed., New Delhi: Laxmi Publications (P) Ltd.

[15] Wikipedia contributors (2024), '*Euro NCAP*' Available at: `https://en.wikipedia.org/wiki/EuroNCAP`. (Accessed 16 Feb 2024).

[16] Rainer Hoffmann, SafetyWissen (2020), '*Oblique Pole Side Impact - Left Hand Drive (UN R135)*' Available at: `https://www.safetywissen.com/requirement/W02.u2w735779jwm0w8s9kf499\52mkorja63571269152/`. (Accessed 22 March 2024).

[17] Rainer Hoffmann, SafetyWissen (2020), '*Full Width Frontal - Left Hand Drive (UN R137)*' Available at: `https://www.safetywissen.com/requirement/W02.c2w735940r6pog4rym95388\155cku163585183481/`. (Accessed 22 March 2024).

[18] Rainer Hoffmann, SafetyWissen (2020), '*Safety Companion 2022*' Available at: `https://online.flippingbook.com/view/11872285/`. (Accessed 22 March 2024).

[19] Euro NCAP, (2015), '*EUROPEAN NEW CAR ASSESSMENT PROGRAMME (Euro NCAP) OBLIQUE POLE SIDE IMPACT TESTING PROTOCOL*', Chapter 6, pp: 17. Available at: `chrome-extension://efaidnbmnnnibpcajpcglclefindmkaj/https://cdn.euroncap.com/\media/20874/oblique-pole-side-impact-test-protocol-v702.pdf`. (Accessed 22 March 2024).

[20] '*Vehicle crashworthiness and occupant protection*', slide 9-10 Available at: `https://web.iitd.ac.in/~achawla/public_html/736/5-VEHICLE_CRASHWORTHINESS.pdf`(Accessed 22 April 2024).

[21] Euro NCAP(2020) '*Mobile progressive Deformable Barrier*' Available at: https://www.euroncap.com/en/car-safety/the-ratings-explained/adult-occupant-protection/frontal-impact/mobile-progressive-deformable-barrier/ (Accessed 23 Feb 2024).

[22] Euro NCAP(2020) '*Full Width Rigid Barrier*' Available at: https://www.euroncap.com/en/car-safety/the-ratings-explained/adult-occupant-protection/frontal-impact/full-width-rigid-barrier/ (Accessed 23 Feb 2024).

[23] Euro NCAP, (2013), '*EUROPEAN NEW CAR ASSESSMENT PROGRAMME Assessment Protocol- Adult occupant protection*', Chapter 1-3, pp: 1-6. Available at: https://cdn.euroncap.com/media/1568/euro-ncap-assessment-protocol-aop-v-60.pdf

[24] Henrikke Baumann and Anne-Marie Tillman (2012) *The Hitch Hiker's Guide to LCA*. Edition 1:7, Malmö, Sweden: Holmbergs i Malmö AB.

[25] Henrikke Baumann and Anne-Marie Tillman (2012) *The Hitch Hiker's Guide to LCA*, pp. 109. Edition 1:7, Malmö, Sweden: Holmbergs i Malmö AB.

[26] Henrikke Baumann and Anne-Marie Tillman (2012) *The Hitch Hiker's Guide to LCA*, pp. 386. Edition 1:7, Malmö, Sweden: Holmbergs i Malmö AB.

[27] Henrikke Baumann and Anne-Marie Tillman (2012) *The Hitch Hiker's Guide to LCA*, pp. 387-388. Edition 1:7, Malmö, Sweden: Holmbergs i Malmö AB.

[28] Arcelor Mittal(2020) '*Steels for hot stamping - Usibor and Ductibor*' Available at: https://automotive.arcelormittal.com/products/flat/PHS/usibor_ductibor (Accessed 04 Feb 2024).

[29] Arcelor Mittal(2020) '*Stress-Strain Curves Hot forming Steels - Usibor 1500 treated*' Available at: chrome-extension://efaidnbmnnnibpcajpcglclefindmkaj/https://automotive-b5-is.aware.be/sites/default/files/Usibor1500--3a82a9aa69487763bbbba1a960151cc0.pdf (Accessed 04 Feb 2024).

[30] Arcelor Mittal(2020) '*7108 (7108-T6) Aluminum*' Available at: https://www.makeitfrom.com/material-properties/7108-7108-T6-Aluminum (Accessed 04 Feb 2024).

[31] Arcelor Mittal(2020) '*6063-T6 Aluminum*' Available at: https://www.makeitfrom.com/material-properties/6063-T6-Aluminum (Accessed 04 Feb 2024).

[32] Arcelor Mittal(2020) '*7003-T6 Aluminum*' Available at: https://www.makeitfrom.com/material-properties/7003-T6-Aluminum (Accessed 01 Apr 2024).

[33] Euro NCAP(2020) '*Side Mobile Barrier*' Available at: https://www.euroncap.com/en/car-safety/the-ratings-explained/adult-occupant-protection/lateral-impact/side-mobile-barrier/ (Accessed 01 Apr 2024).

[34] Euro NCAP(2020) '*Side Pole*' Available at: https://www.euroncap.com/en/car-safety/the-ratings-explained/adult-occupant-protection/lateral-impact/side-pole/ (Accessed 01 Apr 2024).

[35] Milan Brozek (2015), '*RESISTANCE SPOT WELDING OF STEEL SHEETS OF DIFFERENT THICKNESS* ', pp. 76, ENGINEERING FOR RURAL DEVELOPMENT, Jelgava, 20.-22.05.2015.

[36] '*Applications-Car Body- Crash Management Systems* ', pp: 2, The Aluminium Automotive Manual (2013)

[37] John W. Creswell, J. David Crewell. (2018), 'Review of Literature', *Research Design*, Chp. 1, pp. 14-16. Sage Publication, Inc., Los Angeles (5th edition).

[38] John W. Creswell, J. David Crewell. (2018), 'Review of Literature', *Research Design*, Chp. 1, pp. 237. Sage Publication, Inc., Los Angeles (5th edition).

[39] H.F Mahmood and A. Paluszny. (2018), *Design of thin walled columns for crash energy management- their strength and mode of collapse*. SAE International

[40] What is a body in white(BIW)? '*BIW*' Available at: https://www.boronextrication.com/2009/10/19/what-is-a-body-in-white-biw/#:~:text=First%20off%2C%20BIW%20stands%20for,is%20referred%20to%20as%20BIW. (Accessed 01 Apr 2024).

[41] Sai Aditya Pradeep, Rakesh.K.Iyer, Hakan Kazan, Srikanth Pilla (2017), *Automotive applications of plastics: past, present, and future*, Pg 651-673, Appplied plastics engineering handbook(second edition)

[42] Priya Prasad, Jamel E Belwafa(2004), *Vehicle crashworthiness and occupant protection*, pp. 1-10, automotive applications committee american iron and steel institute Southfield, Michigan

[43] Dai Heng Chen(2016), *Crush Mechanics of Thin Walled Tubes*, pp. 3-4, CRC Press, Taylor and Francis group

[44] Dai Heng Chen(2016), *Crush Mechanics of Thin Walled Tubes*, pp. 91-95, CRC Press, Taylor and Francis group

[45] Wikipedia contributors (2024), '*Multiple-criteria decision analysis*' Available at: `https://en.wikipedia.org/wiki/Multiple-criteria_decision_analysis`. (Accessed 08 Apr 2024).

[46] Docol, The automotive steel '*DP800*' Available at: `https://www.ssab.com/api/sitecore/Datasheet/Get?key=385dcdc160144229aef7f2bb02836793_en` (Accessed 01 Apr 2024).

[47] DiCicco-Bloom, B., & Crabtree, B. F. (2006, 4). The qualitative research interview. Medical Education, 40(4), 314–321. doi: 10.1111/j.1365-2929.2006.02418.x

[48] Benjamin F. Crabtree, William L. Miller. (1999), *Doing Qualitative Research*. Sage Publication, Inc., California, U.S.A. (2nd edition).

[49] OPTEL '*What is Life Cycle Assessment (LCA)?*' Available at: `https://www.optelgroup.com/en/blog/what-is-a-life-cycle-assessment-lca/` (Accessed 01 Apr 2024).

[50] R.K Bansal, (1996), *Strength of materials*,pp 292-553, Laxmi Publications

[51] Misono, (1998), *United States Patent*, available at: `https://patents.google.com/patent/US4826238A/en`

[52] Yusof, Sapuan, Sultan, Jawaid, Maleque (2017), *Design and materials development of automotive crash box: a review*, available at:`https://www.elsevier.es/en-revista-cienciatecnologia-dos-materiais-226-resumen-design`

[53] Baumann, Tillman(2012), *Hitch hiker's guide to LCA*. The authors and studentlitteratur 2004.

[54] Ecochain '*What is Ecoinvent? – Meet the LCI Database*' Available at: `https://ecochain.com/blog/what-isecoinvent/#:~:text=Ecoinvent%20is%20the%20World's%20leading%20LCI%20database%20containing%20over%2017.000,resource%20extraction%20to%20waste%20management.` (Accessed 06 Apr 2024).

[55] ReCiPe '*ReCiPe-Life Cycle Assessment*' Available at: `https://pre-sustainability.com/articles/recipe/` (Accessed 06 Apr 2024).

[56] Eco-Invent '*Eco-Invent Database*' Available at: `https://ecoinvent.org/` (Accessed 13 Apr 2024).

[57] Mohamed Harhash,Moritz Kuhtz, Jonas Richter, Andreas Hornig, Maik Gude,Heinz Palkowsk (2021)'*Trigger geometry influencing the failure modes in steel/polymer/steel sandwich crashboxes: Experimental and numerical evaluation*' Available at: https://www.sciencedirect.com/science/article/pii/S0263822321000805 (Accessed 16 Apr 2024).

[58] RCAR '*RCAR*' Available at: https://rcar.org/about (Accessed 16 May 2024).

[59] Carhs, empowering engineers (2021)'*Safety Companion*',pp 100-105.

[60] Jaramporn, Theera (2021) *Modelling of aluminium profile extrusion yield: pre-cut billet size.*

[61] Halvor Kvande(2014) *The Aluminum Smelting Process and Innovative Alternative Technologies.*

[62] Efthymios Balomenos(2011) *Energy and Exergy Analysis of the Primary Aluminum Production Processes: A Review on Current and Future Sustainability.*

[63] Cabletec '*Aluminum extrusion machine*' Available at: https://www.chinacabletec.com/Product/Aluminum-extrusion-machine.html .

[64] Briganto, the precision saw '*Aluminium extrusion and sawing machine*'

[65] Energy use in US steel manufacturing '*Energy consumed for pr*' Available at: http://large.stanford.edu/courses/2016/ph240/martelaro1/

[66] Iron ore '*BHP*' Available at: https://www.bhp.com/what-we-do/products/iron-ore

[67] Qiang Dai, Jarod C. Kelly, and Amgad Elgowainy (2017), '*Update of Process Energy Requirement and Material Efficiency for Steel and Al Stamping in the GREET Model*

[68] EIain P. Flint, Julian M. Allwood, Andre Cabrera Serrenho(2019) *Scrap, carbon and cost savings from the adoption of flexible nested blanking.*

[69] Chalmers University of Technology, 2023. *Regulations for the use of AI tools in thesis work.* [online] Available at: https://www.chalmers.se/en/education/your-studies/masters-and-bachelors-thesis/regulations-for-the-use-of-ai-tools/ [Accessed 27 June 2024].

[70] ChatGPT, 2015. *Introducing ChatGPT.* [online] Available at: https://openai.com/index/chatgpt/ [Accessed 27 June 2024].

[71] Perplexity.ai, 2015. *About Perplexity.* [online] Available at: https://www.perplexity.ai/hub/about [Accessed 27 June 2024].

A
Appendix

A.1 Framework of themes for interviews

This section presents all qualitative study interview questions. Specific questions were tailored to each interviewee's competencies and expertise.

To stakeholders from Zeekr Technology Europe

Systems engineer

- Which of the designs made for beams and crash boxes are feasible for manufacturing?
- What should be the distance considered for transportation for the LCI and LCA model?
- What could be the potential material alternative that can be considered for redesigning?
- What are the process parameters that need to be included in the LCI analysis system boundary?
- What could be the potential number of cars that could be manufactured in a year?
- Are the input values that we presented to you in context to LCI of Phase 1, valid and bear resemblance with real-life scenarios at the supplier end?

CAD Engineer

- How should the CAD model be placed in Catia's global coordinate system?
- Do the presented dimensional and physical attributes accurately reflect the real-world case?

CAE Engineer

- When triggers are included in the crash box design how close/ far should these be placed from the area of impact?
- Is the simplification of the beam's cross-section valid to be used?
- Can you share the performance parameters of the current CMS for the sake of benchmarking?
- Can only stress values be considered for crash box simulation in Phase 1?
- Do the stress values obtained from the crash box simulation in Phase 1 align with the calculated values and fall within acceptable ranges?

To stakeholders from Chalmers University of Technology

- For validating the designs and selection of parameters of the beam, is the trial and error method a valid approach?
- Is the theoretical calculation method designed for sill correct?

A.2 Processes and inputs for datasets in life cycle inventory

For current CMS- aluminium extruded

Bumper beam

Process 1: Producing Al ingots/ billets

It has to be noted that the extrusion process generally requires billets as standard feedstock, though it is not uncommon to use ingots. For the sake of performing LCA with available datasets, the existing process of manufacturing aluminium ingot instead of aluminium billet was opted. Moreover, the production of ingots is often done by batch casting whereas billets are produced in a continuous casting machine. Essentially, the processes can be classified under the umbrella of casting and hence are used interchangeably in this context.

Given the knowledge of the final bumper weight and the percentage of scrap generated in each process, a reverse calculation could be performed to determine the input material needed to produce 'x' kilograms of the final bumper beam.

The dataset (GLO) for the process involved in producing Al ingot contains;

- Pre-treatment of hot metal,
- Recovery and handling of internal process scrap,
- Batching, metal treatment and casting operations,
- Homogenizing, sawing and packaging activities,
- Maintenance and repair of plant and equipment,
- Treatment of process air, liquids and solids and,
- Production of infrastructure (through rough estimate) was also added.

The output of this unit process (within dataset) is packaged aluminium ingots which are ready for transport.

Process 2: Extrusion process (preheating to ageing)

The dataset (ROW) for the process involved in the extrusion process contains steps from cutting of billet to ageing. Detailed process list are;

- Sawing of billet (to required length),
- Scalping and preheating,
- Extrusion,
- Stretching and sawing,
- Ageing and packaging,
- Amount of scrap lost in waste (balanced as primary aluminium input) and,
- Transport of the materials to the plant.

The output of this unit process (within dataset) is profile extruded aluminium bumper.

Process 3: Section rolling or forming

The dataset (ROW) for the process involved in the section rolling or forming contains;

- Heating,
- Descaling,
- Roughing, intermediate and finishing standards and,
- Hydraulic rollers.

The output of this unit process (within dataset) is a formed profile of the extruded aluminium bumper.

Following this process, the bumper beam is prepared at the supplier's facility and is now primed for transportation to the Zeekr manufacturing plant.

Process 4: Transportation- Supplier to Zeekr

Transportation is generally measured in 'tkm' which is essentially tonnes times kilometre.

The freight truck selected for transportation boasts a weight carrying capacity of 32 metric tonnes and adheres to the EURO 5 standard.

The dataset (ROW) for processes involved in transportation contains;

- OPEX,
- Production and maintenance of the truck,
- Construction of road,
- Energy use, combustion emissions and fuel consumption.

Crash boxes

The crash boxes undergo the same manufacturing processes as the bumper beam. Therefore, each of the dataset processes involved—both GLO and ROW—in Process 1 (Producing Al ingots/billets), Process 2 (Extrusion process), and Process 3 (Transportation) remain the same. It should be noted that the crash boxes do not undergo the process of Section rolling or forming.

The major and only difference between system models of extruded crash box and bumper beam is the input weight.

For redesigned CMS- steel stamped

Bumper beam

Process 1: Producing steel coils (for C Section & flat plate)

Given the knowledge of the final weight of the bumper and the percentage of scrap generated in each process, a reverse calculation was performed to determine the input material needed to produce 'x' kilograms of the final bumper beam. Also, note that the procedure to produce C Section and flat plate are the same and the only difference comes in values of input and output.
Furthermore, the steel coil rolling step was not a part of this particular process, hence another process was added that involved rolling of produced steel coils.

The dataset (GLO) for the process involved in producing steel coil (from ore mining to producing steel) includes;

- Emissions from blast furnace,
- Infrastructure emissions and,
- Emissions from burning coal

The dataset (ROW) for the process involved in steel sheet rolling (from produced steel to rolled coils);

- Emissions from pickling line, cold rolling,
- Emissions from annealing, tempering and,
- Emissions from inspection, packaging and maintenance

Process 2: Blanking (for C Section & flat plate)

The dataset (ROW) for the process involved in blanking includes;

- Emissions from factory infrastructure, electricity, OPEX,
- Losses in energy,
- Emissions from ancillary processes,
- Emissions from electricity, compressed air,
- Emissions from infrastructure and OPEX,
- Emissions from water treatment plant, energy used,

Process 3: Heating (for C Section & flat plate)

Note here that a proxy process for metal heating was considered from datasets as an exact process for heating metal parts was not available in the possessed version.

The dataset (ROW) for processes involved in heating includes;

- Emissions from ancillary process,
- Emissions from electricity, and
- Emissions from general water consumption.

Process 4: Hot stamping and quenching (for C Section & flat plate)

It has to be noted that a proxy process for stamping was employed, i.e. deep drawing instead of stamping. Hence, the results may have varied from standard norms. Furthermore, the quenching step was not a part of this particular process of deep drawing, hence another ancillary process was added that involved the use of treated water (with chemicals and oils).

The dataset (ROW) for the process involved in hot stamping and quenching includes;

- Emissions from ancillary processes,
- Emissions from electricity, compressed air,
- Emissions from infrastructure and OPEX,
- Emissions from water treatment plant, energy used,
- Emissions from oils, solvents and chemicals used in treated water, and
- Transportation emissions (from carrying treated water).

Process 4: Section rolling or forming

The dataset (ROW) for the process involved in the section rolling process contains;

- Heating,
- Descaling,
- Roughing, intermediate and finishing standards and,
- Hydraulic rollers.

Process 5: Transportation- Supplier to Zeekr

The same transportation method used for the bumper beam was employed here as well. The freight truck used for transportation has a weight carrying capacity of 32 metric tonnes and adheres to the EURO 5 standard.

The dataset (ROW) for processes involved in transportation contains;

- OPEX,
- Production and maintenance of the truck,
- Construction of road,
- Energy use, combustion emissions and fuel consumption.

Process 6: Welding of C Section and flat plate at Zeekr

The sub-assembly of the bumper is often done by spot welding but in this case, as established under Delimitations, it was done by (steel) arc welding.

The dataset (ROW) for the process involved in (steel) arc welding are;

- Emissions from filler rods and their transport,
- Energy used for arc welding, and
- Emissions from use and production of protective gases

Crash boxes

Except for excluding the rolling or forming process, all other processes are the same as those for the bumper beam. The only other difference is in the welding of the upper and lower half of the crash box, which is as follows;

Process 6: Welding of upper and lower half at Zeekr

The sub-assembly of the crash box was done by steel (arc) welding.

The dataset (ROW) for the process involved in (steel) arc welding are;

- Emissions from filler rods and their transport,
- Energy used for arc welding, and
- Emissions from use and production of protective gases

A.3 Phase 1 and 2 appendices

		Parameters				Parameters	
Dimensions (if increase	Value/ Slope	IXX	NA	Dimensions (if increase	Value/ Slope	IXX	NA
d1	Value	Inc	Inc	h1	Value	Dec	Dec
d1	Slope	4,33,696.0	0.4465	h1	Slope	-4,58,193.0	-0.4718
d2	Value	Inc	Inc	h2	Value	Dec	Dec
d2	Slope	4,33,696.0	0.4465	h2	Slope	-2,22,804.0	-0.2294
d3	Value	Inc	Inc	h3	Value	Dec	Dec
d3	Slope	4,33,696.0	0.4465	h3	Slope	-2,22,804.0	-0.2294
d4	Value	Dec	Dec	h4	Value	Dec	Dec
d4	Slope	-4,33,696.0	-0.4465	h4	Slope	-80,00,000.0	-8.3525
d5	Value	Dec	Dec	h5	Value	Dec	Dec
d5	Slope	-4,33,696.0	-0.4465	h5	Slope	-80,00,000.0	-8.3525
d6	Value	Inc	Inc	h6	Value	Dec	Dec
d6	Slope	4,33,696.0	0.4465	h6	Slope	-80,00,000.0	-8.3525
a1	Value	Inc	Inc	Ig1	Value	Inc	Inc
a1	Slope	2,834.6	0.0029	Ig1	Slope	1,134.6	0.0012
a2	Value	Inc	Inc	Ig2	Value	Inc	Inc
a2	Slope	24,094.0	0.0248	Ig2	Slope	9,643.9	0.0100
a3	Value	Inc	Inc	Ig3	Value	Inc	Inc
a3	Slope	24,094.0	0.0248	Ig3	Slope	9,643.9	0.0100
a4	Value	Inc	Inc	Ig4	Value	Inc	Inc
a4	Slope	6,114.5	0.0063	Ig4	Slope	14.6	0.0000
a5	Value	Inc	Inc	Ig5	Value	Inc	Inc
a5	Slope	6,114.5	0.0063	Ig5	Slope	14.6	0.0000
a6	Value	Inc	Inc	Ig6	Value	Inc	Inc
a6	Slope	3,706.8	0.0038	Ig6	Slope	1,483.7	0.0015
y1	Value	Inc	Inc	IG11	Value	Inc	Inc
y1	Slope	8,67,391.0	0.8931	IG11	Slope	1,483.7	0.0000
y2	Value	Dec	Dec	IG21	Value	Inc	Inc
y2	Slope	-8,67,391.0	-0.8931	IG21	Slope	3.5	0.0001
y3	Value	Dec	Dec	IG31	Value	Inc	Inc
y3	Slope	-8,67,391.0	-0.8931	IG31	Slope	3.5	0.0001
y4	Value	Inc	Inc	IG41	Value	Inc	Inc
y4	Slope	8,67,391.0	0.8931	IG41	Slope	49.9	0.0000
y5	Value	Inc	Inc	IG51	Value	Inc	Inc
y5	Slope	8,67,391.0	0.8931	IG51	Slope	49.9	0.0000
y6	Value	Inc	Inc	IG61	Value	Inc	Inc
y6	Slope	8,67,391.0	0.8931	IG61	Slope	13.6	0.0000

Figure A.1: Slope matrix for attributes v/s Ixx and N.A.

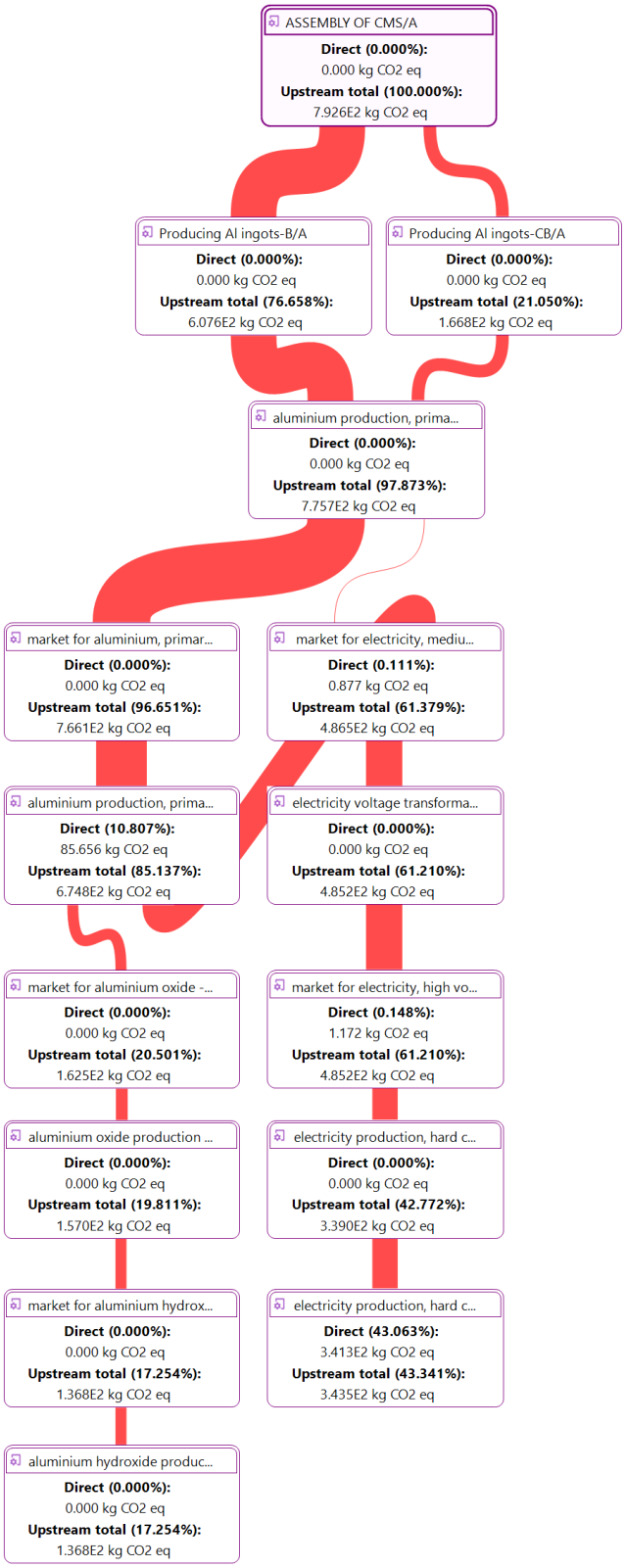

Figure A.2: Sankey diagram of aluminium CMS with top 20 processes and min. 15% contribution

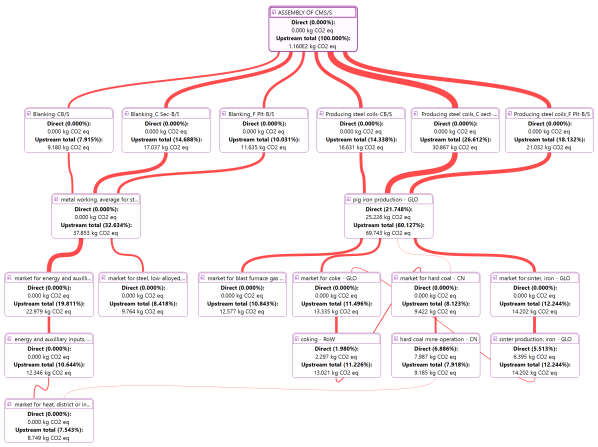

Figure A.3: Sankey diagram of steel CMS with top 20 processes and min. 15% contribution

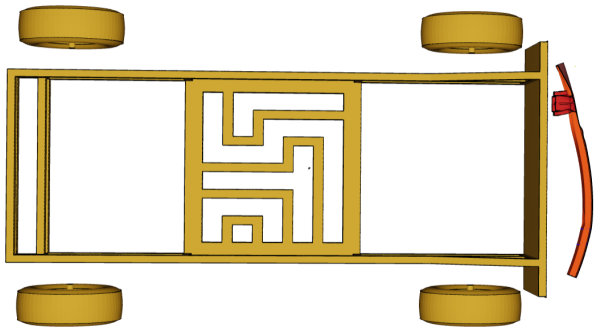

Simulation for steel crash box M bead design in LS Dyna

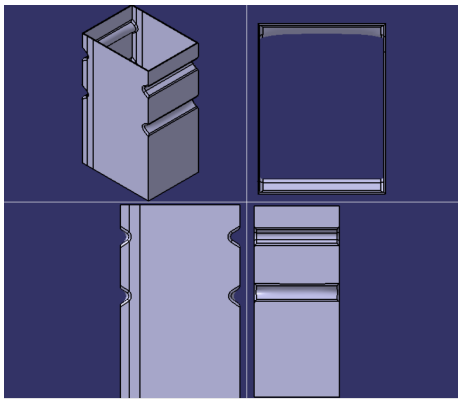

Initial design for steel crash box